CHARACTERIZATION OF THE ROLE OF TANDEM UBIQUITIN BINDING MOTIF (TUBM) OF E3 LIGASE HUWE1

YI WEN

A THESIS SUBMITTED TO THE FACULTY OF GRADUATE STUDIES
IN PARTIAL FULFILLMENT OF THE REQUIREMENTS
FOR THE DEGREE OF
MASTER OF SCIENCE

GRADUATE PROGRAM IN BIOLOGY
YORK UNIVERSITY
TORONTO, ONTARIO

December 2021

Abstract

As an E3 ligase, HUWE1 regulates various cellular processes including protein stability, DNA repair, and transcription regulation through ubiquitinating its substrate proteins. Mutation and deregulation of HUWE1 are associated with many diseases including neuronal disorders and cancers. However, the structure and function of HUWE1 protein has not been fully revealed. The tandem ubiquitin binding motif (tUBM), a novel domain of HUWE1, hypothetically modulates E3 ligase activity of HUWE1 through recognizing ubiquitin or ubiquitin chains. HUWE1 R2981H missense mutation within the tUBM domain was reported as one of the causes of X linked Intellectual Disability thus highlighting the importance of the tUBM domain. Therefore, tUBM domain was characterized in this project and the main findings were that: (1) tUBM interacts all eight types of ubiquitin di-chains; (2) the tUBM domain could modulate HECT domain activity without altering its Ub linkage preference in vitro, and (3) the HECT domain was found to be capable of synthesizing polyUb chains not only using linkage specific monoUb, but also using different diUbs as reactants. Additionally, two ubiquitin variants being developed to target UBM1 were discovered to be capable of modulating tUBM-HECT catalysis in a dose dependent manner. Therefore, the novel HUWE1 tUBM domain may serve as a Ub chains enrichment module and thus be targeted to modulate HUWE1 function.

Acknowledgement

I would like to give thanks to my supervisor, Dr. Yi Sheng, for providing me with the opportunity of MSc. Biology study and a corner of the bench in Sheng lab which allowed me to complete this project. I would like to thank her for her supervision as well as the demonstration of protein purification and the in vitro ubiquitination assay procedure. As a mature student, I cherished this study opportunity by putting in great effort to the project. Only part of my work is stated in this thesis. Although other assigned work such as cell culture, TBARS assay, Mdm2/MdmX dimerization trial, tryptic in-gel digestion and proteomic analysis were excluded, those practices enriched my skills. I would not have built such a grit and independent personality without this study experience. My intrinsic passion on scientific research was proved through this long-journey study.

Meanwhile, I would like to express my sincere appreciation to my advisor, Dr. Terrance Kubiseski, for his suggestions and advice throughout my graduate study as well as his great support on my thesis revision and defence. I would also like to thank Dr. Vivian Saridakis, and Dr. Gerald Audette for being the examiners of my thesis defence. Their comments on improving my thesis writing are highly appreciated. The guidance of the thesis examination procedure provided by Dr. Bridget J. Stutchbury is sincerely appreciated. Additionally, I feel gratitude to Dr. Vivian Saridakis, Dr. Gerald Audette, Dr. Peter Cheung, Dr. Chun Peng, Dr. Emanuel Rosonina, and their lab members for sharing laboratory equipment. The instruction on Octet instrument provided by Shili Duan (Dr. Arrowsmith Lab), the support on MS spectrometry analysis provided by Dr. Peter Luani and the UbV plasmids provided by Dr. Wei Zhang (University of Guelph) are also greatly appreciated.

The graduate courses taught by Dr. Vivian Saridakis, Dr. Emanuel Rosonina, Dr. Arthur Hilliker, Dr. John McDermott and Dr. Peter Backx allowed me to learn in-depth knowledge and techniques of molecular biology about which I feel very grateful. The training and support for my TA ship provided by Dr. Nicole Nivillac, Dr. Tanya Da Sylva and Dr. Mark Vicari are heartily thanked. I would like to address my special thanks to the researchers and graduate students at LSB - Farnaz, Nick, Saptarshi, Mohamed, Vu Hong, Jessica, Anna, Helen, Sukhdeep, Krstina, Neha, Joon, Cindy, Grace, Jyoti, Benjamin, for their generous support on my project by sharing their knowledge and experience. The great administrative support provided by Dhati Patel and Henrietta Erabhahiemen from Biology Department as well as Ebrahim Narimani from Dean Office of Science Faculty are very much appreciated. I am privileged to be a York student from undergraduate to graduate study and the motto “Tentanda via” (The way must be tried) of my Alma Mater will keep inspiring me in the next journey of my life.

Last but not least, my deep appreciation is beyond words to my families - my mother, my husband and my daughter, for their sacrifice and unconditional love. I would not have been able to complete my study by overcoming difficulties and adversities especially during the pandemic in the past two year without their constant encouragement and strong support.

Table of Content

List of Tables

List of Figures

List of Abbreviations

Ab - Antibody
ABC – Ammonium bicarbonate
ABIN - A20-binding inhibitor of NF-κB
AC -Affinity chromatography
ACN – Acetonitrile
APC -Adenomatous Polyposis Coli
APC/C - Anaphase promoting complex/Cyclosome
APS - Ammonium persulphate solution
AMP - Adenosine Monophosphate
AMPK - 5' AMP activated protein kinase
AREL1 -Apoptosis-resistant E3 ubiquitin protein ligase 1
ARLD - Armadillo Repeat Like Domain
ARF - ADP-ribosylation factor
ARF-BP1- ARF Binding Protein 1
ATP - Adenosine Triphosphate
BARD1-BRCA1 associated RING domain 1
BCA - Bicinchoninic Acid
Bcl-2 – B cell lymphoma 2
BH3 - Bcl-2 homology 3
BLI – BioLayer Interferometry
BRCA-1 -Breast cancer type 1 susceptibility protein
BSA – Bovine serum albumin
DMSO - Dimethyl sulfoxide
DTT – Dithiothreitol
DUB -Deubiquitinating Enzyme
Dvl - Dishevelled
E1 - Ubiquitin-activating enzyme
E2 - Ubiquitin-conjugating enzyme
E3 - Ubiquitin-ligase
ERAD - Endoplasmic Reticulum Associated Degradation
FBS - Fetal bovine serum
FBXW1A – F Box/WD repeat containing protein 1A
GSH - Glutathione
GST - Glutathione S-transferase
HECT – Homologous to E6-AP C-terminus
HEK – Human Embryonic Kidney
HERCs - HECT and RCC1 like domain-containing proteins
His tag - Hexa histidine tag
HRP - Horseradish peroxidase
HUWE1- HECT, UBA and WWE Domain containing protein 1
IMAC- Immobilized metal ion affinity chromatography
kDa – Kilo Dalton
LB – Lysogeny Broth
LRRK2 -Leucine Rich Repeat Kinase 2
LUBAC -Linear Ubiquitin Chain Assembly Complex
MB -Medulloblastoma
Mcl 1- Myeloid Cell Leukemia 1
MDM2 - Murine Double Minute 2
1
MULE - Mcl-1 Ubiquitin Ligase E3
MW – Molecular weight
MWCO -molecular weight cut-off
Myc - Myelocytomatosis
NCBI -National Center for Biotechnology Information
NEDD8 - Neuronal precursor cell-expressed developmentally down-regulated protein 8
NEM- N-Ethylmaleimide
NEMO - NF-κB essential modulator
NF-kB -Nuclear Factor kappa light chain enhancer of activated B Cells
NMR – Nuclear Magnetic Resonance
Npl4 -Nuclear protein localization 4
NZF -Npl4 Zinc Figure domain
PAGE - Polyacrylamide gel electrophoresis
PBS – Phosphate buffered saline
PCNA- Proliferating Cell Nuclear Antigen
PH - Pleckstrin Homology Domain
PI – Protease Inhibitor
PIP -PCNA interacting peptide
PPI -Protein Protein Interaction
pre-RC - pre-Replicate Complex
PTM - Post-translational modification
RBR – RING Between RING
RCC1 - Regulator of Chromosome Condensation 1
rpm– Revolutions Per Minute
RING - Really Interesting New Gene
RT – Retention time, room temperature

SDS - Sodium Dodecyl Sulphate
SN – Supernatant
SOCS - Suppressor of Cytokine Signalling
SUMO -Small Ubiquitin-like Modifier
TCEP - Tris(2-carboxyethyl) phosphine hydrochloride
TCR -T cell receptor
TEMED -Tetramethylethylenediamine
tHECT – tUBM-HECT domain
TLS -Translesion Synthesis
TNFα - Tumor necrosis factor alpha
Ub - Ubiquitin
UBA- Ubiquitin Associated Domain
UBD - Ubiquitin Binding Domain
UBM - Ubiquitin Binding Motif
UIM - Ubiquitin Interacting Motif
UV – Ultraviolet
WD - tryptophan-aspartic acid dipeptide
Wnt - Wingless-related integration site
WT – wild type
XLID - X-linked Intellectual Disability

Chapter 1

Introduction

1.1 Multifaceted physiological roles of HUWE1 E3 ligase

HUWE1 (also called Mule, ARF-BP1, LASU, Ureb1 or HectH9) is an E3 ligase named after its HECT, UBA and WWE domains. The *HUWE1* gene is located at Xp11.22 [1] and its mutation has been associated with neurodevelopmental disorder XLID (X-linked intellectual disability) [2-4](Figure 1.1). Through orchestrating its multiple substrate proteins, HUWE1 is required in a wide array of cellular bioprocesses through regulating its substrates thus playing crucial roles maintaining homeostasis of cellular function and development.

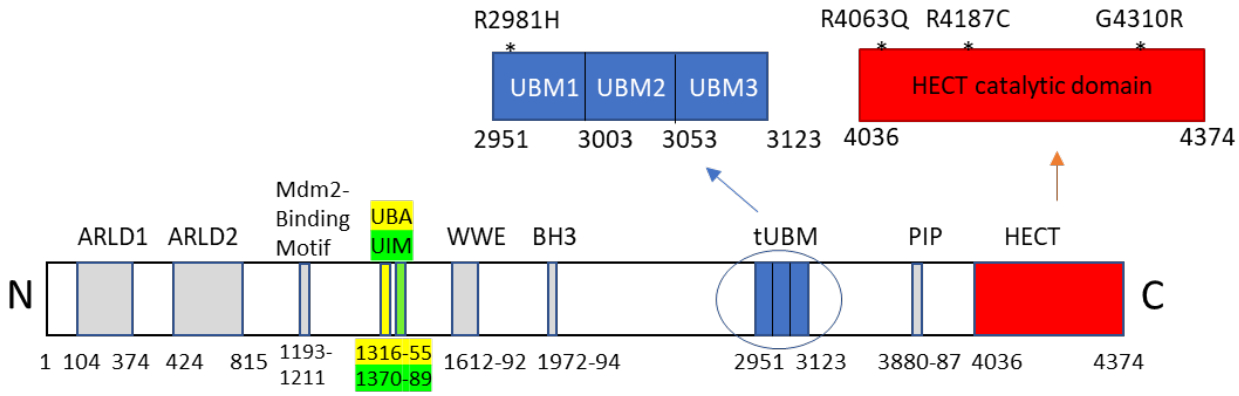

Figure 1.1 Schematic structure of HUWE1 E3 ligase. The identified domains are shown in this figure including ARLD (armadillo-repeat-like domain)(PDB: 5LP8), Mdm2 Binding Motif, UBA (ubiquitin associated)(PDB: 2EKK) colored yellow, UIM (ubiquitin interacting motif) colored green; WWE (tryptophan tryptophan glutamate)(PDB: 6MIW), BH3 (Bcl2 Homology)(PDB: 5C6H), tUBM (Tandem Ubiquitin Binding Motif)(UBM1 PDB:2MUL), PIP (PCNA interacting peptide)(PDB:6QC0), HECT (Homologous to the E6-AP Carboxyl Terminus) domains (PDB:3H1D). The blue colored tUBM and red colored HECT catalytic domain can be viewed from the enlarged presentation. The missense mutation sites involved in X-linked Intellectual Disability (XLID) have been marked with asterisks (*).

1.1.1 HUWE1 in neurogenesis

HUWE1 is a vital player in neurogenesis. *HUWE1* mutations are linked to XLID. Three missense mutations in *HUWE1* c.8942 G > A p. (Arg2981His), c.12037 C > T p. (Arg4013Trp) and c.12559 C > T p. (Arg4187Cys) have been reported to be related to XLID [2, 3]. Segregation

analysis indicates that those *HUWE1* mutations are associated with this disease [2]. The role of HUWE1 in neurogenesis is associated with its regulation of N-Myc [5]. N-Myc is a member of MYC transcription factors which is highly expressed in cerebellar primordium and is critical for neuron progenitor proliferation and neuronal differentiation inhibition [6, 7]. HUWE1 was identified as the E3 ligase which mediates proteasomal degradation of N-Myc via K48 linked polyubiquitination (ubiquitin signaling refers to section 1.2.5 of this chapter) [5].

1.1.2 HUWE1 in tumorigenesis and cell proliferation

HUWE1 has been reported to be broadly involved in tumorigenesis and it plays multifaceted roles as both oncoprotein and tumor suppressor in the context of its substrate proteins. The roles of HUWE1 in tumorigenesis relevant to this project can be introduced in two aspects: (1) Downregulating Wnt/β-catenin pathway; and (2) Ubiquitinating tumor suppressor p53 for the proteasomal destruction.

1.1.2.1 HUWE1 downregulates Wnt/β-catenin pathway

Wnt (Wingless/int-1) signaling pathway is essentially associated with embryonic development and tissue homeostasis regulating cell proliferation, cell fate specification and axis patterning [8-10]. Abnormality of Wnt cascade has been observed in cancer development [11-13]. The oncoprotein β-catenin acts as a key effector in the canonical Wnt signaling pathway [14]. Normally the level of β-catenin is tightly controlled via FBXW1A (F-box/WD repeat-containing protein 1A) mediated proteasomal degradation after β-catenin being phosphorylated by the destruction complex. Upon Wnt ligand binds Fz (Frizzled) receptor and LRP5/6 (low-density-lipoprotein-related protein 5/6) co-receptors, destruction complex becomes disrupted and

Dvl (Dishevelled) is activated via phosphorylation to inhibit destruction complex [8,9]. Thus β-catenin gets accumulated in the cytoplasm and translocated to the nucleus to transactivate its target genes [10, 15].

In Wnt/β-catenin signaling cascade, HUWE1 ubiquitinates Dvl at DIX domain via K63 ubiquitin linkage in a Wnt3a- and CK1e-dependent manner. This prevents multimerization of Dvl and inhibits Wnt/β-catenin pathway [16] (Figure 1.2). In the hyperactive Wnt pathway condition, HUWE1 mediates β-catenin degradation through K48 linked polyubiquitination as the secondary E3 ligase [17]. By negatively regulating Wnt/β-catenin pathway, HUWE1 demonstrates the feature of a tumor suppressor.

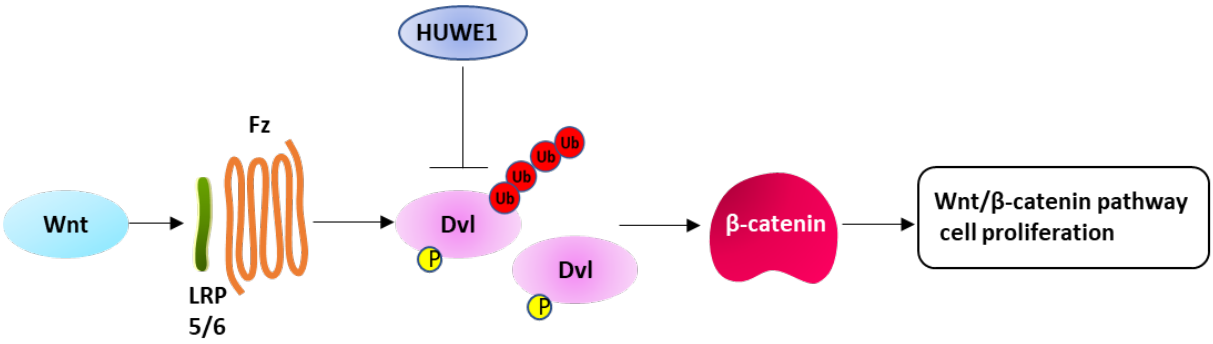

Figure 1.2 Simplified schematic representation of HUWE1 in Wnt/β-catenin pathway. Upon Wnt binds to Fz receptor and LRP5/6 co-receptor, the function of destruction complex is disrupted. Thus, Dvl becomes activated to inhibit GSK3 (Glycogen Synthase Kinase 3) of the destruction complex resulting in the accumulation of β-catenin which is followed by the translocation of β-catenin to the nucleus promoting target gene transactivation. HUWE1 ubiquitinates Dvl via K63 ubiquitin linkages inhibiting multimerization of phosphoprotein Dvl thus downregulates the Wnt/β-catenin pathway.

1.1.2.2 HUWE1 mediates tumor suppressor p53 for proteasomal degradation

The tumor suppressor p53 is another substrate protein of HUWE1. It regulates multiple cellular responses, including DNA repair, cell cycle arrest and apoptosis, thus is known as the "guardian of the genome" [18-22]. Loss of p53 by gene mutation or deletion has been observed

in around 50% of human cancers [23-25]. Despite E3 ligase Mdm2 primarily downregulates p53 [26-29], HUWE1 can also ubiquitinates p53 facilitating its proteolytic destruction thus suppressing p53-dependant apoptosis [30]. Inactivation of HUWE1 leads to p53 stabilization and transactivation [30].

In addition, HUWE1 also interacts with the tumor suppressor ARF ($p14^{ARF}$ in human and $p19^{ARF}$ in mouse) which is how HUWE1 is also named ARF-BP1 [30, 31]. The cellular ARF is made from the alternative reading frame transcript of INK4 (Inhibitor of Cyclin Dependent Kinase 4) locus. ARF protects p53 from being proteasomal degraded by inhibiting both Mdm2 and HUWE1 [32, 33]. In p53 null tumor cells, ARF induces cell growth arrest [34-36], in part through inactivation of HUWE1, indicating HUWE1 may be the mediator in the p53 independent ARF tumor suppression [30] (Figure 1.3).

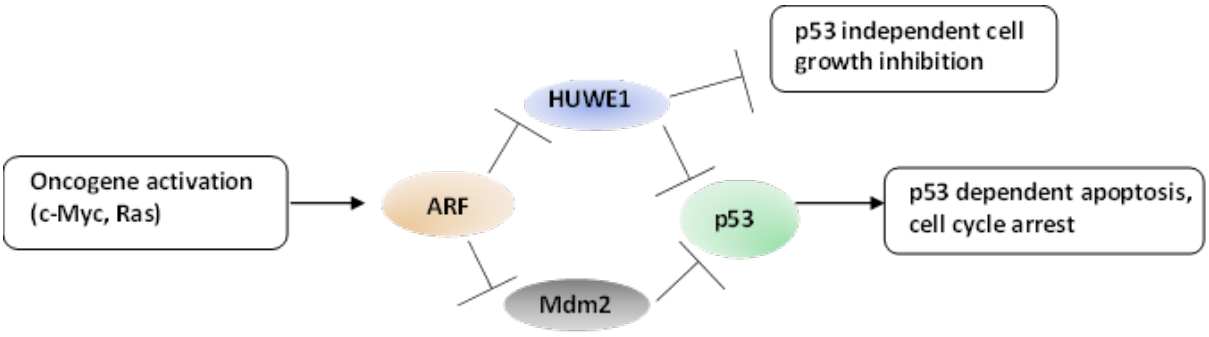

Figure 1.3 Schematic representation of roles of HUWE1 in p53/ARF pathway. In p53 wild types of cells, HUWE1 ubiquitinates p53 for proteasomal degradation in addition to the p53 primary negative regulator Mdm2 does. Consequently, p53 dependent apoptosis and cell cycle arrest are suppressed. In presence of oncogene activation, elevated expressed ARF inhibits HUWE1 and Mdm2 thus reinforces p53 stability.

In summary, HUWE1 is an important and multifaceted E3 ligase involved in tumorigenesis acting as an oncoprotein or tumor suppressor in accordance with its substrate proteins. Besides, the expression level of HUWE1 alters in different types of cancers. In primary and predominantly solid tumors including lung, breast, colorectal carcinoma, and multiple myeloma, HUWE1 exhibits higher than normal expression level [30, 37-40]. However, in thyroid cancer, HUWE1 is downregulated [41]. Therefore, it is essential to reveal the structure and the relevant biological function of HUWE1.

1.2 Biochemical background of HUWE1 as an E3 ligase

1.2.1 Introduction of ubiquitin

Discovered as a "heat-stable and non-dialysable" small protein in 1978 [42], ubiquitin is identified as a regulatory protein consisting of 76 amino acids with a highly conserved sequence for almost all eukaryotes. Human ubiquitin is encoded by four genes: UBB, UBC, UBA52 and UBA80 [43-45]. Expression of UBB and UBC genes resulting four and nine tandem repeats (head to tail multimers) of ubiquitin precursor respectively whereas UBA52 and UBA80 gene codes for ubiquitin fused to RPL40 (Ribosomal Protein L40) and RPS27a (Ribosomal Protein S27a) at C-terminal extension respectively [46, 47]. After being processed by ubiquitin hydrolases, the ubiquitin precursors eventually become conjugation competent ubiquitin molecules [48].

1.2.2 Ubiquitination

Ubiquitination, also called ubiquitylation, is one of the most common post-translational modifications, which attaches ubiquitin molecules to the substrate protein. "The reaction"

(ubiquitination) was first described by Aaron Ciechanover, Avram Hershko and Irwin Rose in 1980, and ubiquitin was termed as "APF-1" in their initial research [49]. From then on, more and more ubiquitination functions have been revealed, and it engages in almost all aspects of eukaryotic cellular processes such as protein proteasomal degradation, DNA damage signalling, protein cellular relocation, and signaling transduction [50-53].

1.2.3 Ubiquitination through an ATP dependent, E1-E2-E3 tri-enzyme mediated cascade

The process of ubiquitination is achieved through three main steps: activation, conjugation, and ligation, sequentially catalyzed by three major types of enzymes: E1 (ubiquitin activating enzyme), E2 (ubiquitin-conjugating enzyme) and E3 (ubiquitin ligase) [54] (Figure 1.4).

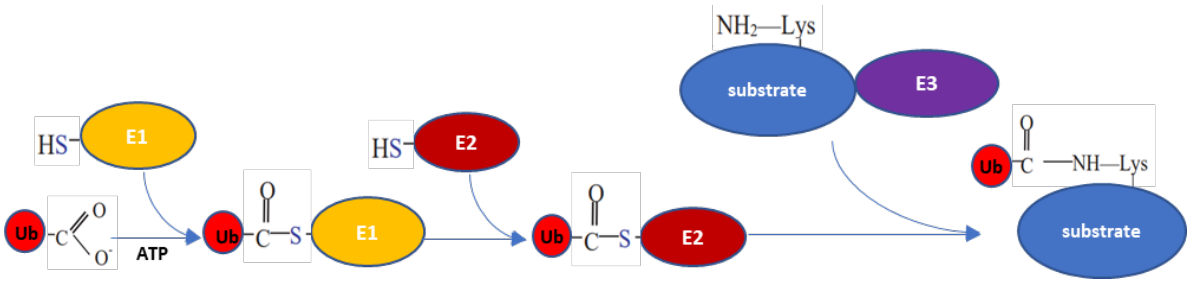

Figure 1.4 Cartoon representation of ubiquitination pathway. Ubiquitination is an ATP dependant post translational modification. The process of attaching ubiquitin molecule to the substrate protein are catalyzed sequentially by three major enzymes: E1, E2 and E3 in three steps.

1.2.3.1 E1- ubiquitin activating enzymes

The E1-E2-E3 cascade is initiated by the E1 ubiquitin activating enzymes. Two human genes: UBA1 and UBA6 encode Uba1 (also known as Uae) and Uba6 two enzymes, respectively. These two enzymes are collectively referred to as E1 enzymes [55-57]. Ube1 works with almost all types of E2 conjugating enzymes except UBE2Z/Use1 whereas Uba6 is

considered the non-canonical E1 that exclusively pairs with UBE2Z/Use1 regulating the transfer of Ub in ubiquitination pathway [55, 58].

E1 activates ubiquitin molecules in presence of ATP (Adenosine triphosphate) and Mg^{2+} by forming an intermediate ubiquitin adenylate at the C-terminal residue (Gly76) of ubiquitin, releasing pyrophosphate (PPi) followed by the attack of catalytic cysteine of E1 to ubiquitin-AMP complex at C-terminus through acyl substitution, resulting in a E1~Ub intermediate linked by a thioester bond and a release of AMP [59, 60].

1.2.3.2 E2- ubiquitin conjugating enzymes

E2 ubiquitin conjugating enzymes (also known as ubiquitin carrier enzymes) take over the activated ubiquitin from E1 and interact with the cognate E3 ligase, performing the second step of ubiquitination [61].

In humans, about 40 types of E2 enzymes are involved in transfer and conjugation of ubiquitin among which the structure of over 30 types of E2 has been solved [62-64]. Each type of E2 contacts E1 as well as one or more types of E3 ligases separately during the ubiquitination process [62, 63, 65, 66]. All 32 structure-solved E2 enzymes contain a 150-amino acid catalytic core (called UBC domain) which contains the catalytic cysteine and part of E3 interacting site which overlaps with the E1 binding region [62, 67].

The cognate E2 is recruited by E1~Ub thus catalyzes transthioesterification reaction transferring the thioester-linked ubiquitin to the catalytic cysteine of E2. Coordinating different types of E3 ligases, E2 catalyzes ubiquitin transfer and conjugation with discriminating mechanisms which will be explained in detail in the following section [62, 63].

1.2.3.3 E3- ubiquitin ligases

At the final step of the tri-enzymatic cascade, E3 ubiquitin ligases mediate the transfer of ubiquitin from a loaded E2 to specific substrate proteins in distinct ways in accordance with different types of E3 ligases [68].

Over 600 human E3 ligases have been identified and can be grouped into three main categories based on their catalytic domain and ubiquitination mechanism: RING (Really Interesting New Gene), HECT (homology to E6AP C terminus) and RBR (RING-between-RING) E3 ligases [68].

1.2.3.3.1 RING E3 ligases

RING E3 ligases indirectly catalyze ubiquitination by providing scaffold for E2~Ub complex. Within the scaffold of RING E3, ligase E2 catalyzes the transferring the ubiquitin to the ε-amino group of lysine residue on substrate protein by forming an isopeptide bond [68-70]. Among 600 E3 ligases in humans, RING E3 ligase is the most abundant E3 ligases in human containing a cross-braced motif that coordinates two Zn^{2+} ions [70]. The well-known E3 ligase Mdm2 (Mouse double minute 2 homolog) is a type of RING E3 ligase which functions as the primary negative regulator of p53 tumor suppressor through ubiquitinating p53 thus mediating its degradation by 26S proteosome [71-73].

1.2.3.3.2 HECT E3 ligases

Different from RING E3 ligases, HECT E3 ligases form an intermediate between the catalytic cysteine and ubiquitin before transferring ubiquitin to the ε-amino group of lysine residue on the target protein [68, 74-76]. HECT E3 ligases have only about 30 members in

humans, all of which contain a conserved C-terminal HECT catalytic domain [77-79]. HECT domain adopts a bilobate structure. N-lobe for E2~Ub binding and a C-lobe carrying the catalytic cysteine for loading ubiquitin. There is a flexible hinge region between N-lobe and C-lobe that allows the C-lobe to achieve its catalytic function through motion [74, 80-83]. Based on the regions before the conserved catalytic domain, HECT E3 ligases can be subdivided into three main classes: (1). NEDD4 family named after E3 ligase NEDD4 (neural precursor cell expressed developmentally down-regulated protein 4) which contains a calcium dependent phospholipid-binding C2 domain, two to four WW protein-protein interaction or substrate recognition domain and a C-terminal HECT domain [80, 83]. (2). HERC family characterized by HERCs (HECT and RCC1 like domain-containing proteins) which contain both HECT domain and RCC1 like domain. There are six members in HERC family. Based on their molecular size and structure, HERCs can be grouped into two categories: Large HERCs and small HERCs. Two large members (HERC1 and HERC2) contain one HECT domain and more than one RLD (RCC1 like domain) whereas four small members (HERC3-6) possess one HECT domain and single RLD domain [84]. (3). Other HECT E3 ligases either lacking conserved N-terminal structures or with N-terminal domains different from NEDD4 or HERC E3 ligases. HUWE1 falls into this catalogue [85].

1.2.3.3.3 RBR E3 ligases

RBR E3 ligases are composed of RING1 domain, IBR (in-between-RING) and RING2 domains [68, 86, 87]. Among 14 types of known RBR ligases, only Parkin, HHARI and HOIP have been well studied. RBR E3 ligases ubiquitinate substrate proteins by a RING/HECT hybrid-like mechanism: RING1 recruits ubiquitin loaded E2, then ubiquitin is first transferred onto the

catalytic cysteine on RING2 forming an intermediate, and eventually attached to lysine residue on the substrate protein [86, 87].

1.2.4 Ubiquitin structure and ubiquitin chain formation

Ubiquitin is a globular protein composed of one α-helix and five stranded β-sheets (Figure 1.5). Through ubiquitination, ubiquitin molecules can be attached to not only substrate protein but also another ubiquitin molecule resulting in polyubiquitin chains. The mechanism of ubiquitin chain conjugation and elongation is that the C-terminal (Gly 76) carboxyl group of donor ubiquitin covalently attaches to the acceptor ubiquitin and subsequently distal donor ubiquitin conjugates to the proximal donor ubiquitin thus forming a polyubiquitin chain [88-90].

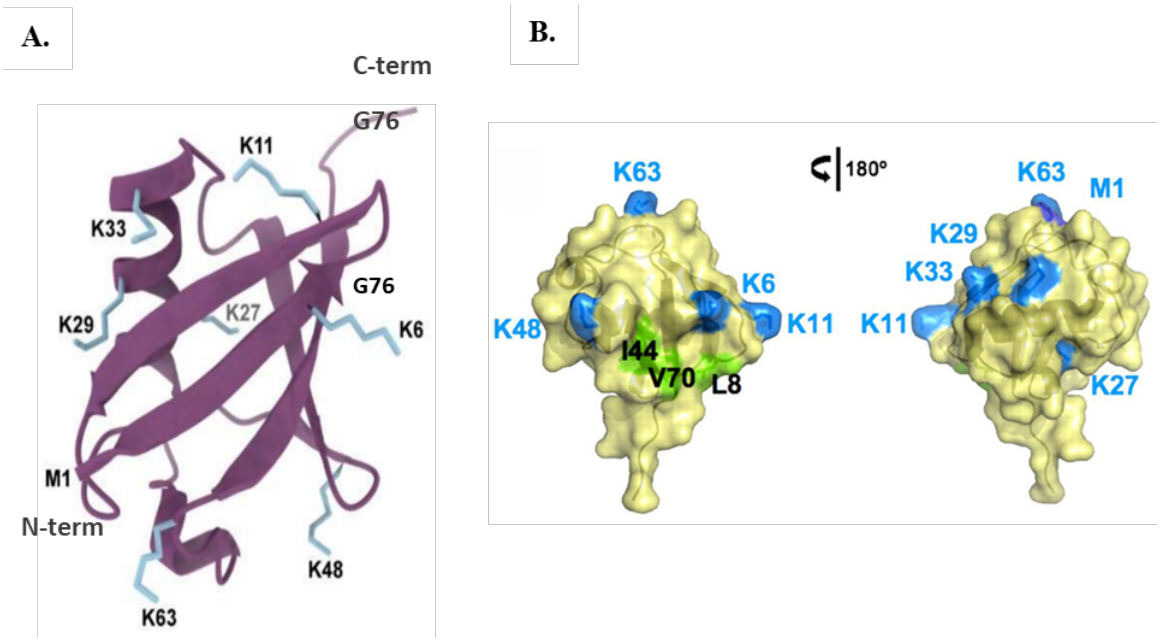

Figure 1.5 Ribbon and surface presentation of ubiquitin structure. A. Ribbon presentation of ubiquitin structure with eight linkage sites labeled (M1, K6, K11,K27, K29, K33, K48 and K63) as well as annotation of C-terminal Glycine 76 (The figure adapted from Dougherty et al., International Journal of Molecular Sciences, 2020). **B.** Surface presentation of ubiquitin molecule with eight linkage sites colored in blue and hydrophobic core L8, I44 and V70 colored in green (The figure is adapted from Messick and Greenberg, The Journal of cell biology, 2009).

1.2.5 Ubiquitin linkages and ubiquitin signaling

Each ubiquitin contains seven lysine residues: K6, K11, K27, K29, K48 and K63. Together with the N-terminal M1 residue, there are a total eight potential linkage sites on each individual ubiquitin (Figure 1.5). For instance, the carboxyl group of ubiquitin tail (Gly 76) of donor ubiquitin forms an isopeptide bond with the ε- amino group of K6 residue on the acceptor ubiquitin is called K6 linkage. The M1 linkage is also called head to tail linkage which is formed between the C-terminus glycine residue of the incoming ubiquitin and the N-terminus methionine of the preceding ubiquitin through a peptide bond. Those eight types of ubiquitin linkages can be involved in assembling di-Ub chains or polyUb chains. Such ubiquitin molecule structure enables the intricate ubiquitination topologies to be formed on substrate proteins including mono-ubiquitination, multi-ubiquitination and homotypic or heterotypic (branched) poly-ubiquitination (Figure 1.6). Different ubiquitin linkages exerting distinct signaling (also known as ubiquitin code) determining function or fate of modified substrate protein [52, 61, 91].

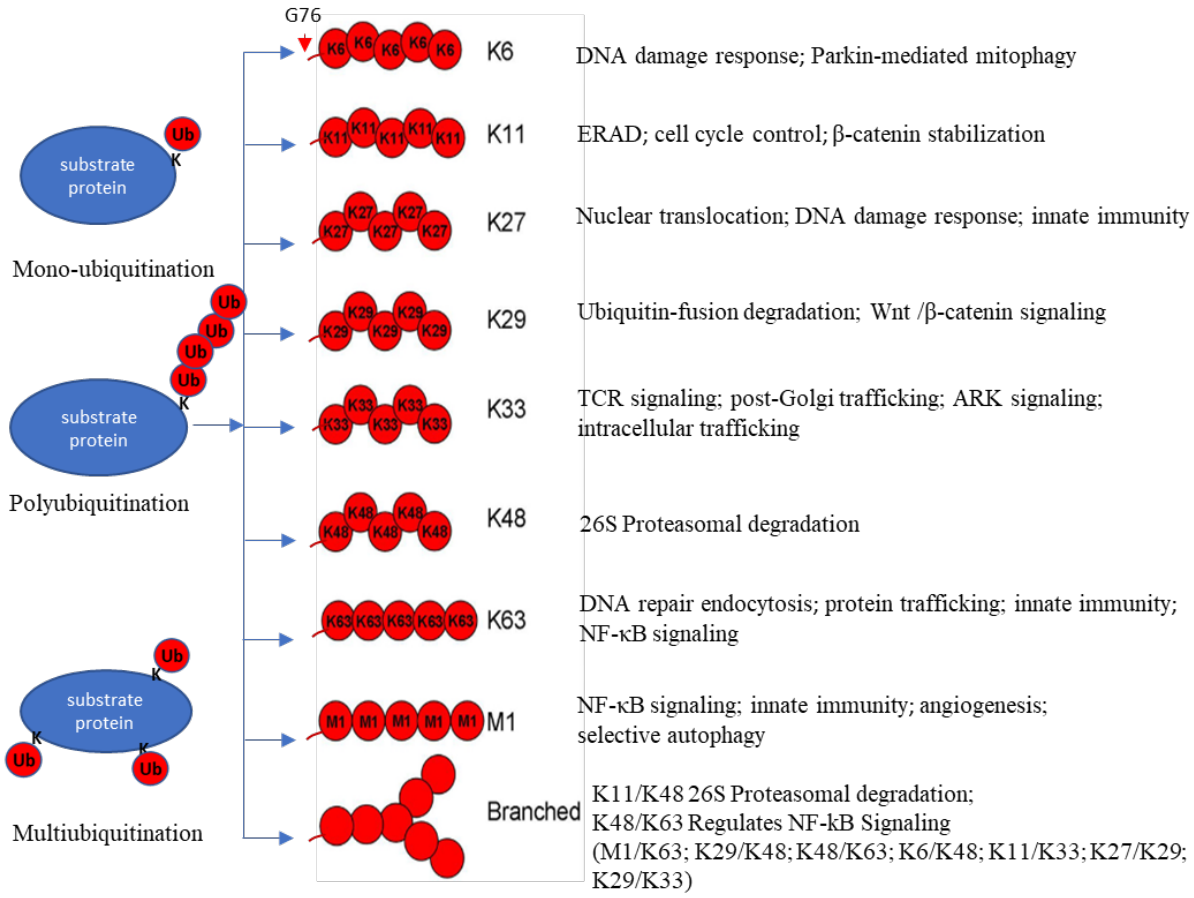

Figure 1.6 Diagram of ubiquitination topologies and the corresponding signaling. Ubiquitin molecules covalently attach to lysine residues in the substrate protein through isopeptide bonds catalyzed by ubiquitination enzymes. Based on the conjugate topologies, ubiquitination can be grouped into three categories: Mono-ubiquitination, Multiubiquitination and Polyubiquitination which includes homotypic polyubiquitination and heterotypic polyubiquitination. Different ubiquitination exerts distinct ubiquitin signaling which endows discriminating function of the substrate protein after modification.

Among those ubiquitin chains, K48 and K63 linked ubiquitination have been well studied whereas other types of linkages (also called atypical linkages) are less known. K48 linked and K48/K11 branched polyubiquitin chains exert signaling for targeted protein to undergo 26s proteasome destruction. K63 ubiquitin linkage is known to be responsible for endocytosis, protein trafficking, innate immunity and NF-κB signaling [50, 92, 93]. K6 linkage is involved in DNA damage response and Parkin-mediated mitophagy. Heterotypic K11 poly-ubiquitination is

considered a powerful degradation signal. K11 linkage is related to human cell cycle control [94], ERAD (endoplasmic reticulum-associated degradation) [95] and β-catenin stabilization [96]. K27 linkage participates nuclear translocation, DNA damage response and innate immunity. K29 linkage is reported to be involved in ubiquitin-fusion degradation and Wnt /β-catenin signaling. K33 linkage plays a role in TCR (T cell receptor) signaling and intracellular trafficking and is associated with post-Golgi trafficking and ARK (AMPK-related kinase) signaling. M1-linkaged Ub chains (also known as linear Ub chains) play crucial roles in inflammatory and immune responses through regulating NF-κB signaling and it is also involved in angiogenesis and selective autophagy [50, 52, 92, 93, 97].

DiUb is the shortest Ub chains including eight different di-Ub linkages (di-M1, di-K6, di-K11, di-K27, di-K29, di-K33, di-K48 or di-K63). Each exhibits distinct confirmation. For instance, di-M1 Ub chain exhibits a head to tail linkage, di-K63 Ub chain adopts an open complex conformation, whereas K48 linked di-Ub chain shows a closed conformation [92, 98, 99] (Figure 1.7). Therefore, these different types of ubiquitin di-chains can be used to characterize the specificity of ubiquitin recognition by different ubiquitin binding proteins. In this project, eight diUb chains have been applied to detect the capability and preference of HUWE1 tUBM domain binding with different Ub linkages.

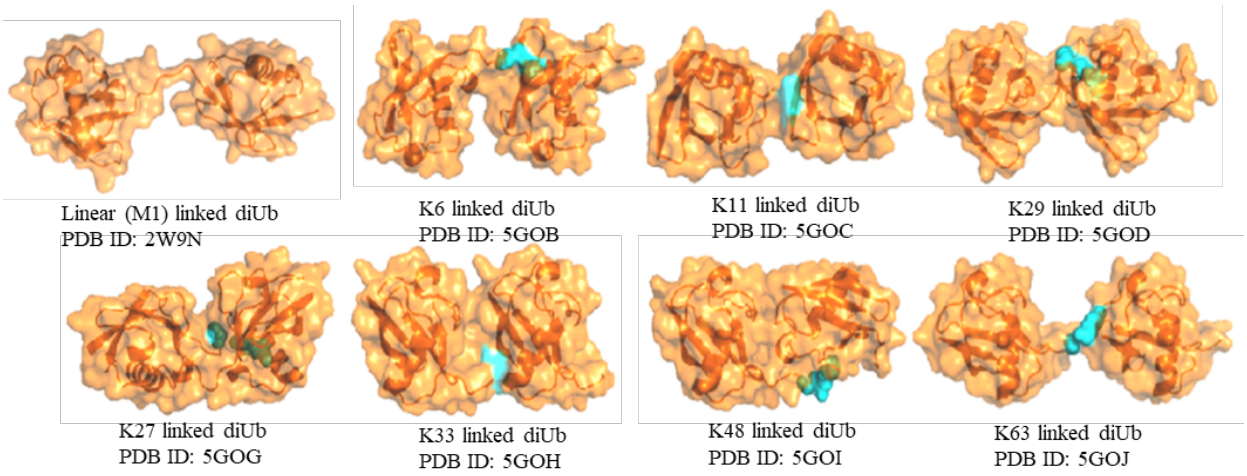

Figure 1.7 View of eight linkage types of diUb. Isopeptide bonds between donor and acceptor ubiquitin are colored in cyan. Di-Ub with different linkages exhibit variant conformations. M1 linked and K63 linked di-Ub adopt open conformation whereas K48 linked di-Ub upholds a close confirmation. Linkage specific di-Ub can be used to characterize the binding recognition of UBD and E3 catalytic specificity (The figure is adapted from Gao et al., The Journal of American Chemical Society 2016).

1.2.6 The linkage specificity of polyubiquitin synthesis

Polyubiquitin synthesis is affected by the selectivity of ubiquitination enzymes. For instance, RBR E3 ligase WSB1 (WD repeat and SOCS box-containing protein 1) ubiquitinates LRRK2 (Leucine-rich repeat kinase 2) forming K27- and K29-linked ubiquitin chains [100]; HECT E3 ligases AREL1 (Apoptosis-resistant E3 ubiquitin protein ligase 1) preferably assembles K33 and K11 linked ubiquitin chains [101]; HECT E3 ligase UBE3C catalyzes K29- and K29/K48 linked polyubiquitin formation [102, 103]; E2~E3 complex Ube2S-APC/C specifically synthesize K11 linked ubiquitin chain [104]; RING-type E3 ubiquitin ligase TRAF6 builds K63 chains together with Ubc13/Uev1A, an E2 complex specific for the K63 linkage synthesis [105], HECT E3 ligase HUWE1 can further add K48 branches on K63 chains being formed by TRAF6 into K48/K63 heterotypic polyubiquitin chains regulating NF-kB signaling which expands the diversity of the ubiquitin code [106].

1.2.7 Reversibility of ubiquitination

The ubiquitin molecules being covalently conjugated to the substrate protein through ubiquitination can be cleaved off by DUBs (Deubiquitinating enzymes), also known as deubiquitinase, ubiquitin hydrolyses or ubiquitin isopeptidases, through a process called deubiquitination [48, 107, 108]. Therefore, ubiquitination is a reversible bioprocess. In fact, the protein ubiquitination is reversible *in vivo* in many cellular processes including but not limited to ubiquitin proteasome pathway.

1.3 Domains and activity of HUWE1

HUWE1 is a large polypeptide composed of 4374 amino acids. Despite its considerable molecular size, only a few domains and motifs of HUWE1 have been characterized. Those known HUWE1 function domains and motifs include C-terminal HECT domain, ARLD 1/2 (Armadillo-repeat-like domain 1 and 2) domains, Mdm2 Binding Motif, UBA-UIM domain, WWE domain, BH3 motif and PIP motif. Also, there is a novel tUBM (Tandem Ubiquitin Binding) which is the research focus of this project [106, 109-115] (Figure 1.1). The cryo-EM structure of the full length HUWE1 shows that HUWE1 adopts a large alpha solenoid architecture to form a scaffold [116] (Figure 1.8). The accessory domains (WWE, UIM, UBA) are connected to the scaffold through flexible links, which are responsible for the substrate proteins recognition and interaction and play crucial roles on modulating HUWE1 enzymatic activity [116].

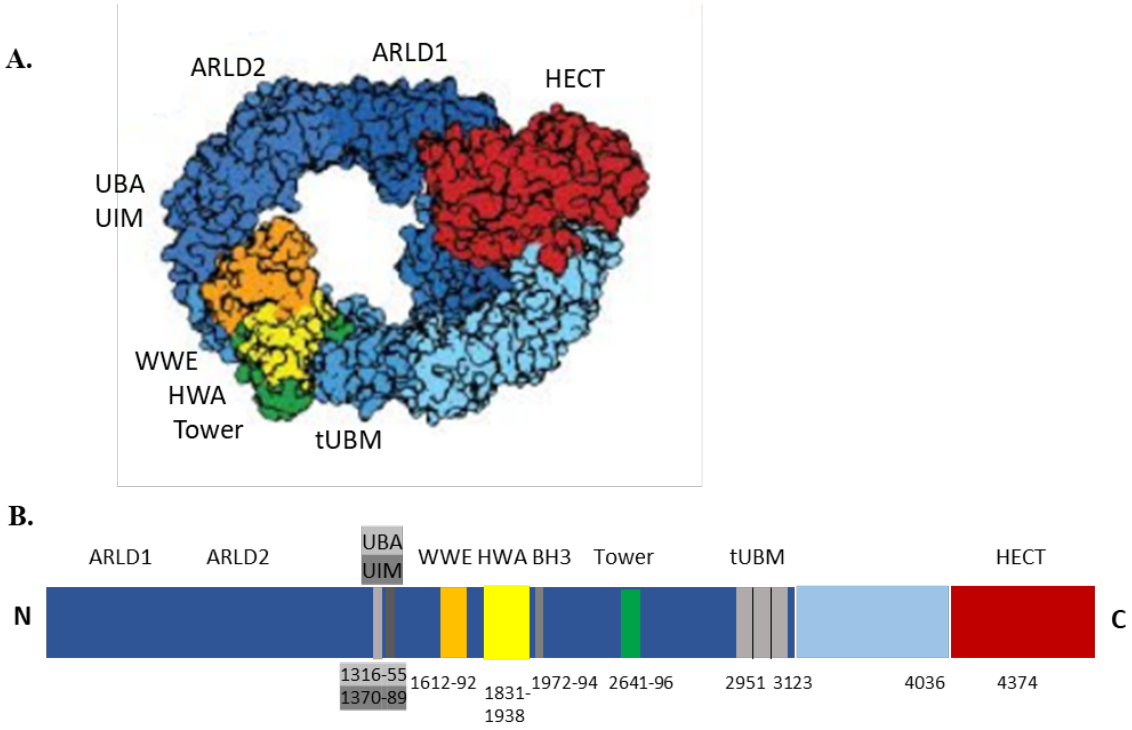

Figure 1.8 Illustration of HUWE1 cryo-EM Structure and domains. A. Ring-shaped cryo-EM structure of full length HUWE1 (EMD-22431). This figure is adapted from Hunkeler, et al., Molecular Cell, 2021 **B.** Schematic representation of linear HUWE1 peptide with illustration of its domains corresponding to the domains demonstrated on the Cryo-EM structure **(A.)** including WWE (orange), HWA (HUWE1 WWE module associated) (yellow), Tower (green), HECT (red) as well as grey colored UBA, UIM, BH3 and tUBM domains.

1.3.1 HUWE1 HECT domain

HUWE1 C-terminal HECT domain is the catalytic domain, responsible for catalyzing the final step of the ubiquitination. The catalytic activity of the HECT domain can be modulated by the other domains of HUWE1 N-terminal to HECT domain through intramolecular regulation.

Like other types of E3 ligases (E6AP, Smurf2, WWP1), HUWE1 HECT domain is also composed of an N-lobe ($HUWE1_{3993–4252}$) which contains the E2 binding domain ($HUWE1_{4150–4200}$), a C-lobe ($HUWE1_{4259–4374}$) carrying the catalytic cysteine (Cys4341) and the two lobes are joined by a flexible hinge region ($HUWE1_{4253–4258}$). The rotary movement of the C-lobe

facilitates the transfer of Ub from the cognate Ub-loaded E2 UbcH7 (also known as UBE2L3 or E2L3) to HUWE1 [113]. The formation of a thioester bond between the catalytic cysteine of HUWE1 and the C-terminus of ubiquitin is an intermediate step before HUWE1 attaches the Ub to the lysine residue of substrate protein through an isopeptide linkage [114].

1.3.2 ARLD 1/2 domains

Two ARLD domains (ARLD 1 and ARLD 2) have been identified at the N terminus of HUWE1 [109] (Figure 1.1). The function of HUWE1 ARLD domains remains to be characterized [109].

1.3.3 Mdm2 Binding Motif

Although both Mdm2 and HUWE1 are E3 ligase, Mdm2 promotes HUWE1 proteasomal degradation through ubiquitination [117, 118]. Mdm2 binding motif on HUWE1 has been identified at residues 1198 to 1205 [117] (Figure 1.1).

1.3.4 UBA-UIM domain

UBA and UIM domains located at the N terminal HUWE1 are two different types of UBD (refers to 1.3.8.1) and both interact with ubiquitin [106, 115]. It has been reported that HUWE1 UBA-UIM domain does not interact with monoubiquitin, but does interact with di-, tri-, and tetra-K63 Ub chains in vitro [106].

1.3.5 WWE domain

WWE is termed after its conserved residues of tryptophan, tryptophan and glutamate. WWE domain has been found in proteins involved in two protein post translational modifications: ubiquitination and PARylations including E3 ligases deltex, Trip12 and RNF146 as well as poly-ADP-ribose polymerases PARP11 and PARP14 [110-121]. PARylation refers to the PTM of covalently attaching ADP-ribose units to substrate proteins catalyzed by PAR polymerase thus regulates chromatin remodelling, DNA repair, transcription and other processes [121]. WWE domains from RNF146 and HUWE1 have been reported to be able to recognize PAR (poly-ADP-ribose) through interacting with *iso*-ADPR (*iso*-ADP-ribose) serving as PAR readers [120, 122]].

1.3.6 BH3 motif

BH3 motif is a short peptide found in certain Bcl-2 (B cell lymphoma-2) family proteins which is associated with mitochondrial events leading to apoptosis [109,123, 124]. Bcl-2 family proteins are regulators of apoptosis which can be grouped into three categories: anti-apoptotic proteins containing four BH (Bcl-2 Homology) motifs (BH1-4) such as Bcl-2 and Mcl-1; pro-apoptotic proteins possessing three BH motifs (BH1-3) including BAX and BAK as well as pro-apoptotic proteins with only BH3 motif such as BAD, BID, Noxa and Puma [109,123-125]. HUWE1 ubiquitinates Mcl-1and mediates its proteasomal degradation through interacting with Mcl-1 at BH3 motif [109, 126].

1.3.7 PIP motif

PIP motif is a short linear motif that can be found in many PCNA binding partner proteins. HUWE1 PIP motif is designated for PCNA interaction [127].

1.4 Introduction of UBD

HUWE1 tUBM domain is one type of Ubiquitin Binding Domain (UBD). UBDs are modular elements that bind non-covalently to ubiquitin or ubiquitin chains functioning as decoders of specific ubiquitin signals [128-130]. At present, more than 150 ubiquitin receptor proteins have been identified containing one or more of approximately twenty types of known UBDs [128, 131, 132]. Different UBDs can be grouped into five categories including Helical domain, Zinc finger, Ub-conjugating-like, Pleckstrin-homology and other types of UBD (Table 1.1). Helical motifs are seen in multiple types of UBDs including UIM, UBA and UBM domains [128, 131, 132]. Zinc fingers (ZnF) are involved in the interaction between ubiquitin and ZnF UBDs such as UBZ (Ubiquitin-Binding ZnF) and NZF (Nuclear protein localization 4 Zinc Finger). Pleckstrin-homology (PH) motif, composed of a C-terminal α-helix and a seven-stranded β-sheet as well as attached phosphoinositides (PIs), which has been found in two types of UBDs – GLUE (Gram-Like Ubiquitin-binding in Eap45) and PRU (Rpn13's Pleckstrin-like Receptor for Ubiquitin) [134-136]. Ubiquitin-conjugating (Ubc)-related motif, found in E2 conjugation enzyme. The existence of Ubc-related motif implies that E2 interacts with ubiquitin not only covalently through its catalytic cystine but also non-covalently through its Ubc-related motif containing UBD [132].

Table 1.1 List of Ubiquitin Binding Domains.

Domain Category	UBD Name	Ubiquitin Hydrophobic core binding to the UBD	Proteins Containing Specific UBD
Helical domain	UBM (Ub-binding motif)	Leu8	Polymerase iota, Polymerase Rev1
	UBA (Ub-associated domain)	Ile44	PLIC1/2, HHR23A/B, p62, NBR1, Cbl-b, USP5, UBC1, HERC2, Vps13D, USP25
	UIM (Ub-interacting motif)	Ile44	RPN10, VPS27, USP28, ATAXIN-3, EPS15, STAM1, STAM2, RAP80, DNAJB2, USP37, USP25, EPSINs
	MIU (Motif interacting with Ub)	Ile44	Rabex-5, RNF168
	DUIM (Double-sided UIM)	Ile44	HRS
	CUE (Coupling of Ub to ER degradation domain)	Ile44	Cue2, Vps9
	UBAN (Ub-binding domain in ABINs and NEMO)	Ile44 Phe4 linker	ABIN1, ABIN2, ABIN3, NEMO, OPTN
	VHS (VPS27, HRS and STA domain)	Ile44	VPS27, HRS, STAM1, STAM2,
	GAT (GGA and TOM1 domain)	Ile44	GGA1, GGA2, GGA3, TOM1
	MyUb (Myosin VI UBD)	Ile44	Myosin VI [33]
Zinc finger (ZnF)	UBZ (Ub-binding ZnF domain)	Ile44	TAX1BP1, Polymerase eta, WRNIP1, FAAP20
	NZF (Npl4 ZnF domain)	Ile44	Npl4, Vps36, TAB2, TAB3, HOIP, HOIL-1L, SHARPIN
	ZnF A20 (A20 ZnF domain)	Asp58	A20, Rabex-5
	ZnF UBP (Ub-specific processing protease ZnF domain)	Leu8 Ile36 tail	USP5, USP20, HDAC6, BRAP2
Ub-conjugating-like	UBC (Ub-conjugating domain)	Ile44	UbcH5c
	UEV (Ub E2 variant domain)	Ile44	TSG101, Mms2
Pleckstrin-homology (PH)	GLUE (GRAM-like Ub-binding in EAP45 domain)	Ile44	Eap45
	PRU (Pleckstrin-like receptor for Ub)	Ile44	Rpn13
Other	PFU (PLAA family UBD)	Ile44	Doa1, PLAA

There are many other types of UBDs. The distinct UBD structures determine their preferred interacting ubiquitin linkages. For instance, most C-terminal UBA domains bind to Lys48 linkage [137]. Another type of UBD NZF (Npl4 Zinc Finger domain) of TAB2 (TAK1-binding protein 2) favors Lys63- over Lys48 linkage [102]. Tandem NZF_{1-3} of TRABID (TRAF-binding domain containing protein) are K63 and M1 ubiquitin binders, but individual NZF domain favors K29 and K33 polyubiquitin chains [102]. NEMO contains UBAN (Ub binding domain in ABIN proteins and NEMO) (ABIN refers to A20-binding inhibitor of NF-κB) domain specifically binding to linear ubiquitin linkages [138, 139].

UBM has been found in proteins including Polι, Rev1 and HUWE1. It has some unique characters in addition to some common UBD features [142-145]. UBM adopts a helix-turn-helix structure and the conserved Leu- Pro motif between two alpha helices is vital for UBM to interact with ubiquitin. Similar as other types of UBD, UBM non-covalently bind to ubiquitin on the hydrophobic core (Leu-8, Ile-44, and Val-70) of ubiquitin. However, the hydrophobic interaction between UBM and ubiquitin distinctly centred at Leu-8 instead of at the conventional Ile-44 as most UBDs [142, 143, 146].

1.4.1 Detecting Ub chain or Ub and identifying Ub linkage types through immunological methods

In order to understand the function of the UBD in context of regulation of substrate protein through diverse ubiquitin signaling, recognition specificity of ubiquitin linkages is the most important character of a UBD to be unraveled. Different types of anti-Ub antibodies specifically recognizing Ub modification have been utilized in immunoblot, immunoprecipitation and ELISA to detect free Ub and Ub conjugates. For instance, FK2 antibody recognizes all

conjugated Ub but not free Ub [147]. Ub-ELISA (enzyme-linked immunosorbent assay) method has been applied to measure the amount of total Ub after all conjugated Ub being converted to free Ub by using USP2cc (Ubiquitin-Specific Protease 2 catalytic core) [148]. Moreover, Ub chain types can be distinguished by Ub linkage-specific antibodies [149, 150]. However, only five of eight types of Ub linkages can be recognized by linkage specific antibodies [150-153]. In addition, the affimers with high affinity to the atypic K6- and K33- linkage polyUb have been developed to detect their corresponding polyUb chains [152].

1.4.2 Recognizing and enriching Ub species through selective UBDs

Ub linkage specific UBD recognizes certain types of Ub chains. The UBDs listed in Table 1.2 have been studied for specific Ub chains identification and enrichment. For instance, K29- and K33- linked Ub chains were selectively bound by NZF1 (Npl4 zinc finger 1) of the DUB TRABID (tumor-necrosis factor receptor-associated factor-binding protein domain) [102]; K63 linkage-specific Ub chain can be recognized by NZF domain of TAB2 (TAK1-binding proteins) which is the adaptor subunit of TAK1 (Transforming growth factor beta-activated kinase 1) [153]. Also, K63 linked Ub chain can be selected by UIM domain of VPS27 (Vacuolar protein sorting-associated protein 27) [154, 155]. To enhance the binding affinity between UBD and Ub, TUBEs (Tandem Ub binding entities) have been engineered so that even the low abundant Ub targets can be specifically captured from cellular lysates [156, 157].

Table 1.2 Ub linkage-selective UBD. The UBDs listed in the table specifically recognize certain type(s) Ub chains.

Ub Linkage Types	Selective UBD	Protein Associated with the UBD
K29/K33	NZF1	TRABID
K63	NZF UIM	TAB2 VPS27
M1	UBAN	NEMO ABIN
K48 (Unconjugated polyUb)	ZnF UBP hybrid with UBA	Engineered protein

1.4.3 Development of UBM inhibitor

The ubiquitin variants (UbVs) have been generated as modulators and probes of cellular proteins. UbVs are powerful tools for probing functions of ubiquitination related enzymes including E2, E3 and DUBs [158-162]. UbVs are developed through a technique called phage display.

Phage display was first reported in 1985, in which a filamentous phage gene III was used to express a fusion protein on its surface [163]. pIII is a minor coating protein on surface of the virion. A piece of DNA encoding a peptide can be inserted into pIII and expressed as a PIII-fused foreign peptide, "displaying" on the surface of the phage [164, 165].

UbVs are engineered based on the ubiquitin peptide sequence thus the molecular size and the structure of UbVs are comparable to that of Ub. Through structural analysis and screening process, the peptide sequence of UbVs can be customized to enhance the binding affinity of UbVs at the interaction surface of the target protein. For instance, β1-β2 loop of UbVs tolerates insertions of one, two, or three residues between positions Leu8 and Thr9 promoting affinity enhancement and extended β3- β4 loops of UbVs can specifically increase the binding affinity to USP15 [158].

Development of target specific UbVs undergoes several runs of selection. Briefly, after a library of UbVs is expressed on phages, a high-throughput screening is conducted to select for the specific UbV binders. The UbV candidates flow through the immobilized target protein. Only the UbVs bind to the immobilized protein remain and non-binding UbVs will be washed away. The binding selection cycle can be repeated multiple times to optimize the binding affinity of UbVs (Figure 1.9).

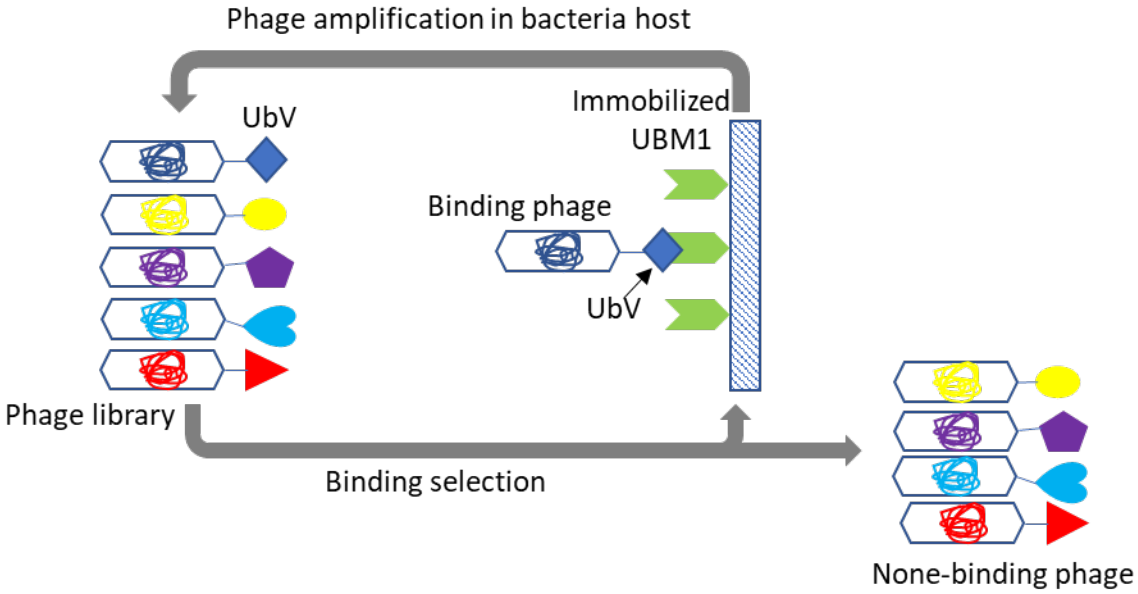

Figure 1.9 Cartoon representation of phage display UbV library high throughput screening cycle targeting UBM1. In phage library, each phage particle displays a unique UbV based on the constructed DNA. The library flow through immobilized target protein, only the protein binding UbVs on the phage are captured whereas non-binding UbVs on the phage are washed away. After several rounds of selection, the UbVs with high binding affinity can be enriched.

1.5 Rationale and aims of the project

Emerging evidence shows that HUWE1 participates in multitudes of physiological processes through ubiquitinating its substrate proteins. However, due to its large molecular size and functional complexity, HUWE1 has not been fully characterized.

HUWE1 tUBM domain ($HUWE1_{2951-3123}$) has been identified based on their sequence homology to the UBM domain of polymerase iota. HUWE1 tUBM containing three tandem repeats UBM1, UBM2 and UBM3 is located ~900 residues upstream of HECT domain ($HUWE1_{4036-4374}$). UBM1 is the first repeat of tUBM domain which is composed of two helices linked by the signature turn containing Leu-Pro motif. The report of R2981H mutation within UBM1 domain leading to XLID highlights the clinic significance of HUWE1 tUBM domain [1, 169]. The focus of this project is to characterize the role of HUWE1 tUBM domain in Ub recognition and its impact on HUWE1 E3 ligase function through modulating HECT catalytic domain.

1.5.1 Aims of the project

Aim 1: Characterization of preference and specificity of ubiquitin and ubiquitin chains interacting with HUWE1 tUBM domain

HUWE1 tUBM domain is hypothesized for recognizing the specific Ub code and recruiting preferred Ub or Ub chains. The preference and specificity of Ub or Ub chains interaction with the tUBM domain are the key characters to be revealed. Furthermore, since tUBM is a Ub binder and a cis molecular modulator of HECT domain, the types of Ub or Ub chains favored by tUBM might impact the HECT domain catalytic specificity of poly Ub chains. Therefore, in vitro analysis including BLI, and native gel electrophoresis were performed to detect the interactions between HUWE1 tUBM domain and each of eight ubiquitin di-chains (M1-, K6-, K11-, K27-, K29-, K33-, K48- and K63- linked). The methods and results of in vitro characterization of the interaction between tUBM and Ub di-chains were summarized in Chapter 2.

Aim 2: Characterization of effect of tUBM on HUWE1 HECT E3 ligase activity and ubiquitin chain specificity

HUWE1 has been reported to mediate multiple types of ubiquitination such as K6, K48, K63 poly-ubiquitination and mono-ubiquitination [152, 170, 171]. Whether it is able to assemble other types of ubiquitin chains need to be explored. In other words, ubiquitin or Ub chains enriched by a UBD may affect the HECT domain catalytic activity in context of linkage specificity and ubiquitination intensity.

As one of the UBD of HUWE1, tUBM domain was hypothesized to modulate HECT domain catalytic function and its preference of Ub linkages. Whether and how tUBM impact HECT domain catalytic activity can be discovered through ubiquitination assay stated in Chapter 4.

Aim 3: The assessment of UbVs as UBM1 modulator to further investigate the effect of tUBM on HECT domain function

Besides comparing the ubiquitination levels catalyzed by tUBM-HECT and HECT alone, the function of tUBM can be further characterized by utilizing a tUBM binding modulator. UbV targeting UBM1 was proposed as the UBM1 modulator in this project based on the hypothesis that UbV competes Ub molecules to bind the tUBM1 thus inhibiting the function of UBM1. An affinity screening test was performed to select the best UBM1 binding UbV through a binding assay. The assessment of UbV on modulating tUBM was conducted through in vitro ubiquitination assay as summarized in Chapter 4.

Chapter 2

Characterization of Preference and Specificity of Ubiquitin and Ubiquitin Chains Interacting with the tUBM Domain

2.1 Introduction

Ubiquitin di-chain (diUb) contains key structure topologies for UBD to recognize [172]. With the processive chain elongation, triUb, tetraUb, pentaUb and even longer Ub chains can be formed with repeating structural topologies as shown in diUb. Comparing to mono ubiquitin, diUb increases the local intensity of Ub around UBD. Therefore, the affinity between diUb and UBD is generally higher than the affinity for mono-Ub [132, 172, 173]. Previous Sheng lab data showed that tUBM binds to triK48 and triK63[174]. In this project, the in vitro binding assay results revealed that tUBM binds to all eight types of diUb chains (diK6, diK11, K27, K29, K33, K48 and diK63) and tUBM favors diM1 and diK63 over other types of diUb chains.

2.2 Materials and methods

2.2.1 Expression and purification of GST-tUBM

The pGEX-4T plasmids containing the gene encoding tUBM ($HUWE1_{2950-3123}$) was transformed into competent BL21 Codon Plus (DE3) -RIPL Escherichia coli (Stratagene) and cultured in Amp+ media.

After induced by 1mM IPTG (Isopropyl β-d-1-thiogalactopyranoside) (Cat#IPT001.50, BioShop), the bacteria culture was kept on the shaker overnight (16 hours) at 16°C to express GST-tUBM protein.

The cells were lysed by using lysis buffer (20 mM Tris, pH 8.0, 150 mM NaCl, 1 mM benzamidine, 0.1% Triton and 10% glycerol). GST-tUBM was purified through GSH (glutathione) Sepharose (GE Healthcare) affinity chromatography. The concentration of purified and dialyzed GST-tUBM was determined through BCA assay (Pierce™ BCA Protein Assay Kit,

Cat#23225, Thermo Scientific). GST-tUBM was concentrated using a concentrator with 30kDa MWCO spinning at 3000rpm until the concentration reached 4.2mg/ml (93µM).

2.2.2 In vitro binding assay using BioLayer interferometry

BioLayer Interferometry employs two-layer optical biosensor to analyze the changes of interference patterns obtained from the light reflected from the layer of the biosensor tip with immobilized protein (known as biocompatible matrix) and the internal reference optical layer. The test was conducted by using the instrument of fortéBIO Octet red 384 (Figure 2.1). The instrument operation was instructed by Shili Duan in Dr. Arrowsmith lab.

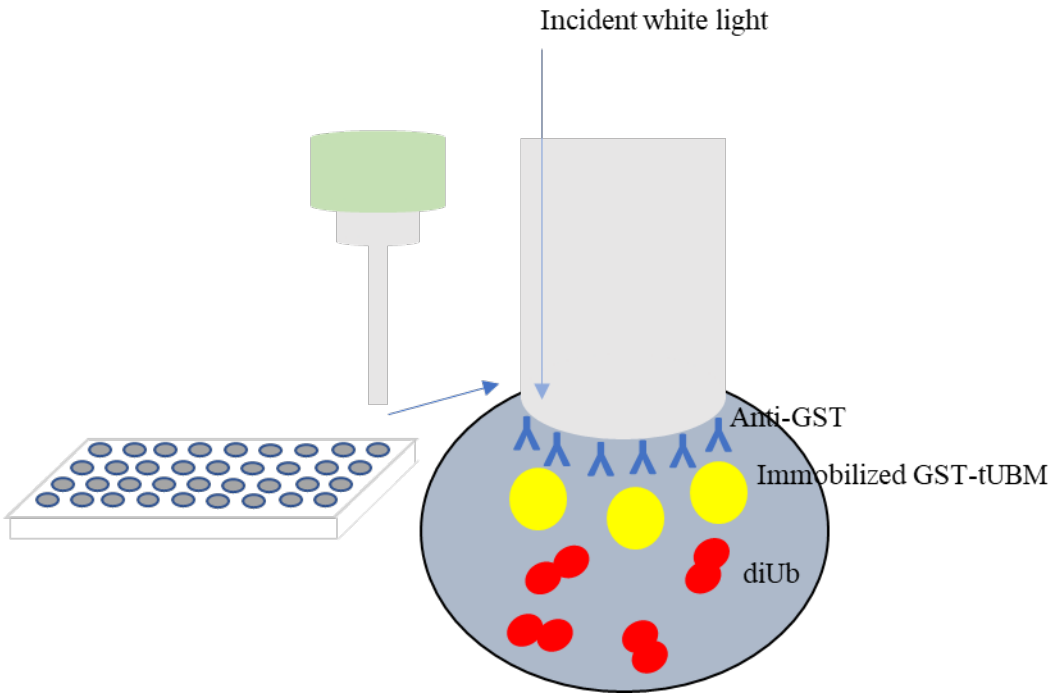

Figure 2.1 Cartoon illustration of the mechanism of fortéBIO Octet instrument in BLI affinity experiment. The surface of biosensor tip is coated with anti-GST antibody that allows GST-tUBM to immobilize on the surface forming a biocompatible matrix. The amount of binder protein diUb interacting with GST-tUBM changes the interference pattern of white light reflected from two surfaces of biosensor tip (biocompatible matrix and inner reference optical layer) which can be detected by the instrument in real time.

Linkage specific di-ubiquitin chain of diM1, diK6, diK11, diK27, diK29, diK33, diK48 and diK63 purchased from UBPBio were applied to Biolayer Interferometry experiments. All eight di-ubiquitin chains as well as WT mono-ubiquitin (Boston Biochem) were tested with GST-tUBM individually. As a bait, GST-tUBM was diluted to 60 µl of 1mg/ml with working buffer (50mM Tris HCl pH 7.5, 150mM NaCl) and loaded into each well of a column of a 384 well plate. As the testing binders, each diUb was diluted to 60 µl of 25µM with 1x HBS-EP buffer as assay buffer (10mM HEPES pH 7.4, 150mM NaCl, 3mM EDTA, 0.005% v/v Surfactant P20) containing 0.02mg/ml BSA, 60µl was loaded into each well. WT mono-ubiquitin was diluted in the same manner.

The eight diUbs were tested in two separate runs. Wild type mono-ubiquitin, di-K48, di-K63 and di-K6 were tested in the first run while di-M1, di-K11, di-K27, di-K29 and di-K33 were tested in the second run. Anti-GST antibody-coated biosensors (Cat# 18-5096 Source: Pall) was placed in assay buffer in designate wells for equilibration before running. The detection, recording and analysis were conducted by fortéBIO Octet instrument OCTET384. During BLI experiment, the biosensors were dipped into GST-tUBM solution and GST-tUBM was immobilized on the surface of the sensor tip. After washed with assay buffer, the biosensor loaded with GST-tUBM was dipped into wells containing each individual linkage specific diUb followed by a wash. The real-time association and dissociation curves recorded the binding between diUb and GST-tUBM.

2.2.3 Analysis of the interaction between GST-tUBM and diUb

The equations describing kinetic interaction between two biomolecules are listed as below:

Eq. 2.1.

$$A + B \underset{k_d}{\overset{k_a}{\rightleftharpoons}} AB$$

A represents the binder protein (analyte) and B is the immobilized protein. AB is the complex formed by binding A to B. Ka is the association rate (also called k_{on}) and k_d is the dissociation rate (also known as k_{off}).

Eq. 2.2.

$$K_D = \frac{[A] \bullet [B]}{[AB]} = \frac{k_d}{k_a}$$

The dissociation constant KD can be calculated as the ration of k_d/k_a. The value of K_D is reverse proportional to the binding affinity of two interacting proteins.

Eq. 2.3. (BLI association phase)

$$Y = R_{max} \frac{1}{1 + \frac{k_d}{k_a * [Analyte]}} (1 - e^{-\left(k_a * [Analyte] + k_d\right) t})$$

Eq. 2.4. (BLI dissociation phase)

$$Y = Y_A e^{-k_d (t - t_A)}$$

$$Y_A = R_{max} \frac{1}{1 + \frac{k_d}{k_a * [Analyte]}} (1 - e^{-\left(k_a * [Analyte] + k_d\right) t_A})$$

For the equation (Eq. 2.3.) and (Eq. 2.4.), Y represents the BLI signal in nm indicating the level of binding as nm shift. Y_A represents the calculated nm shift at the end of association phase. Rmax is the fitted maximum achievable binding response for an analyte to a given level of immobilized protein. Analyte refers to the binder protein. Running time in second is represented by t and t_A represents the time at the end of association which is also the time at the beginning of dissociation.

Eq. 2.5.

$$k_{obs} = k_a * [Analyte] + k_d$$

k_{obs} is the observed overall rate of the combined association and dissociation of two interacting proteins.

Eq. 2.6.

$$R_{eq} = R_{max} \frac{k_a * [Analyte]}{k_a * [Analyte] + k_d}$$

Req (Requilibrium) refers to the fitted response value in nm when the interaction of two proteins reaches equilibrium between association and dissociation for a given analyte (binder) concentration.

The k_a, k_d, and Rmax were provided by Octet Dara Analysis software which indicated the interaction between tUBM and diUb as well as WT Ub (Table 2.2). However, due to lacking equilibrium analysis or steady state analysis, the steady state dissociation constant for preferred type of diUb was not derived from this BLI test (refers to 2.4 discussion section).

2.2.4 Native gel electrophoresis

Native gel is another method that utilizes the PAGE gel electrophoresis free of SDS to display non-covalently interacted proteins based on the mobility shifts of the protein complex because this non-denaturing electrophoresis procedure allows the binding proteins remain intact while migrating in the gel matrix.

Pre-ran a 7% native gel (5.75 ml H2O, 2.5 ml Tris pH 8.8, 1.75 mL 40% Acrylamide: BisAcrylamide 29:1, 50µl 10% APS and 5µl TEMED) in 1×running buffer which was diluted from 5×stock buffer (72g glycine, 15g Tris in 1L H2O) at 125V for 1 hour. 80µg of GST-tUBM

and 4.25µg of each individual diUb (molar ration 1:7.5) as well as wild type ubiquitin were incubated in 4°C cold room for 1 hour and each mixture was loaded onto the native gel and ran at 125V for 2.5 hours. GST tag alone and diUb were proceeded in the same manner concurrently as the negative control. There was no loading dye added to avoid potential interference on protein interaction. The gel was Coomassie stained and de-stained after running.

Eq. 2.7.

$$\mathrm{Rf} = \frac{\text{Migration distance of complex of GST-tUBM and Ub}}{\text{Migration distance of unbound GST-tUBM}}$$

Eq. 2.8.

$$\Delta\mathrm{Rf} = \mathrm{Rf}_{\text{GST-tUBM alone}} - \mathrm{Rf}_{\text{GST-tUBM in presence of Ub}}$$

2.3 Results

2.3.1 Sequence comparison of three UBM repeats of the HUWE1 tUBM domain

The tUBM domain of HUWE1 ($HUWE1_{2951-3123}$) contains three tandem repeats UBM1, UBM2 and UBM3 which is ~900 residues upstream of HECT catalytic domain ($HUWE1_{4036-4374}$) (Figure 1.1). The importance of tUBM was highlighted by the report that single site mutation R2981H led to XLID [4]. Comparing to other ubiquitin binding domains of HUWE1 including UBA (Ubiquitin Associated) ($HUWE1_{1317-1355}$) and UIM (Ubiquitin Interacting Motif) ($HUWE1_{1370-1389}$), the tUBM domain is structurally distinct.

Previously, the structure of the first UBM1was solved in Sheng lab [175] (PDB:2MUL) (Figure 2.2A). Sequence alignment of three repeats was shown in Figure 2.3B. The UBM1, UBM2 and UBM3 of HUWE1 all contain conserved residues LP (L2976 and P2977 in UBM1 numbering) that may be important for the structural integrity of HUWE1 (Figure 2.2B).

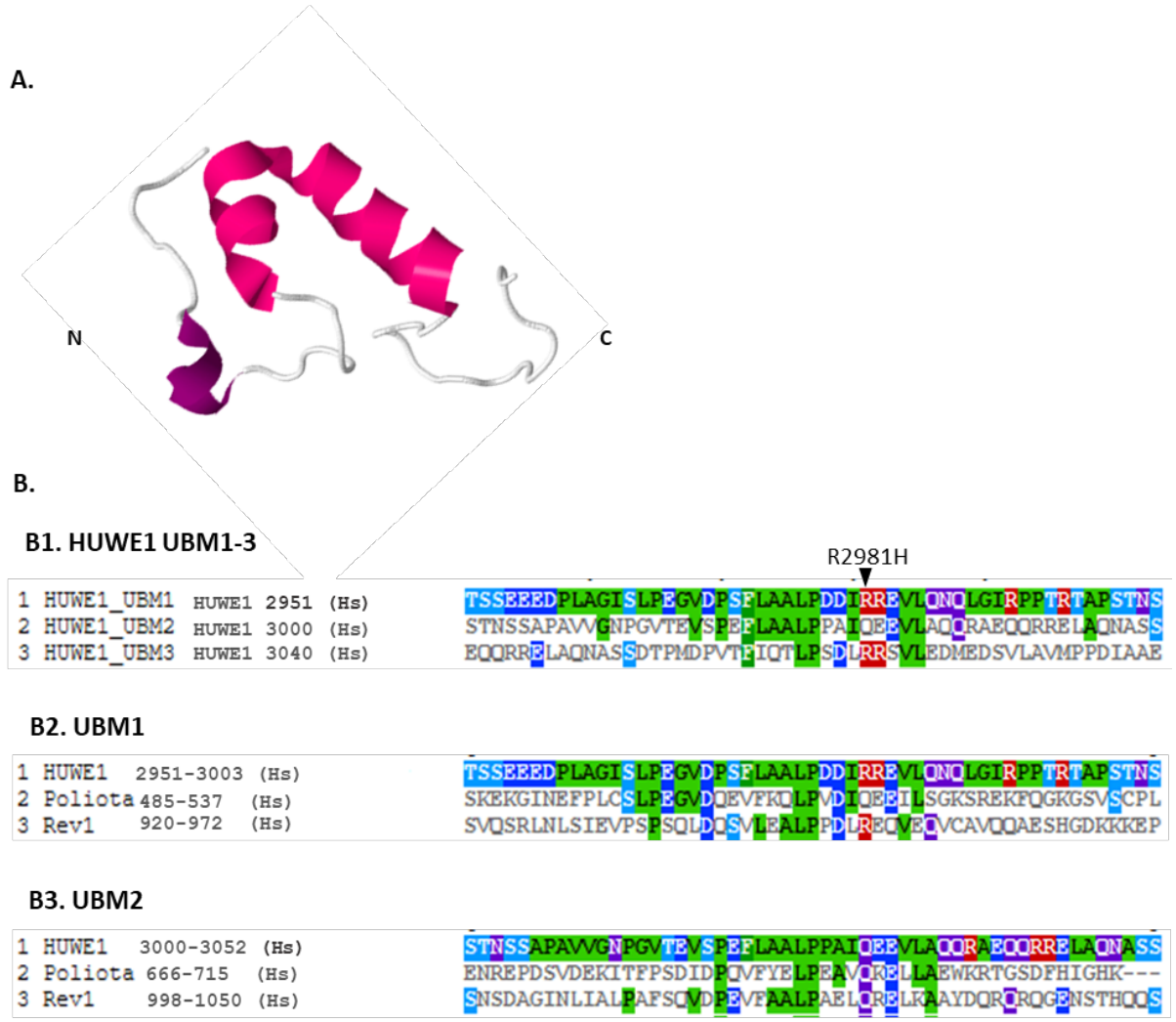

Figure 2.2 Schematic ribbon representation of UBM1 domain and amino acid sequence alignment of UBMs. A. UBM1 is composed of two helices linked by the signature turn containing Leu-Pro motif. The N-terminal helix (colored in purple) is comprised of the six residues (Pro2970 to Ala2975 and the C-terminal helix (colored in pink) contains 11 residues (Asp2978 to Gln2988) (PDB:2MUL)**. B1**. The amino acid sequence alignment of human HUWE1 UBM1, UBM2 and UBM3. R2981H mutation has been reported to be involved in XLID disease. **B2.** UBM1 amino acid sequence alignment of human HUWE1, human Pol iota and human Rev1. **B3.** UBM2 amino acid sequence alignment of human HUWE1, human Pol iota and human Rev1. The listed amino acid sequences are Homo sapiens (Hs) HUWE1 (NCBI Reference Sequence: NP_113584.3), Hs Pol iota (GenBank: AAF63383.1) and Hs Rev1 (GenBank: AAI30412.1). The consensus residues in are shaded with colors. Hydrophobic residues are shaded green, polar residues are shaded purple, negative charge residues are shaded blue and positive charge residues are shaded red. The alignment results are generated by Clustal Omega (1.2.4), viewed by Mview 1.63 (Nigel P. Brown, 2018).

2.3.2 The interaction between the HUWE1 tUBM domain and diUb chains

To test whether diUb chain can bind to tUBM, in vitro binding assay was performed using GST-tUBM as the immobilized bait protein and each of eight types of diUb chains (diM1, diK6,diK11,diK27, diK29, diK33, diK48 and diK63) and WT Ub as binder proteins. The interaction was detected by fortéBIO Octet red 384 instrument and demonstrated through the BLI sensorgram (Figure 2.3). BLI signal (in nm shift) represented the real-time change of the interaction between the immobilized bait protein and the testing binder proteins. The experiment process was recorded for 780 second and included six stages: (i) Equilibrium of the biosensor; (ii) GST-tUBM immobilization on the biosensor; (iii) Washing the biosensor; (iv) Equilibrium of the biosensor in diUb binder solution; (v) Association phase; (vi) Dissociation phase (Figure 2.3). The kinetic binding parameters including association rate (k_a or k_{on}), dissociation rate (k_b or k_{off}) and signal intensity (Response) of each binding curve were analyzed automatically by Octet Data Analysis software through fitting the data to one of the available curve fitting models that best fit to a series of data points based on the mathematical functions and constraints (Figure 2.4 and Table 2.1). The association and dissociation curves displayed in both sensorgram proved that HUWE1 tUBM interacts with all eight types of diUb and WT Ub.

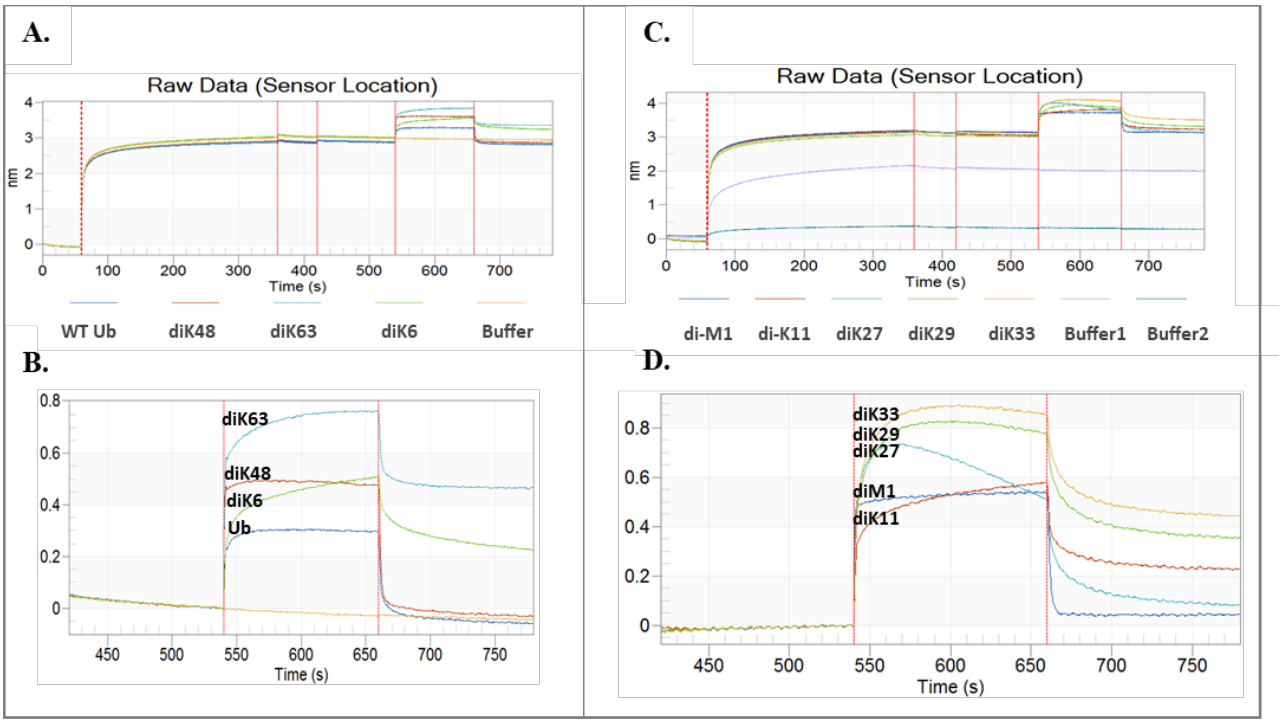

Figure 2.3 BLI Sensorgram – Affinity Binding Curves of eight types of diUb as well as WT ubiquitin binding to GST-tUBM. The binding curves are color coded. **A and B**. The binding of diK63, diK48, diK6 and WT Ub were tested in the first run. **C and D.** The binding of diK33, diK29, diK27, diM1 and diK11 were tested in the second run. **A and C**. Overall sensorgram of the process (780 seconds) including Stage 1: equilibrium in GST-tUBM solution from 0 sec to 60 sec; Stage 2: GST-tUBM attached to the surface of biosensor tip and was immobilized from 60 sec to 360 sec; Stage 3: washing from 360 sec to 420 sec; Stage 4: equilibrium in 25uM diUb solution from 420 sec to 540 sec; Stage 5: association phase that diUb bound onto the immobilized GST-tUBM from 540 sec to 660 sec and Stage 6: dissociation phase that diUb was washed off from GST-tUBM from 660 sec to 780 sec. **B and D.** Enlarged sensorgram of association curve and dissociation curve from 540 sec to 780 sec. The association curves indicate the interaction between each of diK63, diK48, diK6, WT Ub (**B**) as well as each of di-M1, di-K11, di-K27, di-K29, di-K33(**D**) and GST-tUBM

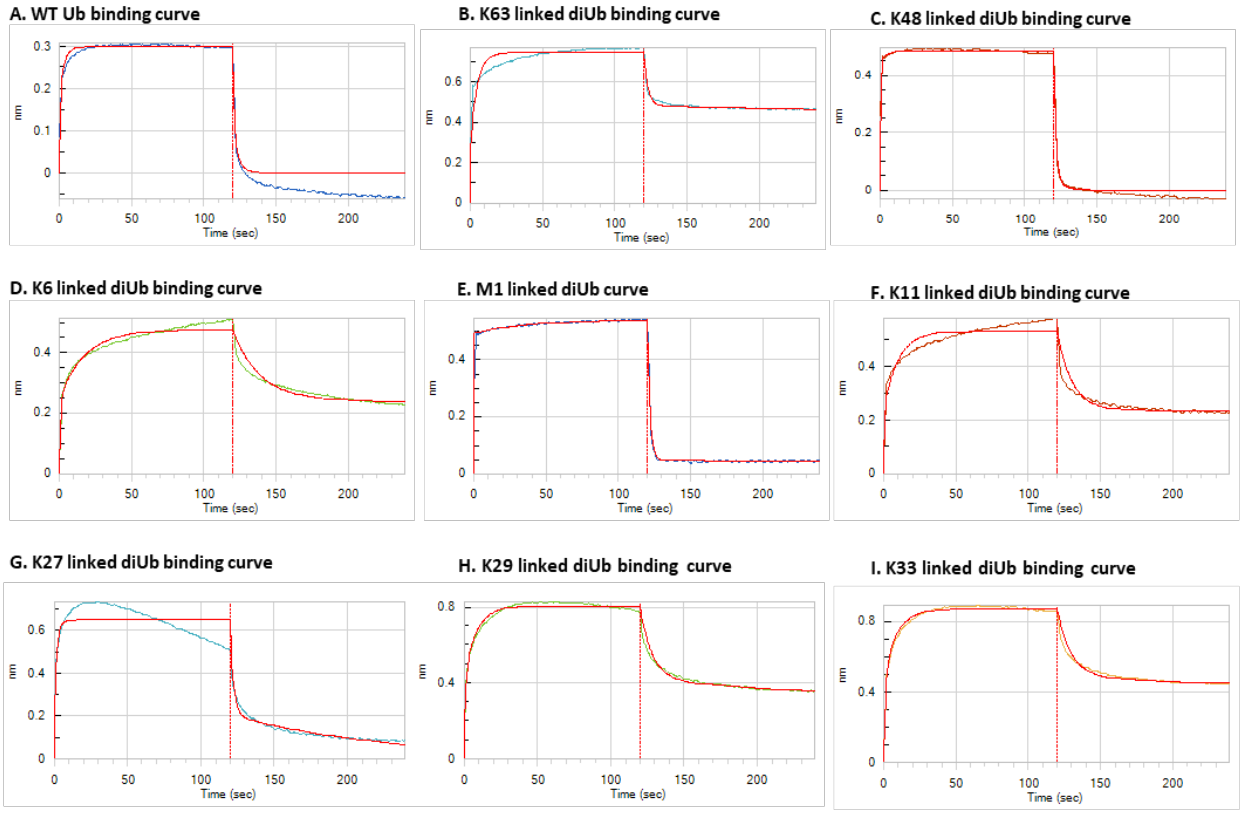

Figure 2.4 Individual binding curve with its associated fitting curve of each diUb. GST-tUBM was immobilized at the surface of the biosensor tip. Each of eight types of diUb as well as WT Ub were tested separately as the binder protein. The association, dissociation curve and the fitting curve were illustrated for each type of Ub.

Table 2.1 The kinetic binding parameters of diUb and WT Ub obtained from the BLI test *.

Ub Type	k_a (1/Ms)	k_d (1/s)	Rmax (nm)
diM1	1.2×10^{6}	5.4×10^{-1}	5.0×10^{-1}
diK6	3.7×10	5.5×10^{-2}	1.4×10
diK11	5.8×10	9.8×10^{-2}	2.0×10
diK27	1.8×10^{4}	4.4×10^{-1}	8.9×10^{-1}
diK29	9.9×10	1.2×10^{-1}	1.9×10
diK33	2.0×10^{2}	1.1×10^{-1}	8.4
diK48	6.4×10^{4}	6.1×10^{-1}	6.2×10^{-1}
diK63	8.9×10^{3}	2.5×10^{-4}	4.8×10^{-1}
WT Ub	7.28×10^{2}	2.8×10^{-1}	1.9

* GST-tUBM was the immobilized protein and each type of diUb as well as WT Ub were the binder proteins. The parameters including association rate (k_a), dissociation rate (k_d), and fitted maximum achievable binding response (Rmax) that indicates the interaction between tUBM and diUb as well as WT Ub.

2.3.3 Characterization of interaction between HUWE1 tUBM and di-ubiquitin chains through native gel electrophoresis

To verify the result of the BLI experiment, native gel electrophoresis was utilized to further examine the interactions of HUWE1 tUBM with diUbs or WT Ub. Native gel electrophoresis displays protein interactions based on the mobility shifts of the protein complex.

The GST-tUBM mobility shift changes were presented by the change of the Retention factor (ΔRf). The ΔRf value illustrated in Figure 2.5A was calculated by subtracting the Rf value of GST-tUBM in presence of Ub from the Rf of GST-tUBM alone (Eq. 2.8). The results confirmed that GST-tUBM interacts with ubiquitin di-chains (diM1, diK11, diK27, diK29, diK33, diK48 and diK63) based on the mobility shifts of GST-tUBM in presence/absence of di-ubiquitin chains (Figure 2.5A). There was no mobility shift of GST tag in presence of diUb or WT mono-Ub (Figure 2.5A). Shown as the bar graph of ΔRf values, the mobility of GST-tUBM

shifted the most in presence of diM1 and diK63 Ub chains, and the least in presence of WT mono-Ub (Figure 2.5B).

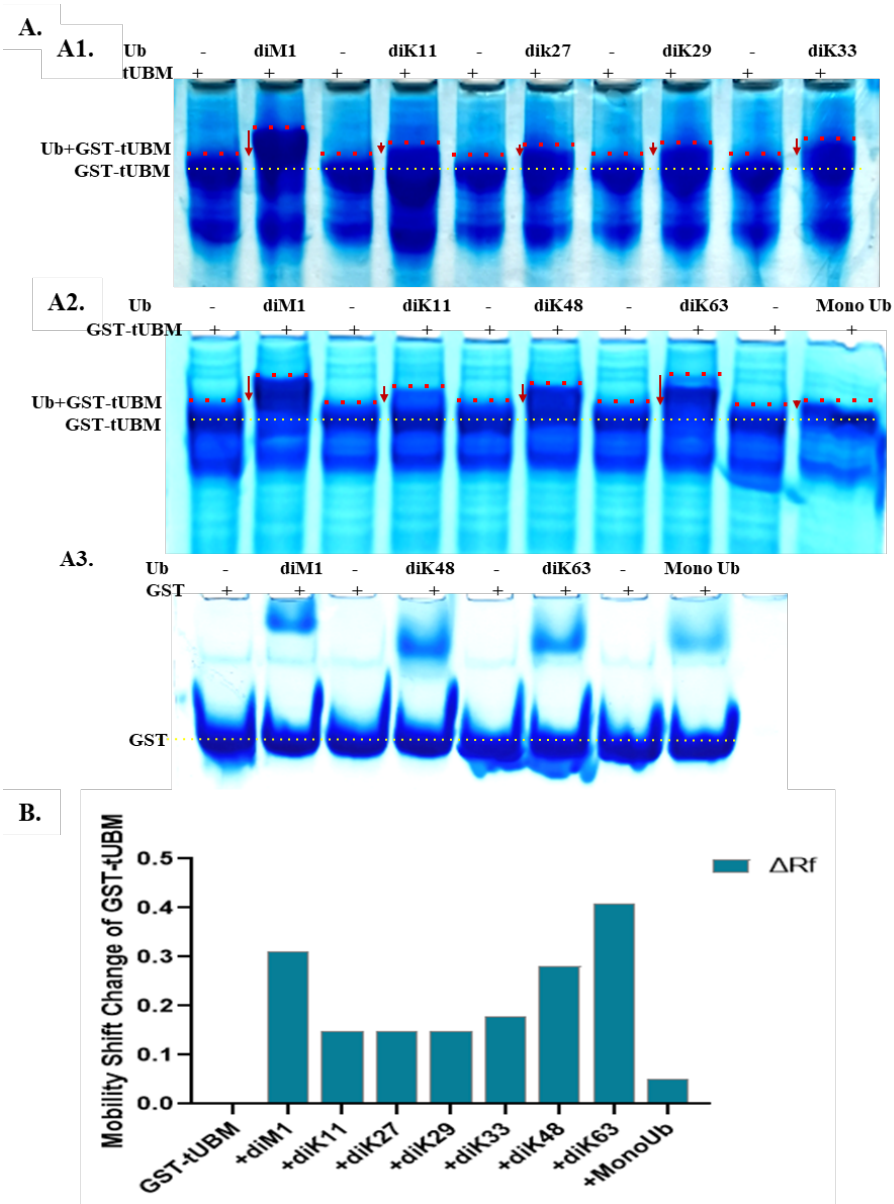

Figure 2.5 Native gel image showing interaction between different types of ubiquitin and GST-tUBM. A. Interaction between GST-tUBM and di-ubiquitin chains. Samples were loaded onto 7% native gel and run at 125V in cold room for 2.5 hours after 1hour pre-run. **A1.**and **A2**. The mobility of GST-tUBM in presence of diM1, diK11, diK27, diK29, diK33 and WT Ub with the molar ration 1:7.5. The mobility shift of GST-tUBM was altered the most by diM1 comparing to other types of diUb chains. **A3.** GST alone was tested with diUb, and no mobility shift of GST was observed indicating no interaction between GST and di-ubiquitin chains. **B.** The migration distance of GST-tUBM in absence/presence of Ub was measured based on the result of native gel and the ΔRf value was calculated based on the equation 2.8.

2.4 Discussion

The result of BLI kinetic binding experiment revealed that HUWE1 tUBM interacts with each of eight types of diUb (diM1, diK6, diK11, diK27, diK29, diK33, diK48 and diK63) as well as WT Ub. The result of the native gel electrophoresis confirmed this result. In addition, GST showed non-binding to Ub in native gel test which means the interaction is between tUBM and Ub but not the GST tag. However, the preferred diUb binding to tUBM still remain unknown due to lacking steady state analysis in BLI experiments. The finding has at least two significant points: (1) HUWE1 tUBM is able to interact with diUb and WT Ub in vitro. (2) HUWE1 tUBM exhibits capability of binding all eight types of diUb (M1, K6, K11, K27, K29, K33, K48 and K63) including canonical and atypical diUb chains in vitro. This observation is different from the precious report of polymerase iota UBM domain that Pol ι UBM domain does not bind to K48 diUb based on the experiment of fluorescence spectroscopy [143]. The further investigation ought to be done to figure out whether this binding disparity is caused by the intrinsic characteristic difference between HUWE1 tUBM domain and Pol ι domain or by different testing methods.

BLI is an efficient, sensitive optical method to detect the PPI (Protein Protein Interaction). However, to obtain a reliable dissociation constant KD value, multiple gradient concentrations of binder protein ought to be tested which was not performed in this project. Therefore, only bindings between diUb and GST-tUBM can be concluded and there was not an assuring ranking of affinity among those eight types of diUbs based on the BLI experiment. One observation in the BLI test was the discrepancy among biosensors may be due to coating issue that the curves of buffer 1 (F1) and buffer 2 (G1) in the second run sensorgram of BLI test were off scale (Figure 2.3C).

The result of the native gel electrophoresis experiment verified that tUBM interacts with all seven types of diUb (diM1, diK11, diK27, diK29, diK33, diK48 and diK63). This was based on the observations that the GST-tUBM and each of the diUb formed a complex which can be seen from the mobility shift of GST-tUBM in presence of diUb, comparing to the migration of GST-tUBM in absence of Ub in the native gel electrophoresis. It appeared that GST-tUBM shifted the most with diM1 and diK63 Ub compared to other types of diUb. The reason can be that diM1 Ub and diK63 adopt open conformation allowing GST-tUBM to access the binding site-hydrophobic core of diUb easier. Different from SDS-PAGE electrophoresis in which protein migration distance is predominantly determined by the size of the peptides and the strength of the electric field, the migration of protein complex in native gel electrophoresis depends on not only intrinsic charges of the native protein complex but also the shape and size of the protein complex. Based on the crystal structures of diUbs, diM1 and diK63 Ub adopt an extended or open conformation whereas diK48 Ub possesses an occluded structure. The diUbs with open conformation may slow down the migration of bound GST-tUBM leading to larger ΔRF than the diUbs with compact and closed conformation.

There are several factors affecting migration rate of the proteins or bound protein complexes in the native gel such as net charge, molecular size, and conformation of the proteins. Electrophoretic migration of the proteins occurs due to the net negative charge of the proteins in alkaline running buffers. The frictional force of the gel matrix exerts a sieving effect regulating the movement speed of proteins according to the molecular size and three-dimensional shape. Small proteins encountering a small frictional force move faster than large proteins. The proteins with occluded conformation facing less obstruction migrate faster than the proteins with open conformation. Therefore, native gel separates proteins based upon the integrated characters of

the net charge, molecular mass, and structure of the proteins. Since the molecular sizes of diUbs are same, the migration rate of the complex of tUBM and diUb depends on the net charge and conformation of the protein complex. According to the native gel test result, the open conformation of diM1 and diK63 Ub contributed to the outstanding mobility shift of GST-tUBM.

Ideally, all eight types of diUb ought to be tested. Due to reagent shortage, diK6 was not tested in this experiment. Also, only three diUbs (diM1, diK48 and diK63) and mono-Ub were tested for their binding with GST-tag and no binding was observed based in this native gel experiment.

Comparing these two PPI test methods, BLI method has several advantages including label-free, real-time, precise kinetic information and efficient test process. Its disadvantage is sensor tip dependent, which demands homogeneity of the coating on the surface of the sensor tip. Ideally, the sensor tips from same manufacturing lot should be used in the experiment to ensure an accurate result [177, 178]. The benefits of native gel electrophoresis method include low-cost and showing difference of protein complex conformation whereas the drawback of the native gel is that no precise binding parameters can be obtained.

2.5 Conclusion

Through BLI and native gel electrophoresis, GST-tUBM was shown to interact not only diM1, diK48 and diK63 but all eight types of ubiquitin di-chains as well as WT mono-ubiquitin molecule whereas GST was unable to bind to these ubiquitin chains.

Chapter 3

Characterization of effect of tUBM on HUWE1 HECT E3 ligase activity and ubiquitin chain synthesis

3.1 Introduction

The results of the HUWE1 tUBM affinity binding experiments stated in Chapter 2 have shown that HUWE1 tUBM is capable to bind all eight types of diUb chains. However, whether and how HUWE1 tUBM affects HUWE1 HECT domain activity ought to be characterized.

Previously, a fused construct of HUWE1 tUBM-HECT which encodes tUBM ($HUWE1_{2951-3123}$) linking with the extended catalytic HECT domain ($HUWE1_{3760-4374}$) was studied in the Sheng lab. The result showed that the polyubiquitination catalyzed by tUBM-HECT was more active than that catalyzed by HECT domain alone, which indicates that tUBM enhances polyubiquitination assembled by HUWE1 HECT domain [176] (unpublished data). However, there were several questions remain unanswered. (1) Whether tUBM promotes the formation of all eight linkage types of polyUb (M1, K6, K11, K27, K29, K33, K48, K63)? (2) Which linkage type(s) of polyUb synthesis is most enhanced in presence of tUBM? (3) Whether tUBM impacts on HECT domain catalysis differently by using linkage specific mono Ub and diUb chains as the reactant, respectively? (4) What type(s) of Ub linkage favored by HECT domain while synthesizing polyUb? (5) What type of ubiquitination (total-, auto- or substrate ubiquitination) is impacted by tUBM? Total ubiquitination refers to the ubiquitin attachment to all protein components in the in-vitro ubiquitination assay including enzymes and substrate proteins which can be detected by using anti-Ub antibody; autoubiquitination refers to the ubiquitin conjugation on E3 ligase which can be probed by using antibody against the tag of the E3 ligase. For instance, anti-GST antibody was used in this project to probe GST-HECT for the auto-ubiquitination level; substrate ubiquitination refers to the ubiquitin added to the substrate proteins which can be detected by using antibody against the substrate.

In vitro ubiquitination assay imitates intrinsic cellular ubiquitination allowing ubiquitination reaction to occur in a tube by including three major enzymes (E1, E2, E3), ATP, ubiquitin molecules as well as substrate proteins. Linkage specific mono-Ub mutants contains only one specific linkage site (M1 only, K6 only, K11 only, K27 only, K29 only, K33 only, K48 only or K63 only) to form a certain type of polyUb while other seven potential linkage sites (lysine or methionine) being substituted by arginine. For instant, K6 only mono-Ub has only K6 remaining, and the other six lysine residues are mutated, therefore only K6 polyUb chain could be synthesized during the ubiquitination reaction.

In this project, it was hypothesized that tUBM enhances HECT domain enzymatic activity and Ub chain formation. To test this hypothesis, the fused tUBM-HECT domain or HECT domain alone was applied in a series of in vitro ubiquitination assays using Mono-Ub wild type or monoUb lysine mutants or diUb as the reactant to characterize the role of tUBM in modulating HECT domain activity.

3.2 Materials and methods

3.2.1 Subcloning pGEX-tUBM-HECT

The construct tUBM-HECT that encodes of $HUWE1_{2951-3123}$ (5'-tUBM) fused with $HUWE1_{3760-4374}$ (HECT-3') was subcloned from a pcDNA plasmid into the pGEX vector in order to express GST-tagged tUBM-HECT protein in *E. coli*. The pGEX-HECT plasmid carrying HECT alone was previously prepared in Sheng lab before this project.

The tUBM-HECT was PCR amplified by using pcDNA plasmid carrying DNA of tUBM-HECT as the templet DNA, 1μM forward primer (5'-gcggcggcccatatgACA AGC AGT GAA GAA GAA GAT-3'), 1μM reverse primer (5'-gcgcgaattcttaGGC CAG CCC AAA GCC TTC

AGA -3'). The forward primer contains a NdeI site, and the reverse primer has a EcoRI site so that the generated PCR product carried the NdeI site at the 5’ end and EcoRI site at the 3’ end. Agarose gel electrophoresis was performed after PCR amplification to verify the size of the target DNA (2.3kb).

PCR product and pGEX vectors were digested with NdeI (20U/µl Cat#R0111S, NEB) and EcoRI (20,000 units/ml Cat#R0101S, NEB) restriction enzymes. The size of target gene (2.3kb) and linearized pGEX plasmids (4.9kb) was verified through agarose gel electrophoresis. Purification of digested DNA was performed by using GeneJET Gel Extraction Kit (Thermo Scientific). Insert DNA and the vector with molar ratio 3:1 was ligated by using T4 DNA ligase (Cat#M0202S, NEB). Ligation product was transformed to 50µl of DH5α competent cells (Cat#18258012, Invitrogen) and the transformed cells were selected by using ampicillin positive LB agar plate.

Colony PCR was conducted to select the E. coli bacteria with target gene being successfully transformed. Sixteen colonies were picked from the ampicillin selective LB agar plate. 2µl of each bacterial suspension containing picked bacteria and nuclease-free water from each individual tube was transferred to a corresponding new PCR tube filled with 18µl mixture of 10µl 2×PCR Master Mix(Cat#K0171, invitrogen), and 1µl of each forward and reverse primers. A positive control was prepared concurrently using the diluted template pcDNA plasmid. The positive tUBM-HECT DNA was extracted and verified by sequencing.

3.2.2 Protein purification

GST-tUBM-HECT and GST-HECT proteins were expressed and purified as previously described.

The substrate protein p53, was expressed in cultured BL21 DE3-pLysS cells which had previously been transformed with the plasmid pET15b - p53. The Nickel Affinity Gel (Sigma) was used for His-tagged p53 purification. The stock buffer was prepared containing 25mM Tris HCl pH6.5, 300mM NaCl, 6mM $MgCl_2$, 5mM imidazole, 0.5mM TCEP, 5mM BME, 2mM Benzamidine and PI. Triton X-100 was added to 50ml of stock buffer to make 0.1% Triton X-100 buffer as the lysis buffer. The rest stock buffer was used as wash buffer. 500mM imidazole was contained in the elution buffer. The SDS-PAGE gel electrophoresis was performed to verify the size of His-p53.

The molecular sizes of all protein components and eight types of linkage specific monoUb in reaction were verified by SDS-PAGE before the in vitro ubiquitination assay.

3.2.3 In vitro ubiquitination assay by using WT Ub and p53

The protein components involved in this assay included GST-tUBM-HECT, GST-HECT, His-E2L3, His-p53 and WT ubiquitin. In 20 µl of each reaction, the mixture contained buffer (50mM Tris HCl pH7.6, 5mM $MgCl_2$, 2mM DTT, 0.1×Protease Inhibitor), 0.43 µg E1, 0.5 µg E2, 1.0 µg E3, 5.0 µg WT Ub, 0.78 µg p53 and 55 µg ATP disodium salt (MW 551.14) except in negative control. Six reaction mixtures were incubated concurrently at 30°C for 90 minutes. Then SDS loading dye was added to each of the tube to stop reaction followed by SDS-PAGE gel electrophoresis by using 4-20% Tris-Glycine gel (REF# XP04120BOX, invitrogen). After proteins being transferred from gel to membrane, the PVDF membrane (pore size 0.2µm, Amersham™ Hybond™, GE) was subjected to Ponceau S stain (Figure 12SB). Thereafter, the membrane was probed sequentially by 1:1000 primary anti-ubiquitin antibody (clone P4G7,

Mouse mAb, Cat#838704, Covance) and 1:5000 secondary HRP conjugated donkey anti-mouse antibody (Cat#711-035-150, Jackson ImmunoResearch).

3.2.4 In vitro ubiquitination assay with linkage specific monoUb or diUb and substrate protein

Several sets of in vitro ubiquitination assays were performed following the same procedures as described previously. In the assay with the linkage specific monoUb (M1 only, K6 only, K11 only, K27 only, K29 only, K33 only, K48 only and K63 only), each type of mutant mono ubiquitin (UBP Bio Ubiquitin Linkage Screening Kit II, Cat. # J3210) with the final concentration of 50 μM was utilized as building blocks of polyUb. In the assay with linkage specific diUb (diM1, diK6, diK11, diK27, diK29, diK33, diK48 and diK63), each type of the diUb (UBP Bio Di-ubiquitin Explore Kit, product ID: J2000) with final concentration 5.9 μM was used. For the substrate protein, p53 with final concentration of 0.74 μM and β-catenin (0.27 μM) were applied as the substrate protein respectively in the corresponding assays. The total volume of each reaction mixture was 20 μl.

The antibodies used in the assay include Ub antibody (1:1000), p53 antibody (1:200, DO-1, Mouse mAb, Cat# Sc-126, Santa Cruz Biotechnology), GST antibody (1:5000, HRP conjugated, clone DG122-2A7, Cat#16-209, Lot #2444093, EMD Millipore), and β-catenin antibody (1:1000 clone 6B3 Rabbit mAb, #9582S, Cell Signaling).

3. 3 Results

HUWE1 tUBM was hypothesized to enhance the HECT domain catalytic activity. Therefore, in vitro ubiquitination assays were designed to test this hypothesis. In vitro ubiquitination assay imitates intrinsic cellular ubiquitination allowing ubiquitination reaction to

occur in a tube by including three major enzymes (E1, E2, E3), ATP, ubiquitin molecules as well as substrate proteins. Based on previous reports, E2L3 (UbcH7) was selected as HUWE1 cognate E2 [65, 113]; p53 and β-catenin were tested separately as the substrate proteins in the reaction; GST-HECT domain or GST-tUBM-HECT domain was used as E3 (Figure 3.1). Several sets of in vitro ubiquitination assays were performed including (1) assay with WT Ub and p53, (2) assay with linkage specific mono-Ub and p53, (3) assay with linkage specific monoUb and β-catenin, (4) assay with linkage specific diUb and p53.

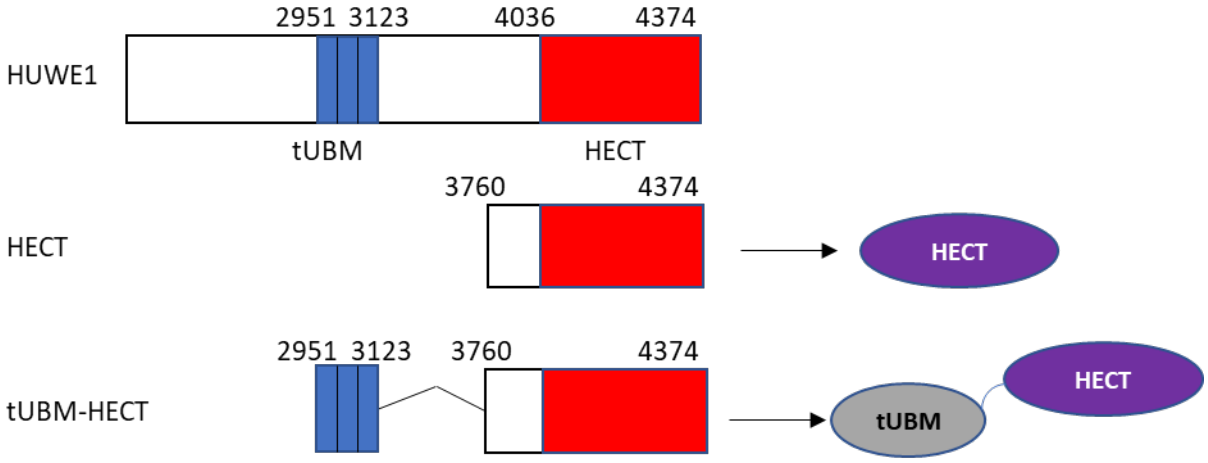

Figure 3.1 Schematic presentation of HUWE1 HECT and tUBM-HECT. HUWE1 HECT catalytic domain only or tUBM fused with HECT domain were used as two E3 ligases in the ubiquitination assay for testing the impact of tUBM on HECT domain catalytic activity.

3.3.1 tUBM enhanced total ubiquitination level in the assay with WT Ub and p53

The in vitro ubiquitination assay with WT Ub and p53 was performed to test the impact of tUBM domain on HECT domain catalytic activity. The reactants without E2 or ATP were used as two negative controls, respectively. As shown in Figure 3.2, the level of ubiquitination presented by intensity of polyUb smear in presence of tUBM was higher compared to the level in

absence of tUBM, indicating that tUBM enhanced the level of total ubiquitination mediated HUWE1 HECT domain.

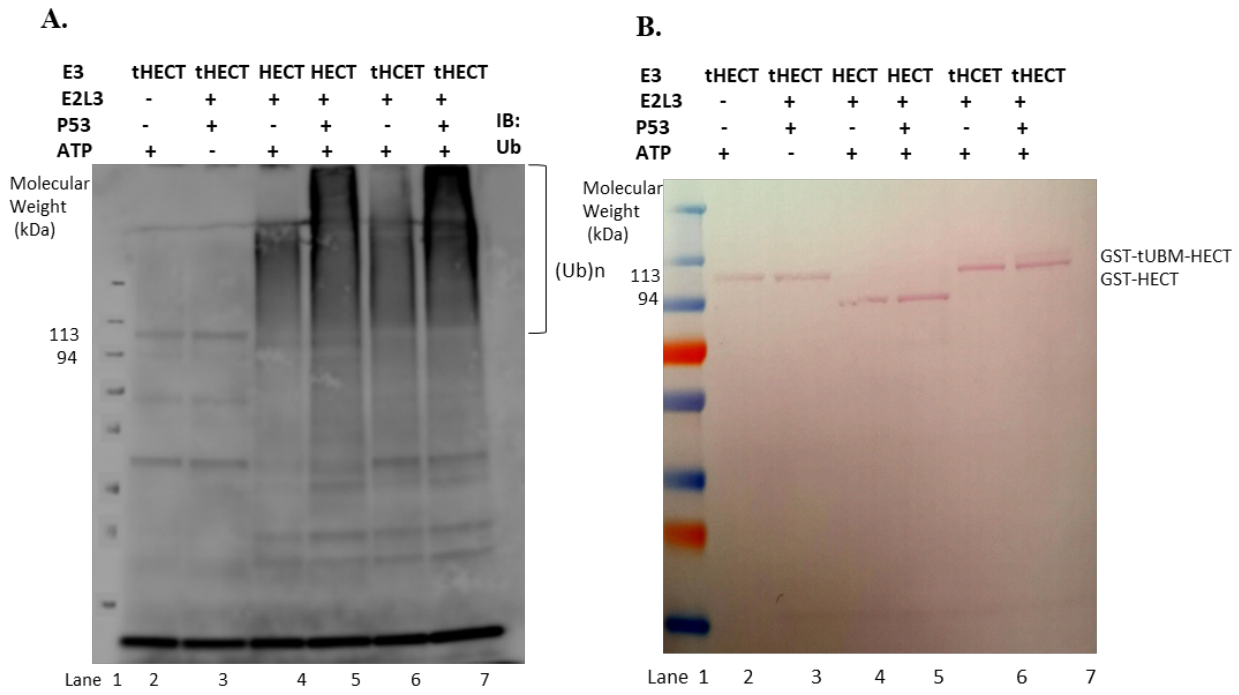

Figure 3.2 Membrane images of the result of the in vitro ubiquitination assay with WT Ub. A. Immunoblot membrane image of in vitro ubiquitination assay after being probed with anti-ubiquitin antibody thus demonstrated total ubiquitination level. E2L3 was skipped in the reaction mixture in lane 2 and ATP was omitted in the reactants in lane 3 both serving as negative controls. **B.** Membrane image after being Ponceau S stained and before being probed with antibody. The pink color bands with MW 113kDa and 94kDa represent GST tagged tUBM fused HECT domain and GST tagged HECT domain, respectively. The same intensity of each protein band implies equal loading of both proteins (n=1).

3.3.2 tUBM enhanced HECT-mediated ubiquitination using linkage specific monoUb

Each of eight types of linkage specific mutant monoUb as the polyUb building blocks was tested in the in vitro ubiquitination assay using either HECT alone or tUBM-HECT as the E3 ligase and p53 as the substrate protein. The results were shown in Figure 3.3. Consistent with the previous assay using WT Ub, tUBM domain enhanced the total and auto ubiquitination level with all ubiquitin linkages which was presented by denser polyUb smears without altering the ubiquitin linkage preference of HECT domain (Figure 3.3).

Several additional observations were also made. (1) The HUWE1 HECT domain was capable to synthesize polyUb chains of many linkages in presence and absence of tUBM (Figure 3.3). Notably, K11 linked polyUb was not detected. This was because K11 only monoUb was not recognized by the Ub antibody used in this project. (2) K6, K27 and K48 were the most favored Ub linkages detected for total ubiquitination, whereas in autoubiquitination more K27-linked polyUb was detected. (3) Despite enhancing total and autoubiquitination, tUBM decreased p53 substrate protein ubiquitination, demonstrated by less polyUb conjugated p53 smear in presence of tUBM (Figure 3.3). The highest level of p53 ubiquitination was found in K27 polyUb conjugated p53.

The in vitro ubiquitination assay with linkage specific monoUb and β-catenin was performed. The results with β-catenin as the substrate protein were very similar to what was observed previously using p53 as the substrate. The main findings were: (1) There were more polyUb chains synthesized in tUBM-HECT present reactions for total and auto ubiquitination. (2) K6, K27 and K48 linked polyUb were found to be the most abundant in total ubiquitination detected by the Ub antibody and the level of K27 linked polyUb was the highest for auto- and substrate ubiquitination (Figure 3.4). (3) K27 polyUb demonstrated the highest level for substrate

ubiquitination and tUBM did not show significant impact on β-catenin ubiquitination (Figure 3.4).

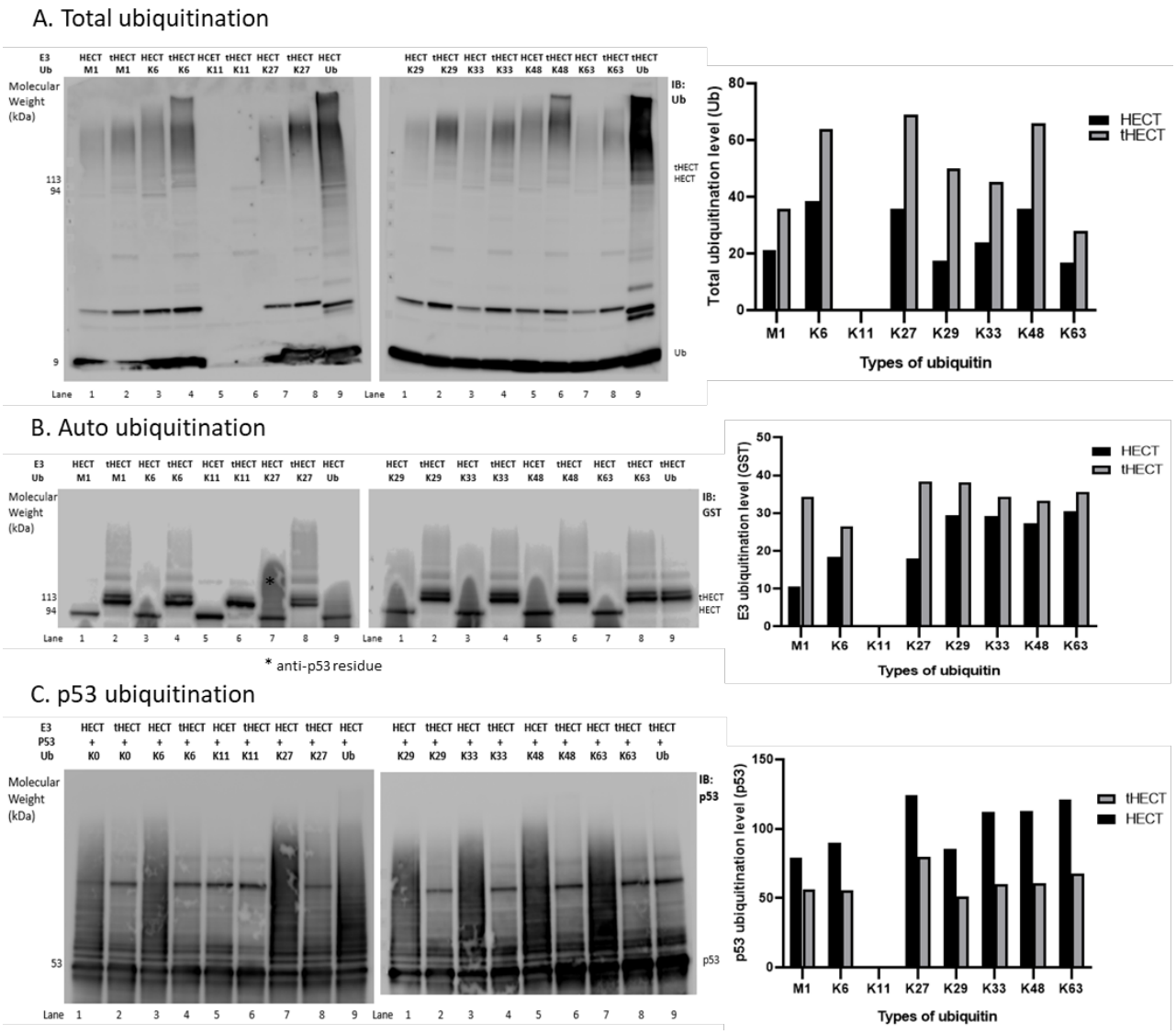

Figure 3.3 In vitro ubiquitination assay with linkage specific monoUb using p53 as the substrate protein. A. Left: Total ubiquitination immunoblotted with the Ub antibody. Right: The bar graph representing the total ubiquitination level quantified using polyUb smear intensity by Image J. **B.** Left: E3 autoubiquitination level immunoblotted using a GST antibody as HECT and tHECT were both GST tagged. Right: Bar graph illustration of autoubiquitination. **C.** Left: The substrate p53 ubiquitination immunoblotted by a p53 antibody. Right: Bar graph illustration of p53 substrate ubiquitination. Notably, K11 linked ubiquitin was not detected by any of three anti bodies. These are the representative images of three independent experiments (n=3).

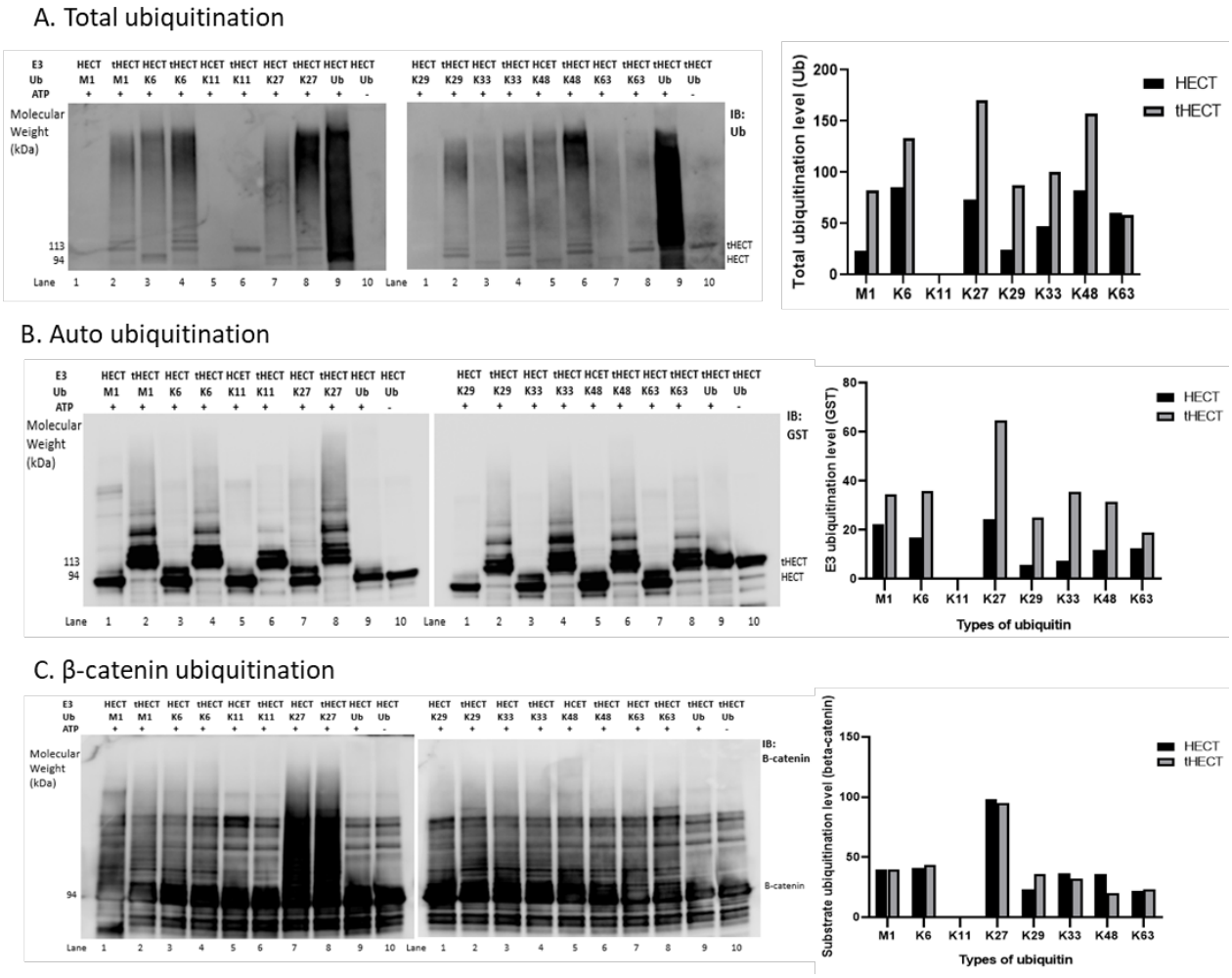

Figure 3.4 Result of in vitro ubiquitination assay with induvial linkage specific monoUb using β-catenin as the substrate protein (n=1). A. Total ubiquitination immunoblotted with the Ub antibody. Right: The bar graph representing the total ubiquitination level quantified using polyUb smear intensity by Image J. **B.** Left: E3 autoubiquitination level immunoblotted using a GST antibody. Right: Bar graph illustration of autoubiquitination. **C.** Left: The substrate β-catenin ubiquitination immunoblotted by a β-catenin antibody. Right: Bar graph illustration of β-catenin substrate ubiquitination.

3.3.3 tUBM enhanced total ubiquitination level in the assay with linkage specific diUb

Eight types of diUb chains were utilized as the source of Ub in this in vitro ubiquitination assay and the results were distinct from those of the previous assays with monoUb. The result showed that (1) the level of K63 linked polyUb was the highest among all Ub linkages whereas K6 and K48 linked polyUb were barely synthesized by HECT for total ubiquitination by using diUb, contrasting to the result by using monoUb as reactant (Figure 3.5); (2) The auto ubiquitination level with diUb as reactant was extremely low (Figure 3.5); (3) As to p53 polyubiquitination, M1 linked polyUb was most favored by HECT domain whereas K6 and K27 linked polyUb were scarcely shown (Figure 3.5) which was also different from the result using monoUb as Ub source. By using diUb as Ub chain building units, tUBM enhanced p53 ubiquitination instead of decreasing p53 polyUb (Figure 3.5). The most significance of this result was that HECT demonstrated the capability of catalyzing not only monoUb but also pre-assembled Ub chain, resulting in different preferred Ub signaling. In the case of diUb chain, the favored Ub linkages were M1 and K63 (n=1).

Taken together, the hypothesis that tUBM enhances HECT domain catalytic activity was supported by the results of five sets of in vitro ubiquitination assay as to total and auto ubiquitination levels but not substrate ubiquitination level. Three significant observations were found from the ubiquitination assay. (1) tUBM domain enhances the total and auto ubiquitination levels catalyzed by HECT applies to multiple Ub linkages including canonical and atypical Ub linkages without altering the Ub linkage preference of HECT domain; (2) The Ub linkage preference of HECT domain was affected by the form of Ub molecule, monoUb or diUb. (3) The presence of tUBM decreases p53 substrate ubiquitination level but did not affect the β-catenin

substrate ubiquitination level when using monoUb as the reactant. However, tUBM enhanced p53 polyubiquitination when diUb chains were used as the reactant.

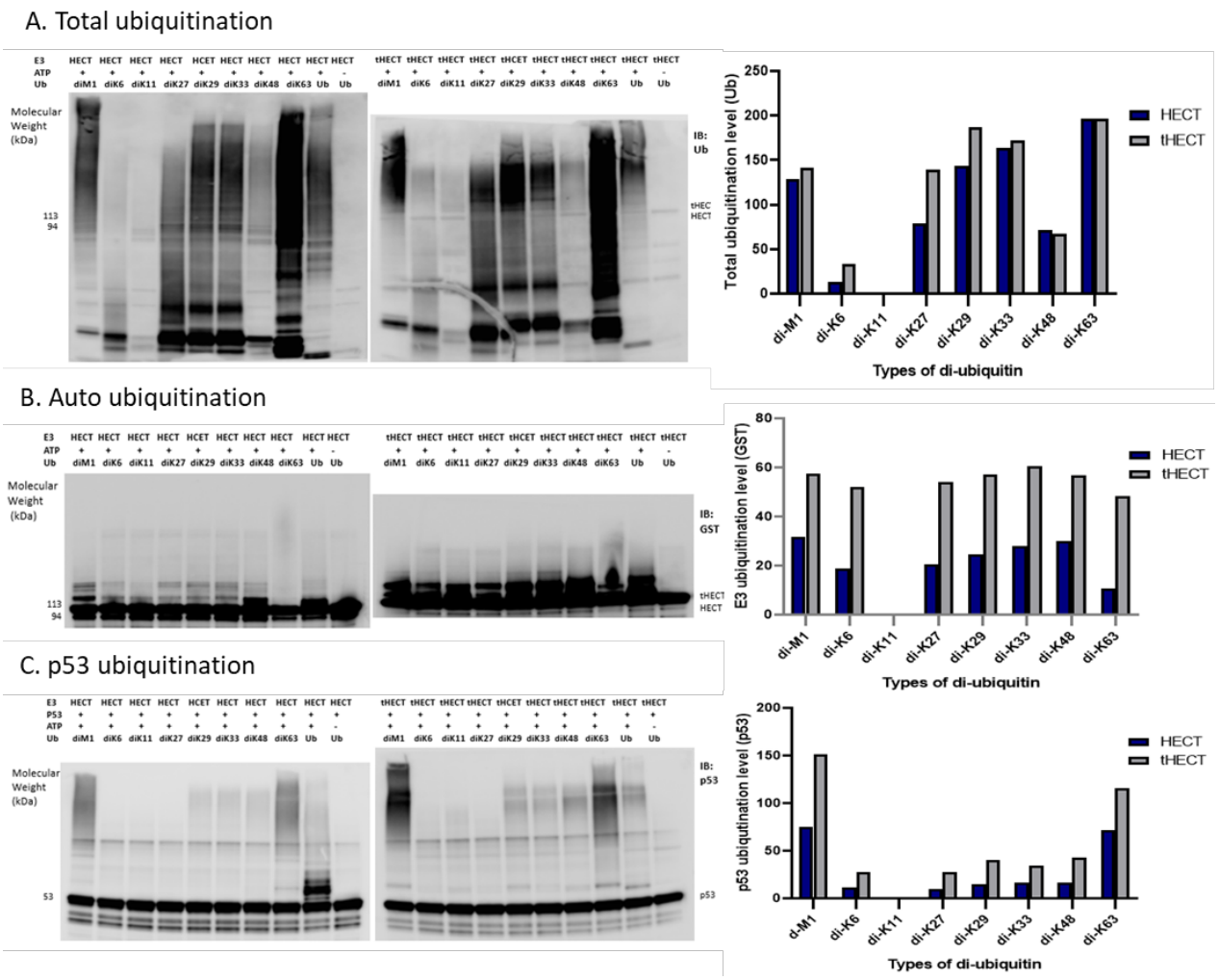

Figure 3.5 Result of in vitro ubiquitination assay utilizing HECT domain as E3 ligase in absence or presence of tUBM domain with induvial linkage specific diUb using p53 as substrate protein. **A.** Left: Two PVDF membranes probed by anti-Ub antibody indicating total ubiquitination level including ubiquitination of all protein components in reaction. Right: The total ubiquitination level of each reaction represented by the quantified polyUb smear intensity are illustrated by the bar graph. **B.** Left: Two membranes re-probed with anti-GST antibody indicating E3 auto ubiquitination level since HECT and tHECT were GST tagged. Right: Bar graph illustration of auto ubiquitination. **C.** Left: Two membranes probed by anti-p53 Ab indicating substrate p53 ubiquitination level. Right: Bar graph illustration of p53 ubiquitination. K11 linked ubiquitin was not detected by any of three types of antibodies (n=1).

3.4 Discussion

It has been reported that HUWE1 assembles K6, K11 and K48 linked polyUb by using linkage specific monoUb in vitro [106]. The results in this chapter confirmed that HUWE1 HECT domain catalyzes K6 and K48 linked polyUb. In addition, K27, K29, K33 and K63 polyUb were also observed being synthesized by HECT in absence and presence of tUBM.

The hypothesis of tUBM enhancing HECT domain catalytic activity was supported by the elevated total and auto ubiquitination level with linkage specific mono ubiquitin. Surprisingly, the presence of tUBM caused the decrease of the p53 ubiquitination level. Yet the reason behind this phenomenon remains unclear. However, tUBM did not show much impact on β-catenin substrate ubiquitination which implies tUBM may discriminatorily affect the substrate ubiquitination level with respect to the type of HUWE1 substrates.

In terms of using monoUb and diUb as building blocks to form polyUb chains, HECT domain demonstrated distinct catalytic preference of Ub linkages in total ubiquitination. K6 and K27 linkages were favored by HECT using mono mutant Ub whereas M1 and K63 linkages were preferred when diUb chain was used as reactant. The significance of this observation was that HUWE1 catalyzes both monoUb and pre-assembled Ub chains, preferring different linkages which leads to corresponding Ub signaling based on the form of Ub molecules. By far, two mechanism of ubiquitination chain elongation has been supported by previous literatures: sequential addition and “en bloc” pre-assembled Ub chain transfer mechanism [181]. The sequential addition refers to ubiquitin molecules being added one at a time to the substrate and then to the distal end of acceptor Ub [182-184] whereas the en bloc refers to the transferring of the pre-assembled Ub chain to the substrate [185-190]. Whether HECT domain catalyzes tri- or poly Ub chains as well as the resulting preference still need to be investigated.

Ubiquitination usually occurs at lysine residue of substrate protein. More lysine residues on substrate protein may increase probability of polyUb formation. However, there is no lysine residue in tUBM domain for polyUb formation. Therefore, the effect of tUBM domain enhancing total and auto ubiquitination is not because tUBM provides lysine residues but through other mechanism which needs to be unveiled.

3.5 Conclusion

Based on the results of the in vitro ubiquitination assays and discussion, several points can be concluded: (1) HUWE1 HECT catalytic domain mediated polyubiquitination occurred with both linkage-specific mono-ubiquitin and di-ubiquitin chains. HECT domain favors K6-, K48- monoUb, and M1-, K63- linked diUb chains in total ubiquitination. (2) tUBM enhances HECT domain catalytic activity without changing the ubiquitin linkage specificity of HECT domain.

Chapter 4

The Characterization of Ubiquitin Variants (UbVs) as the HUWE1-UBM1 modulator

4.1 Introduction

4.1.1 Ubiquitin Variant

Engineered UbVs (Ubiquitin Variants) have been developed as inhibitors or modulators of target proteins [164, 165]. In this project, HUWE1 UBM1-binding UbVs were developed using phage display technology by Dr. Wei Zhang (University of Guelph). Five UbV candidates were subject to GST pull down assay and BLI binding assay to examine their interactions with the HUWE1 UBM1 domain. Two of five UbV candidates were selected as the best binders of UBM1 and further tested for their ability to modulate HUWE1 E3 ligase activity in in vitro ubiquitination assays.

4.2 Materials and methods

4.2.1 UbV protein preparation and GST pull down assay

For prey protein (UbV) preparation, pET 53 plasmids carrying each of five UbVs were transformed into BL21 Condon plus DE3 RIPL competent cells. For bait protein (GST-UBM1) preparation, the pGEX plasmid carrying HUWE1-UBM1 was transformed into BL21 competent cells. The GST-tagged HUWE1 UBM1 purification was performed as previously described. A GST pull-down experiment was performed, and SDS-PAGE electrophoresis was used to check the interaction between each UbV and the HUWE1 UBM1 domain.

4.2.2 BLI binding assay with HUWE1 UBM1-binding UbVs

To further test the interaction between UbVs and UBM1, BLI binding assay was performed. The proteins including five UbV candidates, WT Ub, GST-UBM1 and GST were purified as described previously and concentrated to around 100μM tested by BCA assay. For

BLI binding assay, 200µl of 20µM GST-UBM1 was loaded as immobilized protein. 200µl of 20µM GST was prepared concurrently as a negative control to detect non-specific binding of UbVs.

Each UbV was diluted by serial dilution using HEPES buffer (25mM HEPES pH7.0, 150mM NaCl) with 0.02% BSA (Pierce™ BCA Protein Assay Kit, Thermo) from 10µM to 0.625µM with five concentrations. WT Ub was diluted from 60µM to 3.75µM via serial dilution resulting in five concentrations. 200µl of each binder protein with corresponding concentrations was loaded in the well of a 384-well plate. The interaction was detected by the Octet RED384 instrument (fortéBIO). The parameter of association rate k_a, dissociation rate k_d and R_{max} were provided by Octet Data Analysis software. In addition, the steady state statistical data was also provided by the same software, including dissociation constant K_D, Chi^2 /Degree of Freedom (χ^2/DoF) and coefficient of determination (R^2). Lower K_D value indicates higher affinity between two interacting proteins; Lower χ^2/DoF value (≤ 1) represents a better fit of the measurement model; R^2 measures the amount of variance around the fitted values and the larger R^2 value means the better regression model that fits observations.

4.2.3 In vitro ubiquitination assay with UbV

In vitro ubiquitination assay was performed as previously described in Chapter 3, using GST-HUWE1 tUBM-HECT and HECT as the E3 ligases. Impact of UbVs on HUWE1 E3 ligase activity was tested in the presence or absence of UbVs. The reaction was set up as previously described with 50ng/µl GST-tUBM-HECT and GST-HECT in a reaction volume of 20 µl. Three conditions (no UbV, 1.60µM UbV as the low concentration , 3.19µM UbV as the high

concentration) were tested either with tUBM-HECT or with HECT as the E3 ligase. The reaction mixtures without ATP were prepared as negative controls.

4.3 Results

UbVs were developed to block the ubiquitin interacting site on UBM1 thus disable UBM1 function of decoding ubiquitin signaling. Interaction between each of five UbV candidates and UBM1 was tested through GST-UBM1 pull down assay and BLI binding assay. The modulating effect of UbV on tUBM-HECT was explored through in vitro ubiquitination assay.

4.3.1 The interaction between UbVs and GST-UBM1 characterized by pull-down assay

Five UbVs were tested separately through GST-UBM1 pull-down assay. As shown in Figure 4.1, UbV2, UbV3, UbV4 and UbV5 co-eluted with GST-UBM1, indicating their interaction with GST-UBM1. The GSH columns immobilized with GST alone were utilized to test the non-specific binding between UbVs and GST alone. Compared to the UbV bands eluted from GST-UBM1 columns, there are fainter UbV bands eluted from GST alone columns, indicating some non-specific binding between several UbVs (UbV3, UbV4 and UbV5) and GST alone (Figure 4.1). As the band intensity for UbV2, UbV3, UbV4 and UbV5 co-eluted with GST-UBM1 were stronger than the ones co-eluted with GST alone, it suggested that UbV2, UbV3, UbV4 and UbV5 are the specific binders of GST-UBM1.

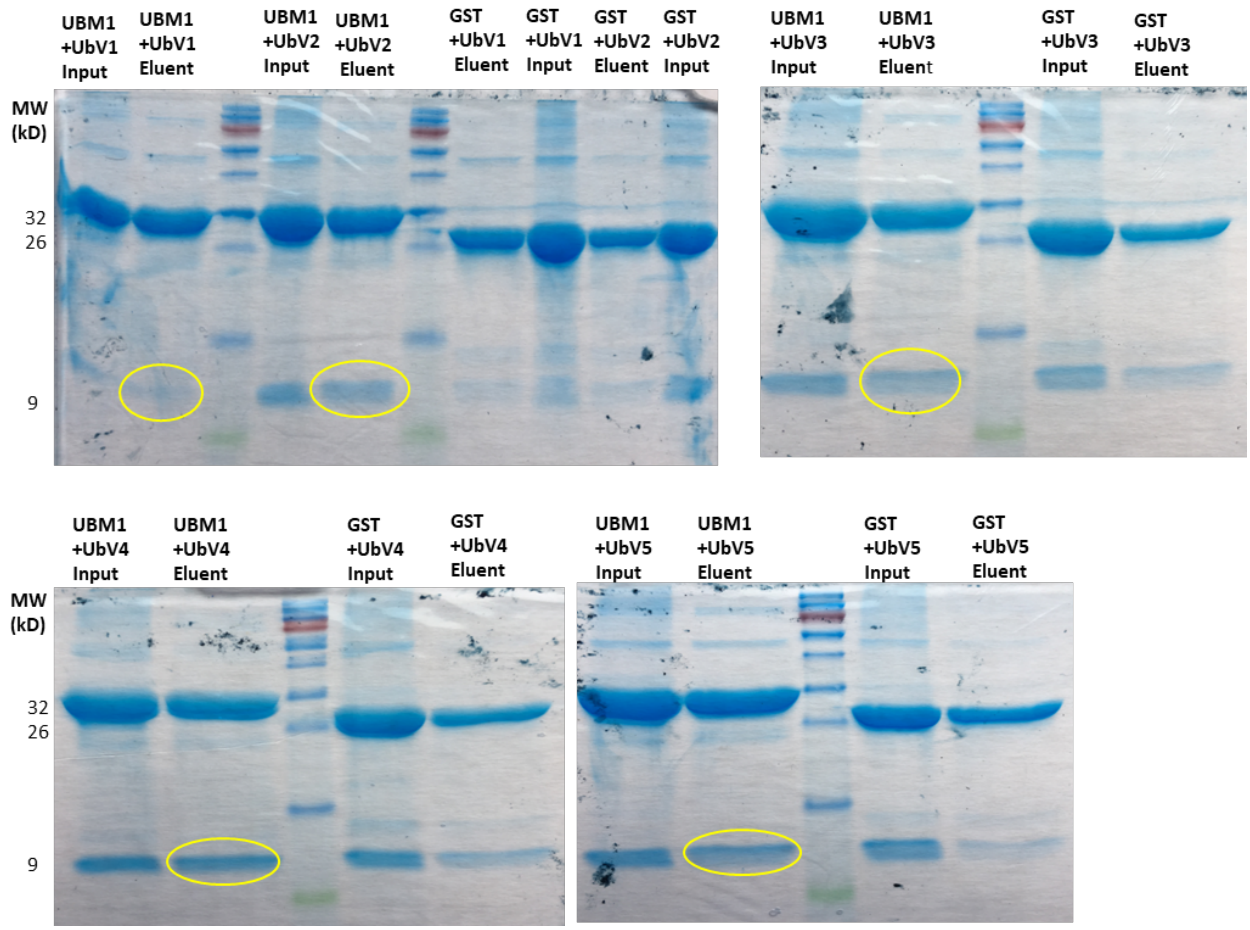

Figure 4.1 Gel images showing the interaction between HUWE1 GST-UBM1 and UbVs using GST pull down assay. The circled bands were UbVs eluted from GST-UBM1 bound GSH column indicating the interaction between UbVs and UBM1. GST tag bound beads were used to test non-specific binding of UbV.

4.3.2 The interaction between UbVs and GST-UBM1 characterized by BLI binding assay

The BLI binding assays were performed using WT Ub, UbV2-4 and GST-UBM1 to further characterize the interaction between UbV candidates and GST-UBM1. The binding parameters including association rate k_a, dissociation rate k_d, observed rate k_{obs}, max binding signal Rmax, equilibrium binding signal Req were obtained from Octet Data Analysis software and summarized in the Table 4.1.

Since these UbV molecules are engineered to bind the target protein HUWE1 UBM1 domain as a modulator, the ideal UbV molecules are expected to have higher affinity than WT Ub interacting with HUWE1 UBM1. The steady state analytical data including KD value, χ^2/DoF and R^2 were provided by the Octet Data Analysis software shown in the Table 4.2. The dissociation constant (KD) of WT Ub was $2.00\times10^{-5}\pm5.6\times10^{-6}$ M. The KD values of UbV2 ($3.10\times10^{-7}\pm7.1\times10^{-8}$ M), UbV3 ($3.30\times10^{-7}\pm7.7\times10^{-8}$ M) and UbV4 ($5.60\times10^{-7}\pm5.7\times10^{-8}$ M) were 100- to 1000- fold lower than the KD of WT Ub implying that UbV2-4 are tight binders that may be able to compete with Ub binding to GST-UBM1. The χ^2/DoF value of three UbV candidates were between 10^{-5} and 10^{-4} (≤1) representing the good fit of the measurement model. Besides its affinity of binding to the UBM1, the optimal UbV candidate should have less non-specific binding to GST tag. UbV3 and UbV4 were selected as the two ideal binders due to their lower non-specific binding to GST which was illustrated in Figure 4.2E represented by comparatively flatter binding curve. The selected UbV3 and UbV4 were proceeded to function characterization in the following in vitro ubiquitination assays.

Table 4.1 The BLI binding assay parameters for WT Ub and UbVs.

Ub Type	Concentration (nM)	Ka (1/Ms)	Kd (1/s)	Kobs (1/s)	Rmax	Req
WT Ub	3750	1.13×10^{4}	4.01×10^{-3}	4.65×10^{-2}	0.0664	0.0607
WT Ub	7500	1.43×10^{4}	5.58×10^{-3}	1.13×10^{-1}	0.0888	0.0844
WT Ub	1.50×10^{4}	8.40×10^{3}	3.63×10^{-3}	1.30×10^{-1}	0.1218	0.1184
WT Ub	3.00×10^{4}	6.65×10^{3}	3.82×10^{-3}	2.03×10^{-1}	0.1517	0.1488
WT Ub	6.00×10^{4}	2.50×10^{3}	8.96×10^{-5}	1.50×10^{-1}	0.2269	0.2268
UbV2	3750	5.00×10^{5}	1.45×10^{-2}	3.27×10^{-1}	0.1467	0.1402
UbV2	7500	3.66×10^{5}	5.19×10^{-3}	4.62×10^{-1}	0.1827	0.1807
UbV2	1.50×10^{4}	2.84×10^{5}	1.94×10^{-2}	7.29×10^{-1}	0.2144	0.2087
UbV2	3.00×10^{4}	2.13×10^{5}	1.26×10^{-2}	1.08	0.1992	0.1969
UbV2	6.00×10^{4}	3.21×10^{5}	6.99×10^{-3}	1.21	0.1995	0.1984
UbV3	3750	5.23×10^{5}	1.32×10^{-2}	3.40×10^{-1}	0.1829	0.1758
UbV3	7500	3.96×10^{5}	9.62×10^{-3}	5.05×10^{-1}	0.2252	0.2209
UbV3	1.50×10^{4}	2.59×10^{5}	5.46×10^{-2}	7.01×10^{-1}	0.2878	0.2654
UbV3	3.00×10^{4}	2.23×10^{5}	8.61×10^{-3}	1.13	0.2503	0.2484
UbV3	6.00×10^{4}	3.54×10^{5}	7.31×10^{-3}	1.34	0.2496	0.2482
UbV4	3750	7.42×10^{5}	1.81×10^{-2}	4.82×10^{-1}	0.1382	0.133
UbV4	7500	5.10×10^{5}	2.77×10^{-2}	6.66×10^{-1}	0.1934	0.1853
UbV4	1.50×10^{4}	3.53×10^{5}	5.32×10^{-2}	9.35×10^{-1}	0.235	0.2216
UbV4	3.00×10^{4}	2.64×10^{5}	4.76×10^{-3}	1.33	0.2306	0.2298
UbV4	6.00×10^{4}	4.14×10^{5}	4.78×10^{-3}	1.56	0.2278	0.2271

Table 4.2 BLI affinity binding assay steady state kinetic parameters for WT Ub, UbV2, UbV3 and UbV4.

Ub Type	**KD** (M)	**KD Error** (M)	**χ^2/DoF**	**R^2**	**Rmax** (nm)	**Rmax Error** (nm)
WT Ub	2.00×10^{-5}	$\pm5.6\times10^{-6}$	3.2×10^{-4}	0.94	0.285	0.033
UbV2	3.10×10^{-7}	$\pm7.1\times10^{-8}$	1.2×10^{-4}	0.88	0.219	0.008
UbV3	3.30×10^{-7}	$\pm7.7\times10^{-8}$	2.1×10^{-4}	0.87	0.276	0.011
UbV4	5.60×10^{-7}	$\pm5.7\times10^{-8}$	4.6×10^{-5}	0.98	0.262	0.006

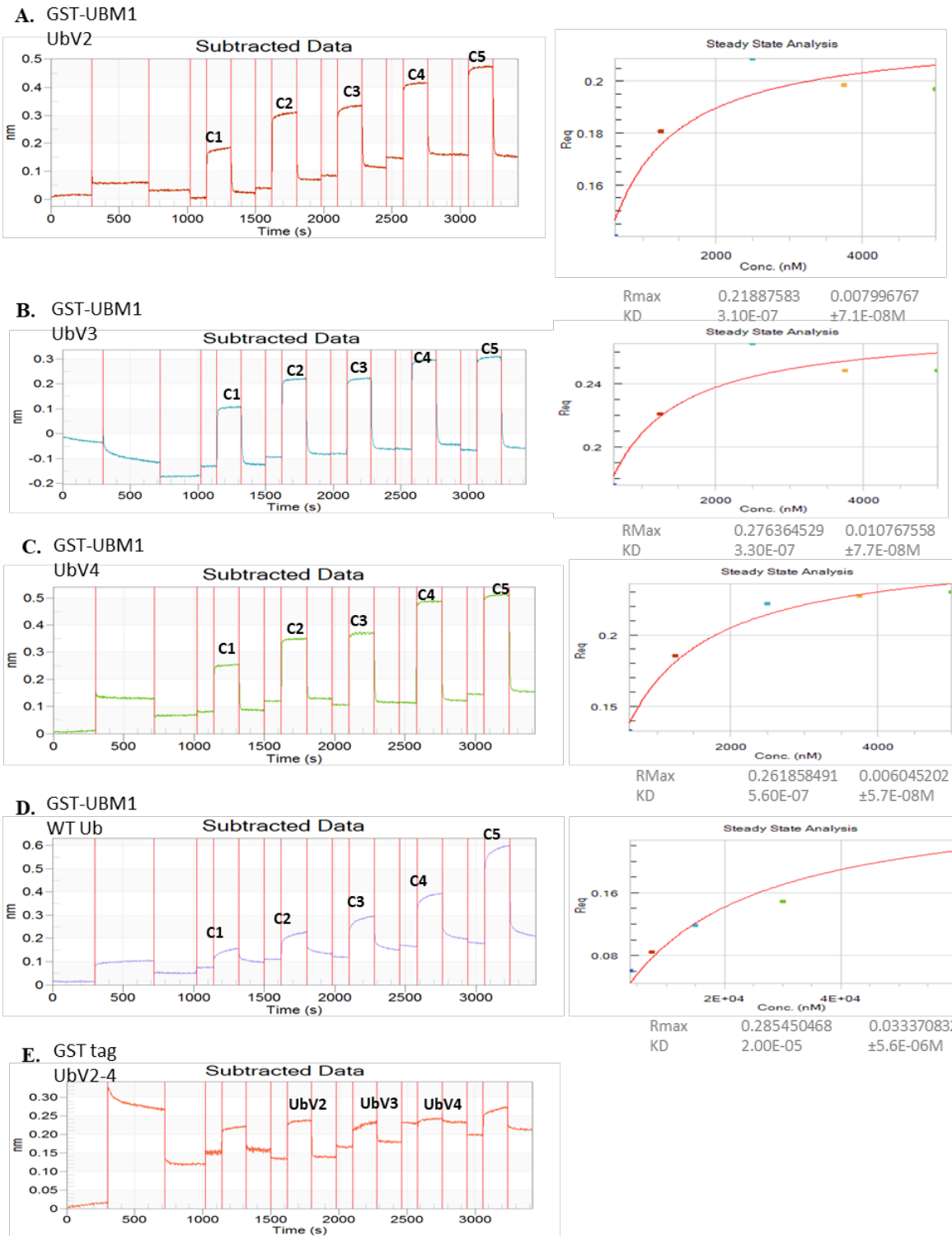

Figure 4.2 Subtracted data of BLI binding assay. A. UbV2 binding curves of five concentrations and its kinetic binding assay result. **B.** UbV3 binding curve and its binding assay result. **C.** UbV4 binding curve and its binding assay result. **D.** WT Ub binding curve and its binding assay result. **E.** The binding curves which indicated possible non-specific binding between UbV2-4 and GST alone.

4.3.3 The modulating effect of UbV on tUBM-HECT found from in vitro ubiquitination assay

To examine whether and how the UbVs affect the HUWE1 catalytic activity, in vitro ubiquitination was performed using HECT domain alone (HECT) or tUBM-HECT (tH) as the E3 ligases, in absence and presence of UbVs.

In vitro ubiquitination assay was performed in presence of UbV3 of two different concentrations 1.60μM and 3.19μM. The reaction mixture without ATP serves as a negative control. The results showed that UbV3 had little effect on HECT catalytic activity and showed bimodal effect on tUBM-HECT mediated ubiquitination. At concentration of 1.60μM, UbV3 boosted tUBM-HECT further, and increased total ubiquitination level (Figure 4.3, lane 3), whereas at 3.19μM, UbV3 exerted negative impact on tUBM-HECT activity and decreased ubiquitination level (Figure 4.3, lane 5).

Similar in vitro ubiquitination assay was performed in presence of UbV4. The results showed that UbV4 slightly enhances HECT catalytic activity and increased ubiquitination level (Figure 4.4 lane 4). At concentration of 1.60μM, UbV4 boosted tUBM-HECT activity and further increased total ubiquitination level (Figure 4.4 lane 3), whereas at 3.19μM, UbV4 lowered the ubiquitination level (Figure 4.4 lane 5).

Therefore, both UbV3 and UbV4 modulated tUBM-HECT domain in dose dependent manner. The dual roles of UbV, activator at low concentration and inhibitor at high concentration, warrant further investigation of the underlying mechanism.

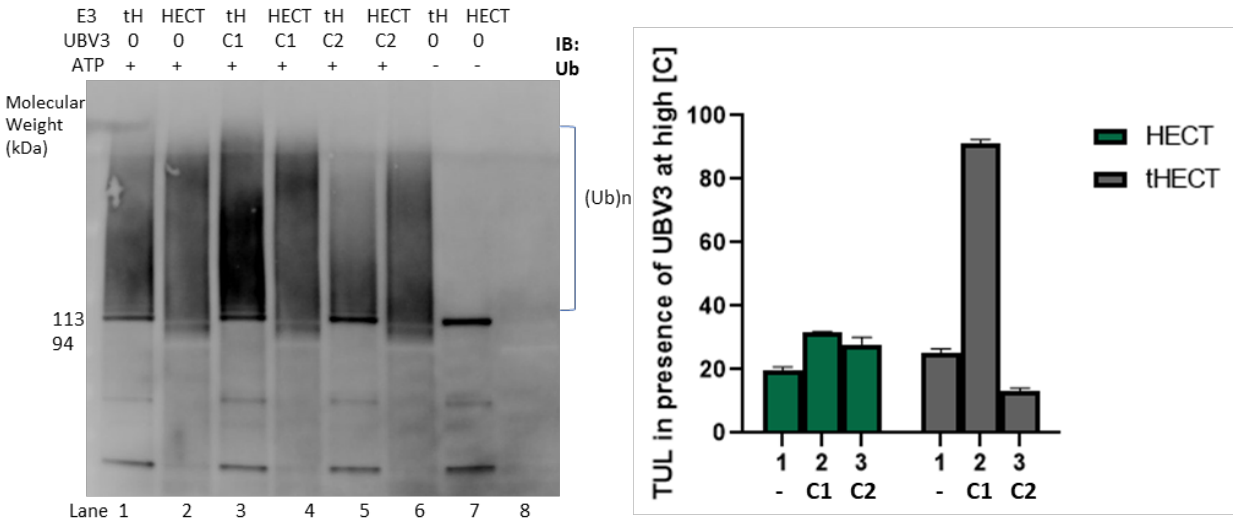

Figure 4.3 In vitro ubiquitination assay with UbV3. In vitro ubiquitination assay in presence of UbV3 with two different concentrations C1= 0.015µg/µl (1.60µM); C2=0.03µg/µl (3.19µM). The reaction mixture without ATP was loaded into lane 7,8 serving as negative control (n=1).

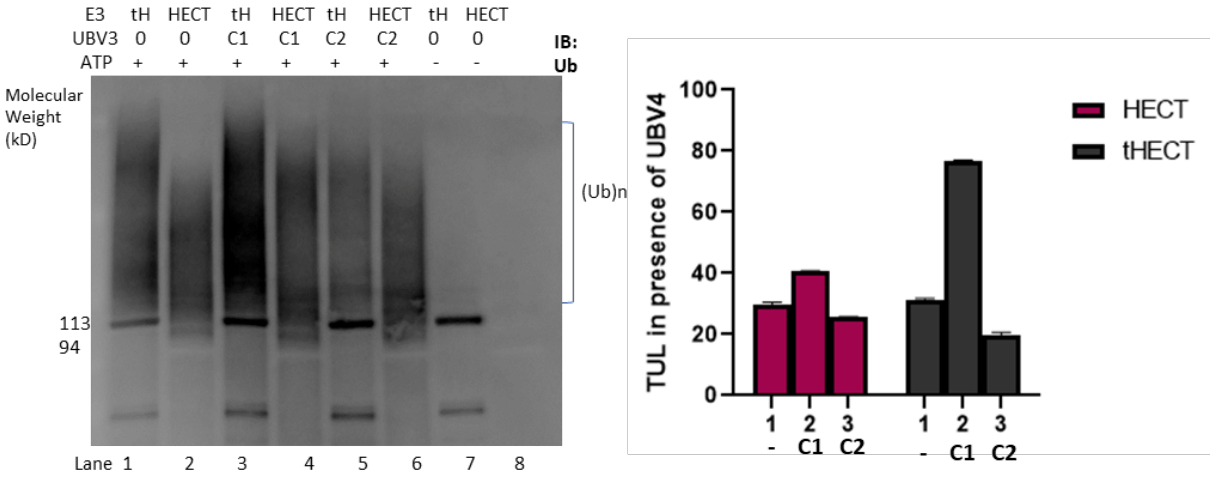

Figure 4.4 In vitro ubiquitination assay with UbV4. The in vitro ubiquitination assay in presence of UbV4 was performed with two concentrations, C1= 0.015µg/µl (1.60µM); C2=0.03µg/µl (3.19µM). This is the representative data of two independent experiments (n=2).

4.4 Discussion and Conclusion

UbV3 and UbV4 were selected as two UBM1 binding molecules. Their interactions with HUWE1 UBM1 were examined first with GST-pull down assay and then with BLI binding assay. Both UbVs showed high affinity binding to HUWE1 UBM1. The modulating effect of UbV3 and UbV4 on tUBM-HECT were then investigated through in vitro ubiquitination assays. Both UbVs can act as the inhibitors of tUBM domain conditionally in the dose dependent manner. At lower concentration (1.60μM), UbV3 and UbV4, as UBM1 activator, boosted the tUBM to enhance HECT domain catalytic activity. However, at high concentration (3.19μM), UbV3 and UbV4 acted as the inhibitor to attenuate the effect of tUBM on HUWE1 HECT mediated polyubiquitination. Therefore, UbV3 and UbV4 affect tUBM domain as modulators in dose dependent manner. Future work needs to investigate the underlying mechanism of the UbV effects on tUBM.

Chapter 5

Final remarks and future direction

5.1 Concluding remarks

The important roles that E3 ligase HUWE1 plays in tumorigenesis, neurogenesis and other pathogenic bioprocess have been characterized and reported by different research groups. HUWE1 R2981H mutation that is involved in XLID disease highlights the significance of the novel tUBM domain of HUWE1.

As a novel UBD, the interaction between the linkage specific Ub chains and tUBM needs to be characterized because Ub signaling and recognition are the critical character of a UBD. Ub signaling is exhibited by different topology of Ub chains via various Ub linkages. In addition, the effect of tUBM on HECT domain catalytic activity also needs to be characterized.

Based on the rationale stated above, an NMR structure analysis of UBM1 had previously performed in Sheng lab. Interaction between tUBM and K48-, K63 linked Ub chains as well as the effect on HECT catalysis in vivo had also been investigated in Sheng lab as a starting point of this research (Figure 5.1).

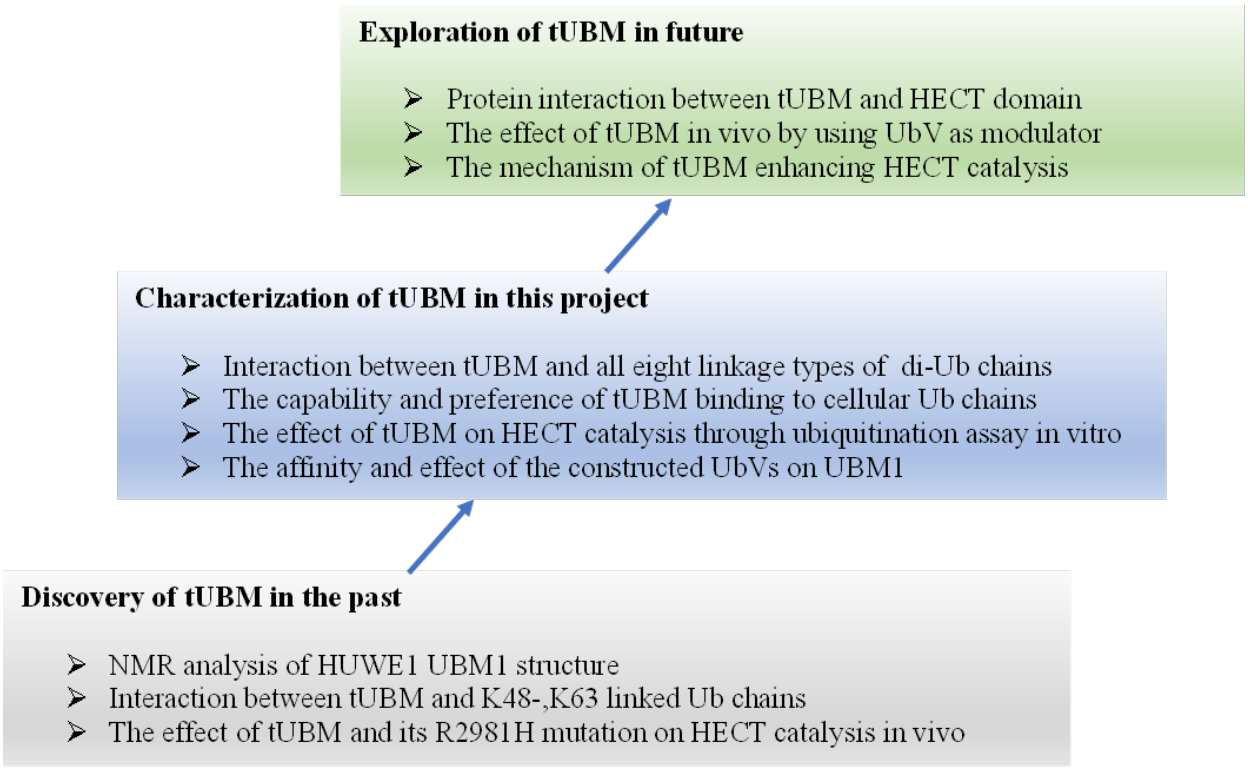

Figure 5.1 Flowchart of the work on HUWE1 tUBM domain characterization in the past, present, and future.

The experiments performed in this project further characterized the HUWE1 tUBM domain mainly from following two aspects: (1) revealed the linkage types of Ub chains interacting with tUBM including atypical Ub linkages; (2) detected the effect of tUBM on HECT catalysis through change of ubiquitination level in presence or absence of tUBM in vitro. The main findings include (1) HUWE1 tUBM domain interacts all eight linkage types of Ub di-chains (di-M1, diK6, diK11, diK27, diK29, diK33, diK48 and diK63); (2) total ubiquitination level mediated by HECT domain is increased by tUBM without altering preferred types of polyUb synthesized by HECT.

Notably, several research methods have been applied in this project such as BLI, native gel electrophoresis and in vitro ubiquitination assay. BLI was proved to be an ideal test method detecting protein-protein interaction with high sensitivity and efficiency. The greatest advantage

of BLI is that multiple samples can be tested in the same run within a short time frame. Therefore, BLI can be further utilized to test protein interactions for tUBM in the future based on the optimal concentrations of immobilized protein and binding protein indicated in this project. Furthermore, as a widely applied method to test the activity of an E3 ligase, the significance of the in vitro ubiquitination assay performed in this project was that by probing with different antibodies (anti-Ub, anti-GST, anti-p53 and anti-β-catenin), the total ubiquitination level, auto-ubiquitination level and substrate ubiquitination level were unveiled accordingly to examine the effect of tUBM or UbVs on HUWE1 HECT domain mediated ubiquitination.

5.2 Further direction

5.2.1 Further investigation on protein interactions of tUBM

Protein-protein interaction is the basis of protein function including signalling, activation, and inhibition. The protein interaction between diUb and tUBM domain as well as the interaction between UbV and UBM1 have been characterized (refer to Chapter 2 and Chapter 4 accordingly). However, to better understand the role of tUBM in modulating HUWE1 activity, more investigations are warranted.

5.2.1.1 Interaction between tUBM domain and HECT domain

The hypothesis that tUBM promotes HECT domain catalytic function thus enhances total ubiquitination levels has been supported through a series of in vitro ubiquitination assay (refers to Chapter 3). However, the mechanism of tUBM enhancing HECT domain catalytic activity remains unclear. Whether or not tUBM interacts with the HECT domain needs to be tested. A

BLI experiment can be an ideal method by using His-HECT as the immobilized protein and GST-tUBM as the binder protein.

5.2.1.2 Interaction between UbV and HECT domain

As the UBM1-binding UbVs, UbV3 and UbV4 were found to affect HECT mediated ubiquitination (refers to Chapter 4). Therefore, the interaction between the two UbVs and HECT domain needs to be investigated. Future work includes using BLI experiment with GST-HECT domain as immobilized protein and UbVs as binder proteins to detect whether the UBM1-binding UbVs binds directly to HUWE1 HECT domain.

5.2.1.3 Interaction between UbV and UBM2/UBM3 repeats of tUBM

The UbV3 and UbV4 were developed as the modulator of UBM1 and the affinity between the two UbVs and UBM1 had been characterized (refers to Chapter 4). However, whether the UbVs bind to UBM2 and UBM3 repeats of tUBM domain still to be tested. The research methods used in this project can be directly applied to characterize the interactions of UbVs with UBM2/UBM3 of tUBM.

5.2.1.4 The modulating effect of UbV on the catalytic activity of HUWE1 in cells

The modulating effect of UbV on catalytic activity of tUBM-HECT have been tested in vitro in this study. To reveal how UbV affect the catalytic activity of HUWE1, an in vivo ubiquitination assay could be performed by using transfected UbV in cells. By comparing the ubiquitination levels in presence and absence of UbV, the modulating impact of UbV on HUWE1 E3 ligase can be characterized.

5.2.2 Proposed hypothesis on the mechanism of tUBM enhancing ubiquitination

Based on the results of the *in vitro* ubiquitination assay stated in Chapter 3, HUWE1 tUBM enhanced the HECT domain catalytic activity without altering its preference of Ub linkages. However, the mechanism of how tUBM affects HECT domain remains unknown. A testing on the interaction between tUBM and HECT was proposed and mentioned in the section 5.2.1. In addition, through amino acid sequences comparison between the tUBM and HECT activation segment, a hypothesis can be proposed that tUBM may enhance the HECT domain catalytic activity by interrupting the auto inhibitory conformation of HECT domain as the HECT activation segment does. The rationale is explained in the following sections and the hypothesis needs verification in the future.

5.2.2.1 Introduction of HUWE1 activation segment

The C-terminal catalytic HECT domain of HUWE1 contains two distinct lobes. N-lobe (residues 3993-4252) contains E2 binding site and C-lobe (4259-4374) contains the conserved catalytic cysteine (Cys 4341). There is a linker region (4253-4258) connecting the two lobes [113]. HECT domain of HUWE1 remains inactive by forming an asymmetric auto-inhibited dimer in solution [114, 194, 195]. An activation segment (3843-3886) containing similar sequence as dimerization region (3951-3994) had been reported as the intramolecular engagement of HUWE1. The auto-inhibition state of HECT domain can be interrupted by presence of the activation segment leading to activation of HUWE1 catalytic activity [114] (Figure 5.2).

Through amino acid sequence alignment of UBM1with the HUWE1 activation segment, several residues were identified in UBM1 that could be aligned with the HUWE1 activation segment sequence (Figure 5.3). This implies that tUBM may enhance HECT domain catalytic activity by interrupting the auto-inhibition state of HECT domain. This hypothesis needs to be verified by further experiments. Mutation of tUBM at the conserved residues that aligned with the active segment can be applied to an in vitro ubiquitination assay to test whether tUBM could interrupt the auto-inhibitory state of HECT as the activation segment does. Due to the potential of tUBM on modulating HUWE1 enzymatic function, besides the work stated in this thesis, it is worth to conduct more future work to further reveal the function of the novel HUWE1 tUBM domain and the mechanism of its modulation.

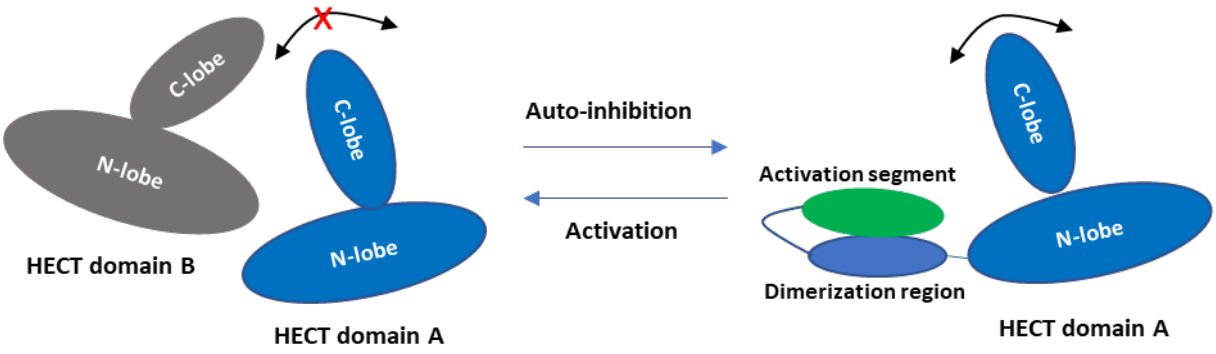

Figure 5.2 Cartoon presentation of auto-inhibition and activation of HUWE1 HECT domain. In solution, HUWE1 HECT domains of dimerize through dimerization region which hinders the movement of HECT domain C-lobe thus adopting an auto-inhibition conformation. Activation segment (green) interrupts the dimerization resulting in the activation of HECT domain.

A.

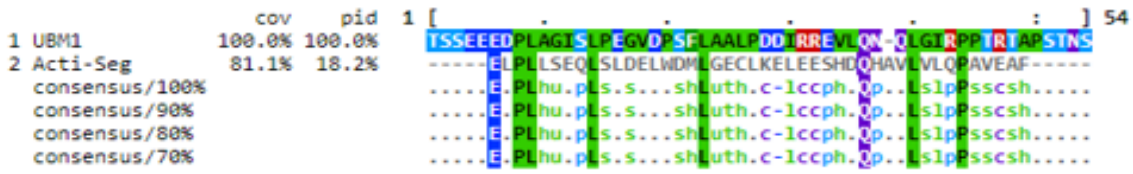

B.

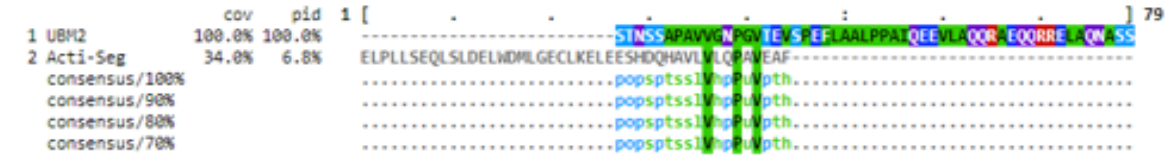

C.

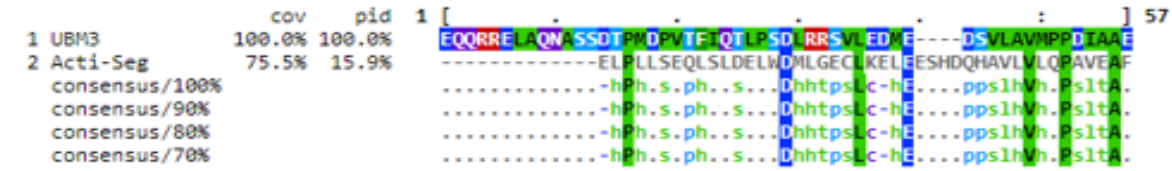

Figure 5.3 Sequence alignment of the activation segment (HUWE1$_{3843-3886}$) with each repeat of tUBM. The result was generated by Clustal Omega (1.2.4), viewed by Mview 1.63 (Nigel P. Brown, 2018). **A.** Sequence alignment of activation segment with UBM1 (HUWE1$_{2951-3003}$). The conserved parts of sequence have been colored. **B.** Sequence alignment of activation segment with UBM2 (HUWE1 $_{3000-3052}$). The colored area represents the conserved sequences. **C.** Sequence alignment of activation segment with UBM3 (HUWE1$_{3044-3096}$). The conserved parts of sequence have been colored.

References

1. Moortgat, S., et al., *HUWE1 variants cause dominant X-linked intellectual disability: a clinical study of 21 patients.* Eur J Hum Genet, 2018. **26**(1): p. 64-74.

2. Froyen, G., et al., *Submicroscopic duplications of the hydroxysteroid dehydrogenase HSD17B10 and the E3 ubiquitin ligase HUWE1 are associated with mental retardation.* Am J Hum Genet, 2008. **82**(2): p. 432-43.

3. Turner, G., A. Gedeon, and J. Mulley, *X-linked mental retardation with heterozygous expression and macrocephaly: Pericentromeric gene localization.* American Journal of Medical Genetics, 1994. **51**(4): p. 575-580.

4. Friez, M.J., et al., *HUWE1 mutations in Juberg-Marsidi and Brooks syndromes: the results of an X-chromosome exome sequencing study.* BMJ Open, 2016. **6**(4): p. e009537.

5. Zhao, X., et al., *The HECT-domain ubiquitin ligase Huwe1 controls neural differentiation and proliferation by destabilizing the N-Myc oncoprotein.* Nat Cell Biol, 2008. **10**(6): p. 643-53.

6. Knoepfler, P.S., P.F. Cheng, and R.N. Eisenman, *N-myc is essential during neurogenesis for the rapid expansion of progenitor cell populations and the inhibition of neuronal differentiation.* Genes & development, 2002. **16**(20): p. 2699-2712.

7. Stanton, B.R., et al., *Loss of N-myc function results in embryonic lethality and failure of the epithelial component of the embryo to develop.* Genes Dev, 1992. **6**(12a): p. 2235-47.

8. Komiya, Y. and R. Habas, *Wnt signal transduction pathways.* Organogenesis, 2008. **4**(2): p. 68-75.

9. MacDonald, B.T., K. Tamai, and X. He, *Wnt/beta-catenin signaling: components, mechanisms, and diseases.* Developmental cell, 2009. **17**(1): p. 9-26.

10. Steinhart, Z. and S. Angers, *Wnt signaling in development and tissue homeostasis.* Development, 2018. **145**(11): p. dev146589.

11. Segditsas, S. and I. Tomlinson, *Colorectal cancer and genetic alterations in the Wnt pathway.* Oncogene, 2006. **25**(57): p. 7531-7.

12. Zhan, T., N. Rindtorff, and M. Boutros, *Wnt signaling in cancer.* Oncogene, 2017. **36**(11): p. 1461-1473.

13. Clements, W.M., et al., *beta-Catenin mutation is a frequent cause of Wnt pathway activation in gastric cancer.* Cancer Res, 2002. **62**(12): p. 3503-6.

14. Valenta, T., G. Hausmann, and K. Basler, *The many faces and functions of β-catenin.* The EMBO journal, 2012. **31**(12): p. 2714-2736.

15. Clevers, H. and R. Nusse, *Wnt/β-Catenin Signaling and Disease.* Cell, 2012. **149**(6): p. 1192-1205.

16. de Groot, R.E., et al., *Huwe1-mediated ubiquitylation of dishevelled defines a negative feedback loop in the Wnt signaling pathway.* Sci Signal, 2014. **7**(317): p. ra26.

17. Dominguez-Brauer, C., et al., *E3 ubiquitin ligase Mule targets β-catenin under conditions of hyperactive Wnt signaling.* Proceedings of the National Academy of Sciences of the United States of America, 2017. **114**(7): p. E1148-E1157.

18. Vogelstein, B., D. Lane, and A.J. Levine, *Surfing the p53 network.* Nature, 2000. **408**(6810): p. 307-10.

19. Inga, A., et al., *Differential transactivation by the p53 transcription factor is highly dependent on p53 level and promoter target sequence.* Mol Cell Biol, 2002. **22**(24): p. 8612-25.

20. Beckerman, R. and C. Prives, *Transcriptional regulation by p53.* Cold Spring Harb Perspect Biol, 2010. **2**(8): p. a000935.

21. Lane, D.P., *Cancer. p53, guardian of the genome.* Nature, 1992. **358**(6381): p. 15-6.

22. Levine, A.J., *p53, the Cellular Gatekeeper for Growth and Division.* Cell, 1997. **88**(3): p. 323-331.

23. Feki, A. and I. Irminger-Finger, *Mutational spectrum of p53 mutations in primary breast and ovarian tumors.* Crit Rev Oncol Hematol, 2004. **52**(2): p. 103-16.

24. Ozaki, T. and A. Nakagawara, *Role of p53 in Cell Death and Human Cancers.* Cancers, 2011. **3**(1): p. 994-1013.

25. Soussi, T. and K.G. Wiman, *Shaping genetic alterations in human cancer: the p53 mutation paradigm.* Cancer Cell, 2007. **12**(4): p. 303-12.

26. Fakharzadeh, S.S., et al., *Structure and organization of amplified DNA on double minutes containing the mdm2 oncogene.* Genomics, 1993. **15**(2): p. 283-90.

27. Montes de Oca Luna, R., D.S. Wagner, and G. Lozano, *Rescue of early embryonic lethality in mdm2-deficient mice by deletion of p53.* Nature, 1995. **378**(6553): p. 203-6.

28. Jones, S.N., et al., *Rescue of embryonic lethality in Mdm2-deficient mice by absence of p53.* Nature, 1995. **378**(6553): p. 206-8.

29. de Rozieres, S., et al., *The loss of mdm2 induces p53-mediated apoptosis.* Oncogene, 2000. **19**(13): p. 1691-7.

30. Chen, D., et al., *ARF-BP1/Mule is a critical mediator of the ARF tumor suppressor.* Cell, 2005. **121**(7): p. 1071-83.

31. Qi, C.F., et al., *Characterization of ARF-BP1/HUWE1 interactions with CTCF, MYC, ARF and p53 in MYC-driven B cell neoplasms.* Int J Mol Sci, 2012. **13**(5): p. 6204-19.

32. Sherr, C.J., *Tumor surveillance via the ARF–p53 pathway.* Genes & Development, 1998. **12**(19): p. 2984-2991.

33. Sherr, C.J., et al., *p53-Dependent and -independent functions of the Arf tumor suppressor.* Cold Spring Harb Symp Quant Biol, 2005. **70**: p. 129-37.

34. Normand, G., et al., *p14ARF induces G2 cell cycle arrest in p53- and p21-deficient cells by down-regulating p34cdc2 kinase activity.* The Journal of biological chemistry, 2005. **280**(8): p. 7118-7130.

35. Yarbrough, W.G., et al., *Human Tumor Suppressor ARF Impedes S-Phase Progression Independent of p53.* Cancer Research, 2002. **62**(4): p. 1171-1177.

36. Eymin, B., et al., *p14ARF induces G2 arrest and apoptosis independently of p53 leading to regression of tumours established in nude mice.* Oncogene, 2003. **22**(12): p. 1822-35.

37. Yoon, S.Y., et al., *Over-expression of human UREB1 in colorectal cancer: HECT domain of human UREB1 inhibits the activity of tumor suppressor p53 protein.* Biochemical and Biophysical Research Communications, 2004. **326**(1): p. 7-17.

38. Confalonieri, S., et al., *Alterations of ubiquitin ligases in human cancer and their association with the natural history of the tumor.* Oncogene, 2009. **28**(33): p. 2959-2968.

39. Wang, Y., et al., *HECT E3 ubiquitin ligases – emerging insights into their biological roles and disease relevance.* Journal of Cell Science, 2020. **133**(7): p. jcs228072.

40. Crawford, L.J., et al., *The E3 ligase HUWE1 inhibition as a therapeutic strategy to target MYC in multiple myeloma.* Oncogene, 2020. **39**(27): p. 5001-5014.

41. Ma, W., et al., *Tumour suppressive function of HUWE1 in thyroid cancer.* Journal of Biosciences, 2016. **41**(3): p. 395-405.

42. Ciehanover, A., Y. Hod, and A. Hershko, *A heat-stable polypeptide component of an ATP-dependent proteolytic system from reticulocytes.* Biochemical and Biophysical Research Communications, 1978. **81**(4): p. 1100-1105.

43. Redman, K.L. and M. Rechsteiner, *Identification of the long ubiquitin extension as ribosomal protein S27a.* Nature, 1989. **338**(6214): p. 438-440.

44. Bianchi, M., et al., *Dynamic transcription of ubiquitin genes under basal and stressful conditions and new insights into the multiple UBC transcript variants.* Gene, 2015. **573**(1): p. 100-9.

45. Kimura, Y. and K. Tanaka, *Regulatory mechanisms involved in the control of ubiquitin homeostasis.* J Biochem, 2010. **147**(6): p. 793-8.

46. Lund, P.K., et al., *Nucleotide sequence analysis of a cDNA encoding human ubiquitin reveals that ubiquitin is synthesized as a precursor.* J Biol Chem, 1985. **260**(12): p. 7609-13.

47. Kirschner, L.S. and C.A. Stratakis, *Structure of the Human Ubiquitin Fusion Gene Uba80 (RPS27a) and One of Its Pseudogenes.* Biochemical and Biophysical Research Communications, 2000. **270**(3): p. 1106-1110.

48. Amerik, A.Y. and M. Hochstrasser, *Mechanism and function of deubiquitinating enzymes.* Biochim Biophys Acta, 2004. **1695**(1-3): p. 189-207.

49. Ciechanover, A., et al., *Characterization of the heat-stable polypeptide of the ATP-dependent proteolytic system from reticulocytes.* J Biol Chem, 1980. **255**(16): p. 7525-8.

50. Haglund, K. and I. Dikic, *Ubiquitylation and cell signaling.* Embo j, 2005. **24**(19): p. 3353-9.

51. Mukhopadhyay, D. and H. Riezman, *Proteasome-independent functions of ubiquitin in endocytosis and signaling.* Science, 2007. **315**(5809): p. 201-5.

52. Swatek, K.N. and D. Komander, *Ubiquitin modifications.* Cell Res, 2016. **26**(4): p. 399-422.

53. Bennett, E.J. and J.W. Harper, *DNA damage: ubiquitin marks the spot.* Nature Structural and Molecular Biology, 2008. **15**: p. 20+.

54. Pickart, C.M. and M.J. Eddins, *Ubiquitin: structures, functions, mechanisms.* Biochimica et Biophysica Acta (BBA) - Molecular Cell Research, 2004. **1695**(1): p. 55-72.

55. Hyer, M.L., et al., *A small-molecule inhibitor of the ubiquitin activating enzyme for cancer treatment.* Nat Med, 2018. **24**(2): p. 186-193.

56. Groettrup, M., et al., *Activating the ubiquitin family: UBA6 challenges the field.* Trends in Biochemical Sciences, 2008. **33**(5): p. 230-237.

57. Liu, X., et al., *The non-canonical ubiquitin activating enzyme UBA6 suppresses epithelial-mesenchymal transition of mammary epithelial cells.* Oncotarget, 2017. **8**(50): p. 87480-87493.

58. Liu, X., et al., *Orthogonal ubiquitin transfer identifies ubiquitination substrates under differential control by the two ubiquitin activating enzymes.* Nat Commun, 2017. **8**: p. 14286.

59. Lee, I. and H. Schindelin, *Structural insights into E1-catalyzed ubiquitin activation and transfer to conjugating enzymes.* Cell, 2008. **134**(2): p. 268-78.

60. Lv, Z., et al., *Crystal structure of a human ubiquitin E1-ubiquitin complex reveals conserved functional elements essential for activity.* The Journal of biological chemistry, 2018. **293**(47): p. 18337-18352.

61. Callis, J., *The ubiquitination machinery of the ubiquitin system.* The arabidopsis book, 2014. **12**: p. e0174-e0174.

62. Stewart, M.D., et al., *E2 enzymes: more than just middle men.* Cell Res, 2016. **26**(4): p. 423-40.

63. Valimberti, I., et al., *E2 superfamily of ubiquitin-conjugating enzymes: constitutively active or activated through phosphorylation in the catalytic cleft.* Sci Rep, 2015. **5**: p. 14849.

64. Ye, Y. and M. Rape, *Building ubiquitin chains: E2 enzymes at work.* Nature reviews. Molecular cell biology, 2009. **10**(11): p. 755-764.

65. Lan Huang, E.K., Guangli Wang, Sylvie Beaudenon, Peter M. Howley, Jon M. Huibregtse and Nikola P. Pavletich, *Structure of an E6AP-UbcH7 Complex: Insights into Ubiquitination by the E2-E3 Enzyme Cascade.* Science, 1999. **286**(5443): p. 1321-1326.

66. Turek, I., et al., *Multi-tiered pairing selectivity between E2 ubiquitin-conjugating enzymes and E3 ligases.* J Biol Chem, 2018. **293**(42): p. 16324-16336.

67. Eletr, Z.M., et al., *E2 conjugating enzymes must disengage from their E1 enzymes before E3-dependent ubiquitin and ubiquitin-like transfer.* Nat Struct Mol Biol, 2005. **12**(10): p. 933-4.

68. Berndsen, C.E. and C. Wolberger, *New insights into ubiquitin E3 ligase mechanism.* Nat Struct Mol Biol, 2014. **21**(4): p. 301-7.

69. Plechanovová, A., et al., *Structure of a RING E3 ligase and ubiquitin-loaded E2 primed for catalysis.* Nature, 2012. **489**(7414): p. 115-120.

70. Metzger, M.B., et al., *RING-type E3 ligases: master manipulators of E2 ubiquitin-conjugating enzymes and ubiquitination.* Biochimica et biophysica acta, 2014. **1843**(1): p. 47-60.

71. Shangary, S. and S. Wang, *Targeting the MDM2-p53 interaction for cancer therapy.* Clinical cancer research : an official journal of the American Association for Cancer Research, 2008. **14**(17): p. 5318-5324.

72. Brooks, C.L. and W. Gu, *p53 ubiquitination: Mdm2 and beyond.* Molecular cell, 2006. **21**(3): p. 307-315.

73. Hock, A.K. and K.H. Vousden, *The role of ubiquitin modification in the regulation of p53.* Biochimica et Biophysica Acta (BBA) - Molecular Cell Research, 2014. **1843**(1): p. 137-149.

74. George, A.J., et al., *A Comprehensive Atlas of E3 Ubiquitin Ligase Mutations in Neurological Disorders.* Frontiers in Genetics, 2018. **9**(29).

75. Huibregtse, J.M., et al., *A family of proteins structurally and functionally related to the E6-AP ubiquitin-protein ligase.* Proceedings of the National Academy of Sciences, 1995. **92**(7): p. 2563-2567.

76. Wenzel, D.M. and R.E. Klevit, *Following Ariadne's thread: a new perspective on RBR ubiquitin ligases.* BMC Biology, 2012. **10**(1): p. 24.

77. Lim, K.-H., J.-Y. Joo, and K.-H. Baek, *The potential roles of deubiquitinating enzymes in brain diseases.* Ageing Research Reviews, 2020. **61**: p. 101088.

78. Zheng, N. and N. Shabek, *Ubiquitin Ligases: Structure, Function, and Regulation.* Annual Review of Biochemistry, 2017. **86**(1): p. 129-157.

79. Metzger, M.B., V.A. Hristova, and A.M. Weissman, *HECT and RING finger families of E3 ubiquitin ligases at a glance.* Journal of cell science, 2012. **125**(Pt 3): p. 531-537.

80. Weber, J., S. Polo, and E. Maspero, *HECT E3 Ligases: A Tale With Multiple Facets.* Frontiers in Physiology, 2019. **10**(370).

81. Huang, L., et al., *Structure of an E6AP-UbcH7 Complex: Insights into Ubiquitination by the E2-E3 Enzyme Cascade.* Science, 1999. **286**(5443): p. 1321-1326.

82. Verdecia, M.A., et al., *Conformational flexibility underlies ubiquitin ligation mediated by the WWP1 HECT domain E3 ligase.* Mol Cell, 2003. **11**(1): p. 249-59.

83. Kamadurai, H.B., et al., *Insights into ubiquitin transfer cascades from a structure of a UbcH5B approximately ubiquitin-HECT(NEDD4L) complex.* Mol Cell, 2009. **36**(6): p. 1095-102.

84. García-Cano, J., et al., *HERCing: Structural and Functional Relevance of the Large HERC Ubiquitin Ligases.* Frontiers in Physiology, 2019. **10**(1014).

85. Scheffner, M. and S. Kumar, *Mammalian HECT ubiquitin-protein ligases: biological and pathophysiological aspects.* Biochim Biophys Acta, 2014. **1843**(1): p. 61-74.

86. Spratt, D.E., H. Walden, and G.S. Shaw, *RBR E3 ubiquitin ligases: new structures, new insights, new questions.* Biochem J, 2014. **458**(3): p. 421-37.

87. Walden, H. and K. Rittinger, *RBR ligase-mediated ubiquitin transfer: a tale with many twists and turns.* Nat Struct Mol Biol, 2018. **25**(6): p. 440-445.

88. Iwai, K. and K. Tanaka, *Ubiquitin chain elongation: an intriguing strategy.* Mol Cell, 2014. **56**(2): p. 189-191.

89. Cotton, T.R. and B.C. Lechtenberg, *Chain reactions: molecular mechanisms of RBR ubiquitin ligases.* Biochemical Society Transactions, 2020. **48**(4): p. 1737-1750.

90. Ries, L.K., et al., *Analysis of ubiquitin recognition by the HECT ligase E6AP provides insight into its linkage specificity.* J Biol Chem, 2019. **294**(15): p. 6113-6129.

91. Winget, J.M. and T. Mayor, *The diversity of ubiquitin recognition: hot spots and varied specificity.* Mol Cell, 2010. **38**(5): p. 627-35.

92. Akutsu, M., I. Dikic, and A. Bremm, *Ubiquitin chain diversity at a glance.* J Cell Sci, 2016. **129**(5): p. 875-80.

93. Suryadinata, R., et al., *Mechanisms of Generating Polyubiquitin Chains of Different Topology.* Cells, 2014. **3**: p. 674-89.

94. Jin, L., et al., *Mechanism of ubiquitin-chain formation by the human anaphase-promoting complex.* Cell, 2008. **133**(4): p. 653-665.

95. Xu, P., et al., *Quantitative proteomics reveals the function of unconventional ubiquitin chains in proteasomal degradation.* Cell, 2009. **137**(1): p. 133-145.

96. Li, Z., et al., *Ube2s stabilizes β-Catenin through K11-linked polyubiquitination to promote mesendoderm specification and colorectal cancer development.* Cell Death & Disease, 2018. **9**(5): p. 456.

97. Huang, H., et al., *K33-linked polyubiquitination of T cell receptor-zeta regulates proteolysis-independent T cell signaling.* Immunity, 2010. **33**(1): p. 60-70.

98. Varadan, R., et al., *Solution conformation of Lys63-linked di-ubiquitin chain provides clues to functional diversity of polyubiquitin signaling.* J Biol Chem, 2004. **279**(8): p. 7055-63.

99. Lai, M.Y., et al., *Structural and biochemical studies of the open state of Lys48-linked diubiquitin.* Biochim Biophys Acta, 2012. **1823**(11): p. 2046-56.

100. Nucifora, F.C., Jr., et al., *Ubiqutination via K27 and K29 chains signals aggregation and neuronal protection of LRRK2 by WSB1.* Nat Commun, 2016. **7**: p. 11792.

101. Kristariyanto, Y.A., et al., *Assembly and structure of Lys33-linked polyubiquitin reveals distinct conformations.* The Biochemical journal, 2015. **467**(2): p. 345-352.

102. Kristariyanto, Y.A., et al., *K29-selective ubiquitin binding domain reveals structural basis of specificity and heterotypic nature of k29 polyubiquitin.* Molecular cell, 2015. **58**(1): p. 83-94.

103. Michel, M.A., et al., *Assembly and specific recognition of k29- and k33-linked polyubiquitin.* Molecular cell, 2015. **58**(1): p. 95-109.

104. Wu, T., et al., *UBE2S drives elongation of K11-linked ubiquitin chains by the Anaphase-Promoting Complex.* Proceedings of the National Academy of Sciences, 2010. **107**(4): p. 1355-1360.

105. Deng, L., et al., *Activation of the IkappaB kinase complex by TRAF6 requires a dimeric ubiquitin-conjugating enzyme complex and a unique polyubiquitin chain.* Cell, 2000. **103**(2): p. 351-61.

106. Ohtake, F., et al., *The K48-K63 Branched Ubiquitin Chain Regulates NF-kappaB Signaling.* Mol Cell, 2016. **64**(2): p. 251-266.

107. Wilkinson, K.D., *Ubiquitination and deubiquitination: Targeting of proteins for degradation by the proteasome.* Seminars in Cell & Developmental Biology, 2000. **11**(3): p. 141-148.

108. Mapa, C.E., et al., *A balance of deubiquitinating enzymes controls cell cycle entry.* Mol Biol Cell, 2018. **29**(23): p. 2821-2834.

109. Zhong, Q., et al., *Mule/ARF-BP1, a BH3-only E3 ubiquitin ligase, catalyzes the polyubiquitination of Mcl-1 and regulates apoptosis.* Cell, 2005. **121**(7): p. 1085-95.

110. Kurokawa, M., et al., *A network of substrates of the E3 ubiquitin ligases MDM2 and HUWE1 control apoptosis independently of p53.* Sci Signal, 2013. **6**(274): p. ra32.

111. Suzuki, Y., Y. Suzuki, and N. Yamamoto, *Molecular Crosstalk between HIV-1 Integration and Host Proteins – Implications for Therapeutics*, in *HIV-Host Interactions*. 2011.

112. Yamamoto, S.P., et al., *Huwe1, a novel cellular interactor of Gag-Pol through integrase binding, negatively influences HIV-1 infectivity.* Microbes Infect, 2011. **13**(4): p. 339-49.

113. Pandya, R.K., et al., *A structural element within the HUWE1 HECT domain modulates self-ubiquitination and substrate ubiquitination activities.* J Biol Chem, 2010. **285**(8): p. 5664-73.

114. Sander, B., et al., *A conformational switch regulates the ubiquitin ligase HUWE1.* Elife, 2017. **6**.

115. Xu, Y., D.E. Anderson, and Y. Ye, *The HECT domain ubiquitin ligase HUWE1 targets unassembled soluble proteins for degradation.* Cell Discov, 2016. **2**: p. 16040.

116. Hunkeler, M., et al., *Solenoid architecture of HUWE1 contributes to ligase activity and substrate recognition.* Mol Cell, 2021. **81**(17): p. 3468-3480 e7.

117. Kurokawa, M., et al., *A network of substrates of the E3 ubiquitin ligases MDM2 and HUWE1 control apoptosis independently of p53.* Science signaling, 2013. **6**(274): p. ra32-ra32.

118. Canfield, K., et al., *Inverse association between MDM2 and HUWE1 protein expression levels in human breast cancer and liposarcoma.* International journal of clinical and experimental pathology, 2016. **9**(6): p. 6342-6349.

119. Aravind, L., *The WWE domain: a common interaction module in protein ubiquitination and ADP ribosylation.* Trends in Biochemical Sciences, 2001. **26**(5): p. 273-275.

120. Wang, Z., et al., *Recognition of the iso-ADP-ribose moiety in poly(ADP-ribose) by WWE domains suggests a general mechanism for poly(ADP-ribosyl)ation-dependent ubiquitination.* Genes & development, 2012. **26**(3): p. 235-240.

121. He, F., et al., *Structural insight into the interaction of ADP-ribose with the PARP WWE domains.* FEBS Letters, 2012. **586**(21): p. 3858-3864.

122. Gatti, M., et al., *The Ubiquitin Ligase TRIP12 Limits PARP1 Trapping and Constrains PARP Inhibitor Efficiency.* Cell Rep, 2020. **32**(5): p. 107985.

123. Giam, M., D.C.S. Huang, and P. Bouillet, *BH3-only proteins and their roles in programmed cell death.* Oncogene, 2008. **27**(1): p. S128-S136.

124. Chittenden, T., *BH3 domains: intracellular death-ligands critical for initiating apoptosis.* Cancer Cell, 2002. **2**(3): p. 165-166.

125. Lomonosova, E. and G. Chinnadurai, *BH3-only proteins in apoptosis and beyond: an overview.* Oncogene, 2008. **27 Suppl 1**(Suppl 1): p. S2-S19.

126. Warr, M.R., et al., *BH3-ligand regulates access of MCL-1 to its E3 ligase.* FEBS Lett, 2005. **579**(25): p. 5603-8.

127. Choe, K.N., et al., *HUWE1 interacts with PCNA to alleviate replication stress.* EMBO Rep, 2016. **17**(6): p. 874-86.

128. Dikic, I., S. Wakatsuki, and K.J. Walters, *Ubiquitin-binding domains - from structures to functions.* Nat Rev Mol Cell Biol, 2009. **10**(10): p. 659-71.

129. Rajalingam, K. and I. Dikic, *Expanding the Ubiquitin Code.* Cell, 2016. **164**(5): p. 1074-1074.e1.

130. Hicke, L., H.L. Schubert, and C.P. Hill, *Ubiquitin-binding domains.* Nat Rev Mol Cell Biol, 2005. **6**(8): p. 610-21.

131. Randles, L. and K.J. Walters, *Ubiquitin and its binding domains.* Frontiers in bioscience (Landmark edition), 2012. **17**: p. 2140-2157.

132. Hurley, J.H., S. Lee, and G. Prag, *Ubiquitin-binding domains.* Biochem J, 2006. **399**(3): p. 361-72.

133. He, F., et al., *Myosin VI Contains a Compact Structural Motif that Binds to Ubiquitin Chains.* Cell reports, 2016. **14**(11): p. 2683-2694.

134. Slagsvold, T., et al., *Eap45 in mammalian ESCRT-II binds ubiquitin via a phosphoinositide-interacting GLUE domain.* J Biol Chem, 2005. **280**(20): p. 19600-6.

135. Husnjak, K., et al., *Proteasome subunit Rpn13 is a novel ubiquitin receptor.* Nature, 2008. **453**(7194): p. 481-8.

136. Schreiner, P., et al., *Ubiquitin docking at the proteasome through a novel pleckstrin-homology domain interaction.* Nature, 2008. **453**(7194): p. 548-52.

137. Raasi, S., et al., *Diverse polyubiquitin interaction properties of ubiquitin-associated domains.* Nat Struct Mol Biol, 2005. **12**(8): p. 708-14.

138. Rahighi, S., et al., *Specific recognition of linear ubiquitin chains by NEMO is important for NF-kappaB activation.* Cell, 2009. **136**(6): p. 1098-109.

139. Lo, Y.C., et al., *Structural basis for recognition of diubiquitins by NEMO.* Mol Cell, 2009. **33**(5): p. 602-15.

140. Sokratous, K., et al., *The role of ubiquitin-binding domains in human pathophysiology.* Crit Rev Clin Lab Sci, 2014. **51**(5): p. 280-90.

141. Vanarotti, M., et al., *Small-molecules that bind to the ubiquitin-binding motif of REV1 inhibit REV1 interaction with K164-monoubiquitinated PCNA and suppress DNA damage tolerance.* Bioorganic & medicinal chemistry, 2018. **26**(9): p. 2345-2353.

142. Bomar, M.G., et al., *Unconventional ubiquitin recognition by the ubiquitin-binding motif within the Y family DNA polymerases iota and Rev1.* Mol Cell, 2010. **37**(3): p. 408-17.

143. Burschowsky, D., et al., *Structural analysis of the conserved ubiquitin-binding motifs (UBMs) of the translesion polymerase iota in complex with ubiquitin.* J Biol Chem, 2011. **286**(2): p. 1364-73.

144. Guo, C., et al., *Ubiquitin-binding motifs in REV1 protein are required for its role in the tolerance of DNA damage.* Mol Cell Biol, 2006. **26**(23): p. 8892-900.

145. Giles, A.C. and B. Grill, *Roles of the HUWE1 ubiquitin ligase in nervous system development, function and disease.* Neural Development, 2020. **15**(1): p. 6.

146. Bienko, M., et al., *Ubiquitin-binding domains in Y-family polymerases regulate translesion synthesis.* Science, 2005. **310**(5755): p. 1821-4.

147. Masahiro Fujimuro, H.S., Hideyoshi Yokosawa, *Production and characterization of monoclonal antibodies specific to multi-ubiquitin chains of polyubiquitinated proteins.* Federation of European Biochemical Societies, 1994. **349**(2): p. 173-180.

148. Ryu, K.Y., R.T. Baker, and R.R. Kopito, *Ubiquitin-specific protease 2 as a tool for quantification of total ubiquitin levels in biological specimens.* Anal Biochem, 2006. **353**(1): p. 153-5.

149. Matsumoto, M.L., et al., *K11-linked polyubiquitination in cell cycle control revealed by a K11 linkage-specific antibody.* Mol Cell, 2010. **39**(3): p. 477-84.

150. Newton, K., Matsumoto, M. L., Ferrando, R. E., Wickliffe, K. E., Rape, M., Kelley, R. F., et al., *Using Linkage-Specific Monoclonal Antibodies to Analyze Cellular Ubiquitylation.* Methods Mol. Biol., 2012. **832**: p. 185-196.

151. Matsumoto, M.L., et al., *Engineering and structural characterization of a linear polyubiquitin-specific antibody.* J Mol Biol, 2012. **418**(3-4): p. 134-44.

152. Michel, M.A., et al., *Ubiquitin Linkage-Specific Affimers Reveal Insights into K6-Linked Ubiquitin Signaling.* Mol Cell, 2017. **68**(1): p. 233-246 e5.

153. Kulathu, Y., et al., *Two-sided ubiquitin binding explains specificity of the TAB2 NZF domain.* Nat Struct Mol Biol, 2009. **16**(12): p. 1328-30.

154. Emmerich, C.H. and P. Cohen, *Optimising methods for the preservation, capture and identification of ubiquitin chains and ubiquitylated proteins by immunoblotting.* Biochem Biophys Res Commun, 2015. **466**(1): p. 1-14.

155. Johnson, A. and G. Vert, *Unraveling K63 Polyubiquitination Networks by Sensor-Based Proteomics.* Plant Physiol, 2016. **171**(3): p. 1808-20.

156. Hjerpe, R., et al., *Efficient protection and isolation of ubiquitylated proteins using tandem ubiquitin-binding entities.* EMBO Rep, 2009. **10**(11): p. 1250-8.

157. Mattern, M., et al., *Using Ubiquitin Binders to Decipher the Ubiquitin Code.* Trends Biochem Sci, 2019. **44**(7): p. 599-615.

158. Teyra, J., et al., *Structural and Functional Characterization of Ubiquitin Variant Inhibitors of USP15.* Structure, 2019. **27**(4): p. 590-605 e5.

159. Ernst, A., et al., *A strategy for modulation of enzymes in the ubiquitin system.* Science, 2013. **339**(6119): p. 590-5.

160. Gabrielsen, M., et al., *A General Strategy for Discovery of Inhibitors and Activators of RING and U-box E3 Ligases with Ubiquitin Variants.* Mol Cell, 2017. **68**(2): p. 456-470.

161. Watson, E.R., et al., *Protein engineering of a ubiquitin-variant inhibitor of APC/C identifies a cryptic K48 ubiquitin chain binding site.* Proceedings of the National Academy of Sciences, 2019. **116**(35): p. 17280-17289.

162. Zhang, W., et al., *System-Wide Modulation of HECT E3 Ligases with Selective Ubiquitin Variant Probes.* Mol Cell, 2016. **62**(1): p. 121-36.

163. SMITH, G.P., *Filamentous Fusion Phage: Novel Expression Vectors That Display Cloned Antigens on the Virion Surface.* SCIENCE, 1985. **228**: p. 1315-1317.

164. Zhang, W. and S.S. Sidhu, *Development of inhibitors in the ubiquitination cascade.* FEBS Letters, 2014. **588**(2): p. 356-367.

165. Zhang, W., et al., *System-Wide Modulation of HECT E3 Ligases with Selective Ubiquitin Variant Probes.* Molecular Cell, 2016. **62**(1): p. 121-136.

166. Vijay-Kumar, S., C.E. Bugg, and W.J. Cook, *Structure of ubiquitin refined at 1.8Åresolution.* Journal of Molecular Biology, 1987. **194**(3): p. 531-544.

167. Burroughs, A.M., et al., *Small but versatile: the extraordinary functional and structural diversity of the β-grasp fold.* Biology Direct, 2007. **2**(1): p. 18.

168. Zuin, A., M. Isasa, and B. Crosas, *Ubiquitin Signaling: Extreme Conservation as a Source of Diversity.* Cells, 2014. **3**: p. 690-701.

169. Bosshard, M., et al., *Impaired oxidative stress response characterizes HUWE1-promoted X-linked intellectual disability.* Sci Rep, 2017. **7**(1): p. 15050.

170. Parsons, J.L., et al., *Ubiquitin ligase ARF-BP1/Mule modulates base excision repair.* EMBO J, 2009. **28**(20): p. 3207-15.

171. Markkanen, E., et al., *Regulation of oxidative DNA damage repair by DNA polymerase λ and MutYH by cross-talk of phosphorylation and ubiquitination.* Proceedings of the National Academy of Sciences of the United States of America, 2012. **109**(2): p. 437-442.

172. Moritsugu, K., et al., *Dynamic recognition and linkage specificity in K63 di-ubiquitin and TAB2 NZF domain complex.* Scientific Reports, 2018. **8**(1): p. 16478.

173. Lee, S., et al., *Structural basis for ubiquitin recognition and autoubiquitination by Rabex-5.* Nat Struct Mol Biol, 2006. **13**(3): p. 264-71.

174. Ramabadran, R., *Structural and Functional Characterization of Novel Ubiquitin Binding Motifs in HUWE1.* Thesis, 2014.

175. Khatun, R., *Structural and functional studies of HUWE1 ubiquitin E3 ligase.* Sheng Lab, 2017. **Dissertation**.

176. Weeramange, C.J., et al., *The strengths and limitations of using biolayer interferometry to monitor equilibrium titrations of biomolecules.* Protein Sci, 2020. **29**(4): p. 1018-1034.

177. Yang, D., et al., *Comparison of biosensor platforms in the evaluation of high affinity antibody-antigen binding kinetics.* Anal Biochem, 2016. **508**: p. 78-96.

178. Choo, Y.S. and Z. Zhang, *Detection of protein ubiquitination.* J Vis Exp, 2009(30).

179. Lapetina, S. and H. Gil-Henn, *A guide to simple, direct, and quantitative in vitro binding assays.* J Biol Methods, 2017. **4**(1): p. e62.

180. Pollard, T.D., *A guide to simple and informative binding assays.* Mol Biol Cell, 2010. **21**(23): p. 4061-7.

181. Deol, K.K., S. Lorenz, and E.R. Strieter, *Enzymatic Logic of Ubiquitin Chain Assembly.* Frontiers in Physiology, 2019. **10**(835).

182. Pierce, N.W., et al., *Detection of sequential polyubiquitylation on a millisecond timescale.* Nature, 2009. **462**(7273): p. 615-9.

183. Lu, Y., W. Wang, and M.W. Kirschner, *Specificity of the anaphase-promoting complex: a single-molecule study.* Science, 2015. **348**(6231): p. 1248737.

184. French, M.E., et al., *Mechanism of ubiquitin chain synthesis employed by a HECT domain ubiquitin ligase.* J Biol Chem, 2017. **292**(25): p. 10398-10413.

185. Wang, M. and C.M. Pickart, *Different HECT domain ubiquitin ligases employ distinct mechanisms of polyubiquitin chain synthesis.* EMBO J, 2005. **24**(24): p. 4324-33.

186. Li, W., et al., *A ubiquitin ligase transfers preformed polyubiquitin chains from a conjugating enzyme to a substrate.* Nature, 2007. **446**(7133): p. 333-7.

187. Ravid, T. and M. Hochstrasser, *Autoregulation of an E2 enzyme by ubiquitin-chain assembly on its catalytic residue.* Nat Cell Biol, 2007. **9**(4): p. 422-7.

188. Masuda, Y., et al., *En bloc transfer of polyubiquitin chains to PCNA in vitro is mediated by two different human E2-E3 pairs.* Nucleic Acids Res, 2012. **40**(20): p. 10394-407.

189. Ronchi, V.P., J.M. Klein, and A.L. Haas, *E6AP/UBE3A ubiquitin ligase harbors two E2~ubiquitin binding sites.* J Biol Chem, 2013. **288**(15): p. 10349-60.

190. Streich, F.C., Jr., et al., *Tripartite motif ligases catalyze polyubiquitin chain formation through a cooperative allosteric mechanism.* J Biol Chem, 2013. **288**(12): p. 8209-8221.

191. LeBlanc, N., E. Mallette, and W. Zhang, *Targeted modulation of E3 ligases using engineered ubiquitin variants.* The FEBS Journal, 2020. **15536**(n/a).

192. LeBlanc, N., E. Mallette, and W. Zhang, *Targeted modulation of E3 ligases using engineered ubiquitin variants.* The FEBS Journal. **n/a**(n/a).

193. Sluimer, J. and B. Distel, *Regulating the human HECT E3 ligases.* Cellular and Molecular Life Sciences, 2018. **75**(17): p. 3121-3141.

194. Lorenz, S., *Structural mechanisms of HECT-type ubiquitin ligases.* Biol Chem, 2018. **399**(2): p. 127-145.

Appendix I

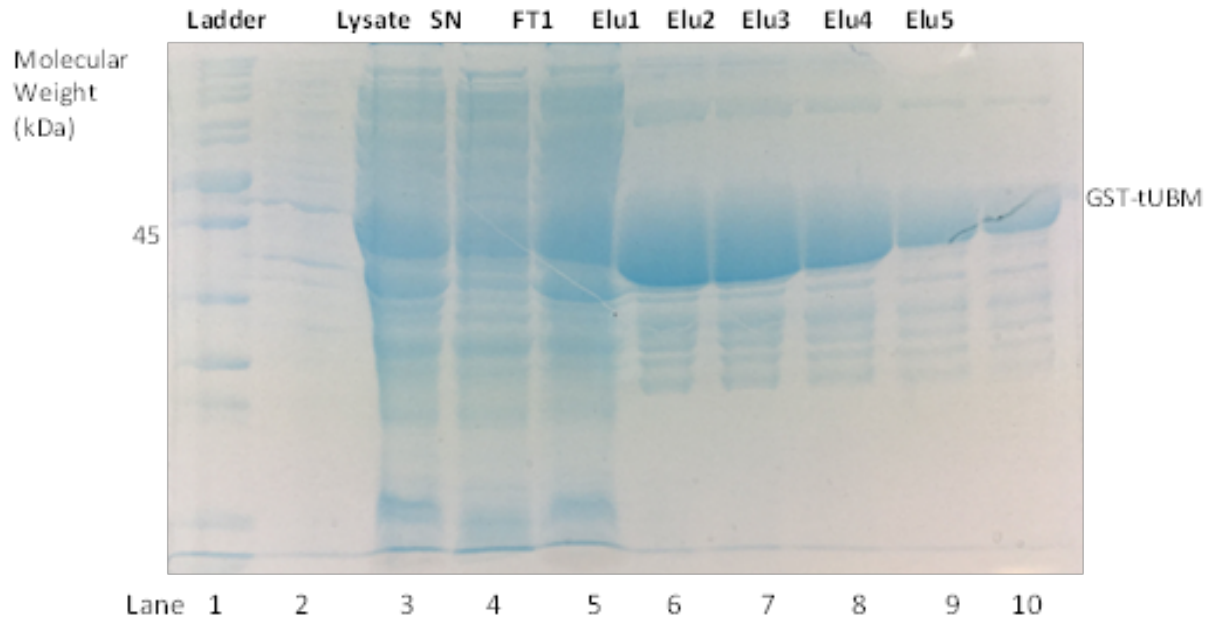

Figure S1. SDS-PAGE gel images of GST-tUBM. BL21 Codon Plus DE3 E. coli containing pGEX plasmids with tUBM gene insertion was cultured and IPTG induced for expression. The cells were lysed and purified by using GSH Sepharose beads. Lysate, supernatant, FT1, Elute1, Elute2, Elute3, Elute4 and Elute5 were separately loaded onto 12% polyacrylamide gel. The gel was run at 130V until the dye front approached the bottom of the gel followed by Coomassie stained and de-stained.

Appendix II

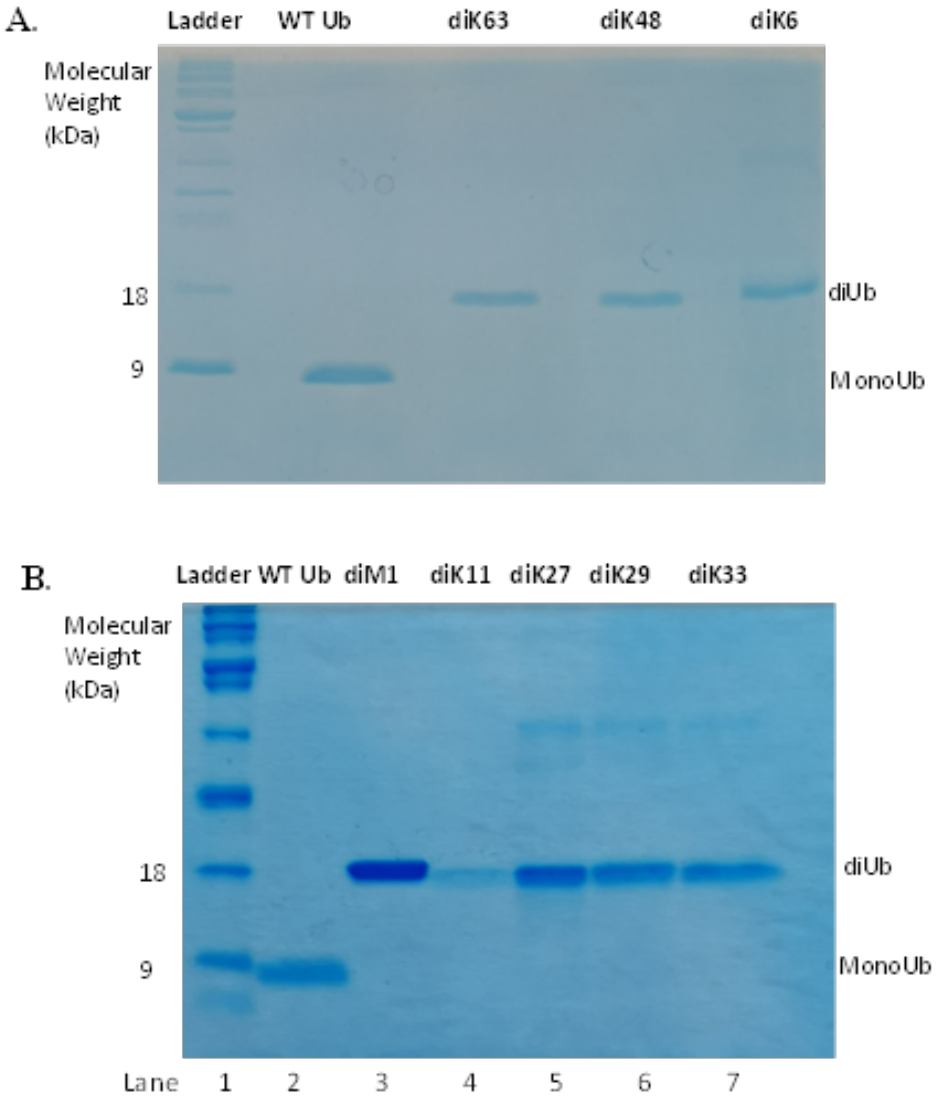

Figure S2. SDS-PAGE gel images of diUb chains. Eight types of di-ubiquitin chains as well as WT Ub from the same sample preparation for BioLayer Interferometry experiment were tested by 15% SDS PAGE gel. 5µl of each di-ubiquitin chain (25µM), 15µl PBS and 5µl of 5×SDS loading dye was mixture individually followed by boiling for 5 min. The gel was run at 120V until the dye front reached to the bottom of the gel. The gel was Coomassie stained

Appendix III

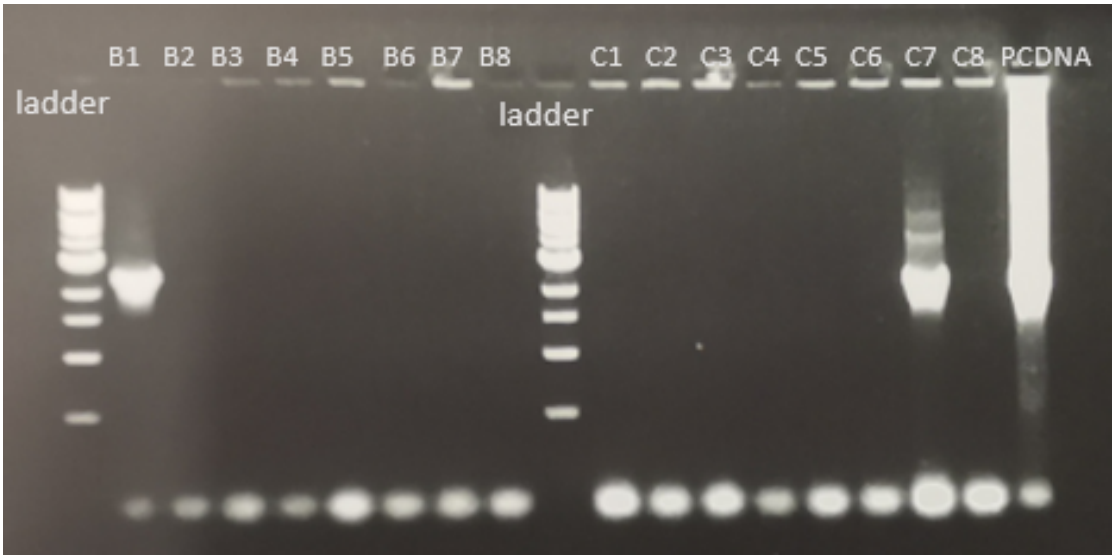

Figure S3. Agarose gel image of colony PCR result. Subclone of GST-tUBM-HECT from pcDNA to pGEX plasmid was performed through several steps: target gene PCR amplification, double digestion, ligation, ampicillin selection. 16 colonies were picked to test whether the gene being successfully transformed into the bacteria. Only two colonies (B1 and C7) showed positive result.

Appendix IV

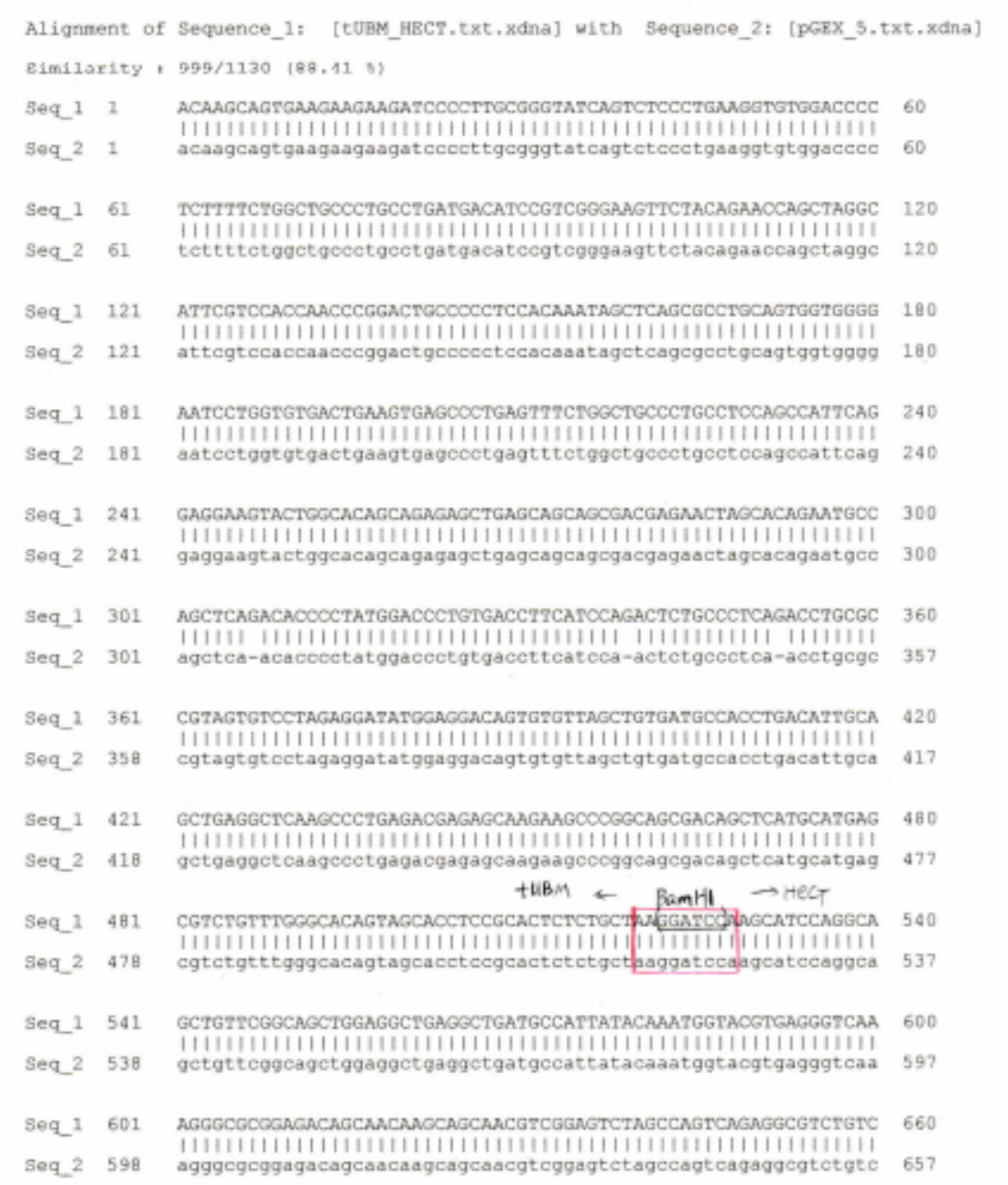

Figure S4. Sequence check of subcloned GST-tUBM-HECT (5' end). The sequence of 5' tUBM cDNA along with 5' end HECT cDNA and plasmid sequencing result (5') aligned thus the sequence of tUBM gene in acceptor pGEX plasmids was confirmed. The linker between tUBM and HECT which contained a BamH1 restriction site was also identified. The forward and reverse sequences were co-examined, and the correctness of nucleotides was manually verified with the sequencing chromatogram.

Appendix V

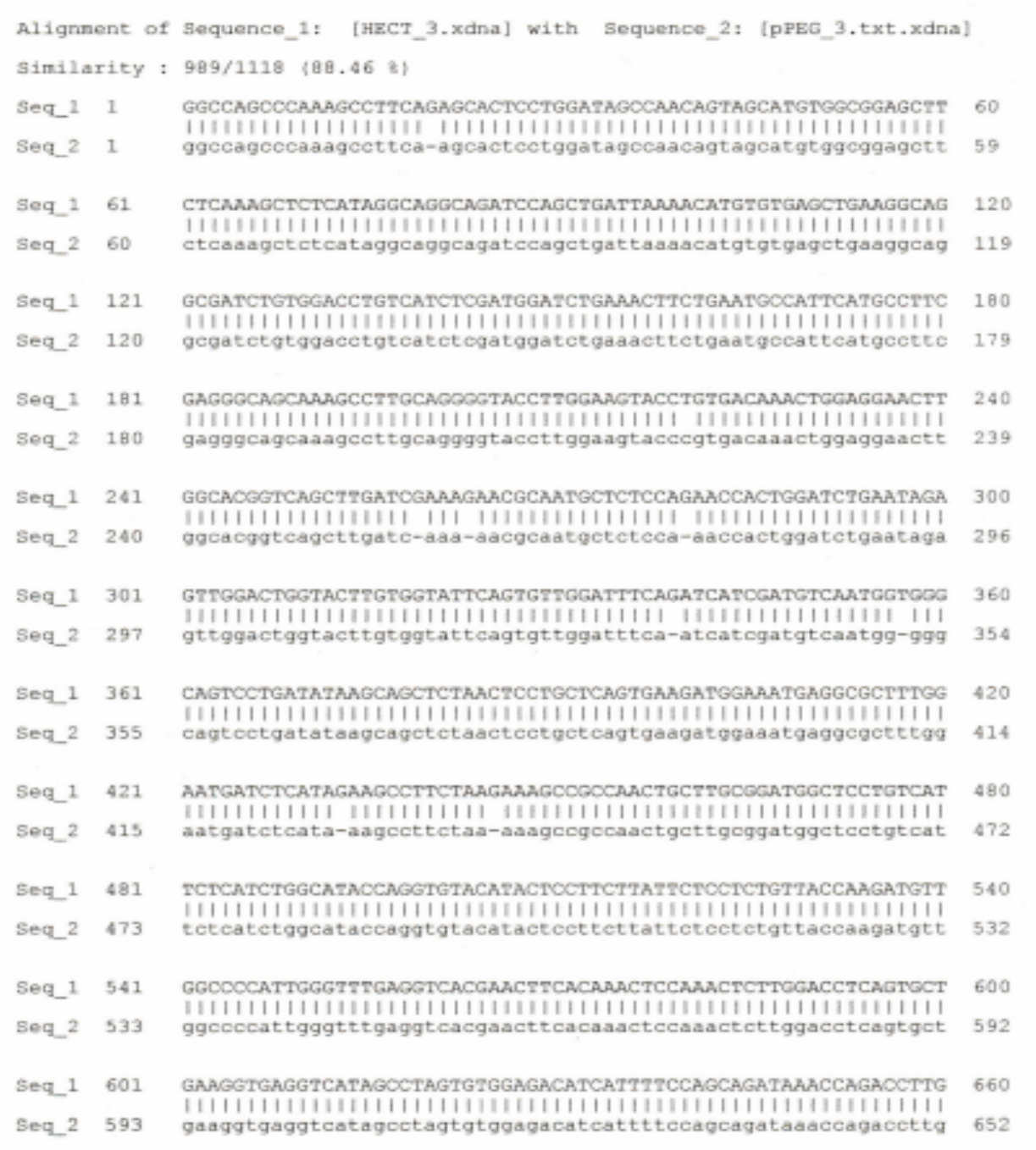

Figure S5. Sequence check of subcloned GST-tUBM-HECT (3' end). The sequence of 3' HECT cDNA and plasmid sequencing result (3') were aligned. Therefore, the sequence of HECT gene in acceptor pGEX plasmids was confirmed. The forward and reverse sequences were co-examined, and the correctness of nucleotides was manually verified with the sequencing chromatogram.

Appendix VI

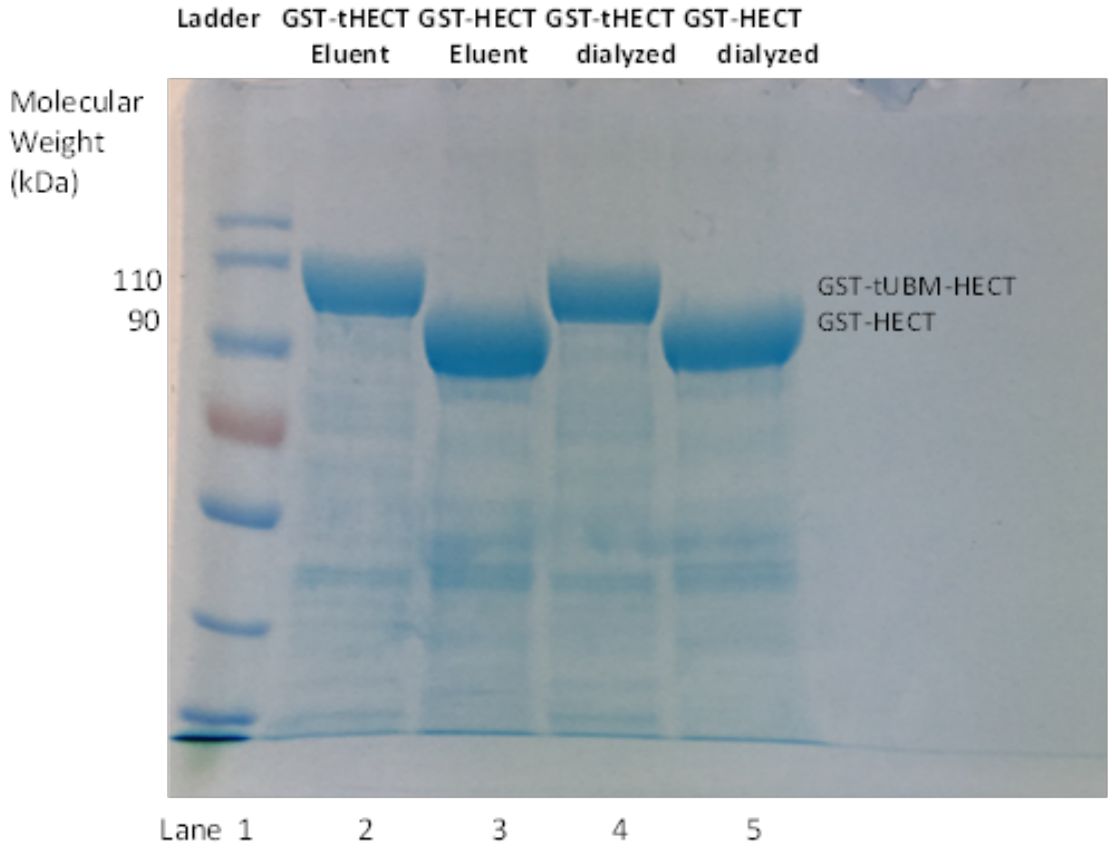

Figure S6. SDS-PAGE gel (7.5%) image of purified GST-tUBM-HECT and GST-HECT proteins.

Appendix VII

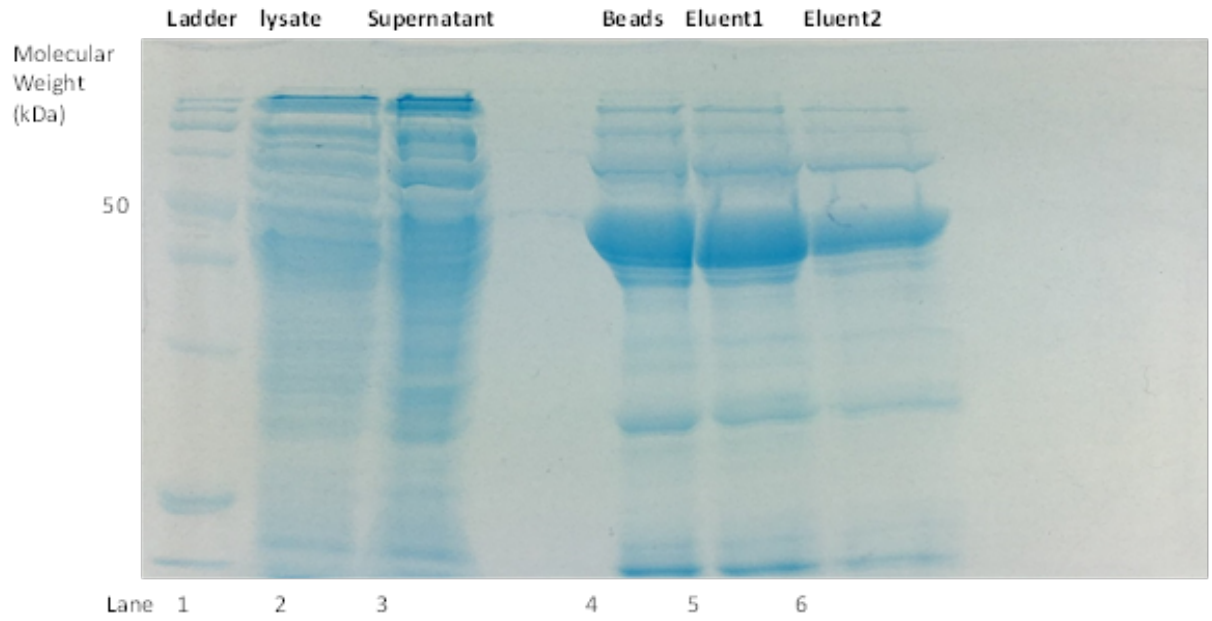

Figure S7. SDS-PAGE gel (12%) image of purified His-p53.

Appendix VIII

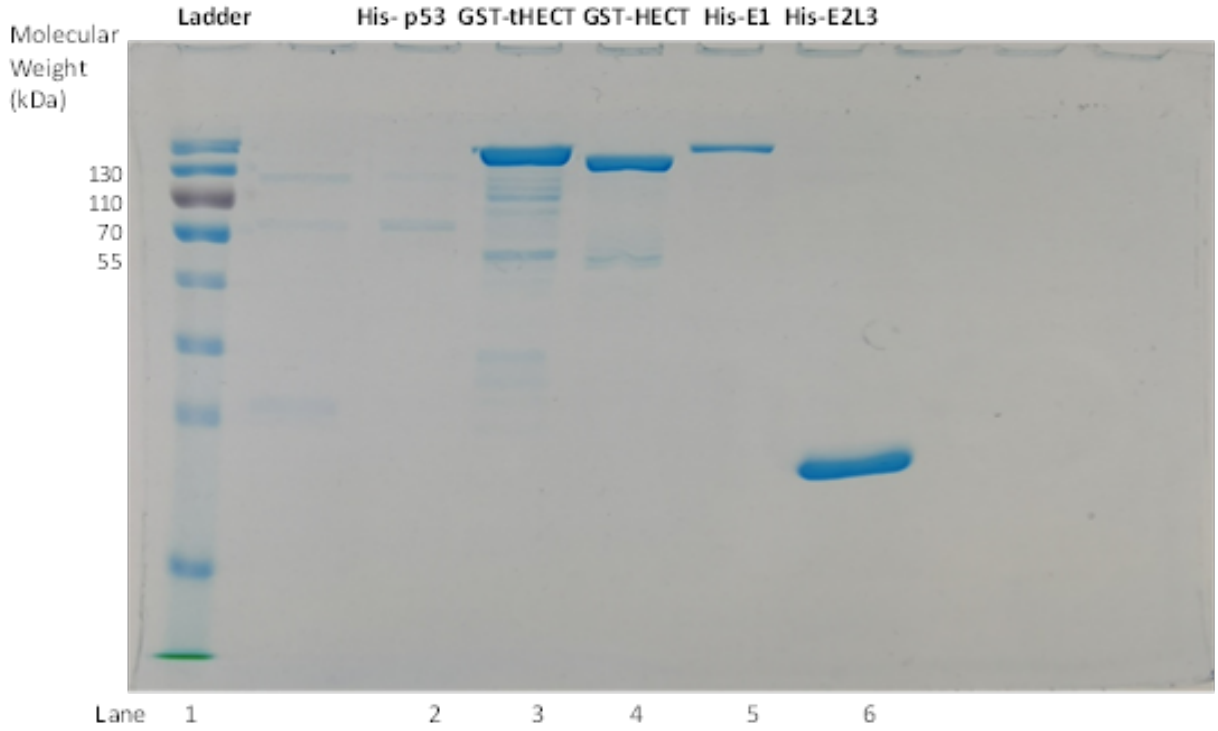

Figure S8. SDS-PAGE gel image of protein components in the in vitro ubiquitination assay. The molecular weight of His-p53 (53kDa), GST-tUBM-HECT (GST-tHECT) (113kDa), GST-HECT (94kDa), His-E1 (118kDa) and His-E2L3(18kDa) were verified.

Appendix IX

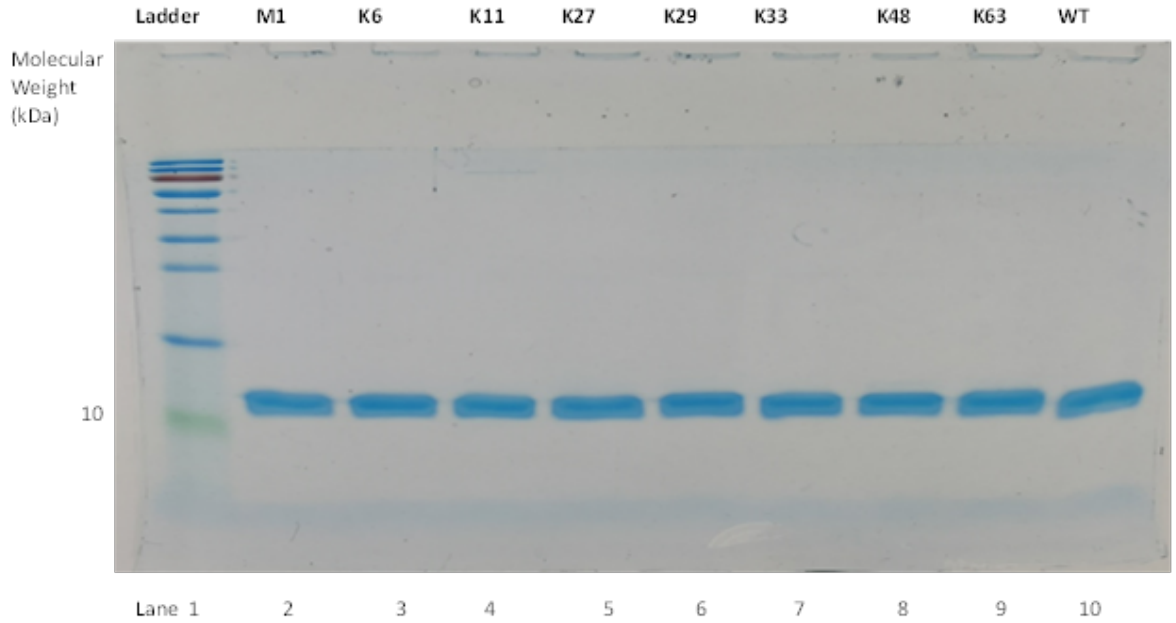

Figure S9. SDS-PAGE gel (15%) image of eight types of mutant mono-ubiquitin. Eight types of linkage specific mono-Ub as well as WT Ub were run on the 15% polyacrylamide gel for MW verification. For each linkage specific Ub, only one linkage site remains while seven other linkage sites were altered from lysine residues to arginine residue hence only one type of polyUb chain can possibly be assembled by using each individual linkage specific mono-Ub as the source of Ub in the in-vitro ubiquitination assay.

Appendix X

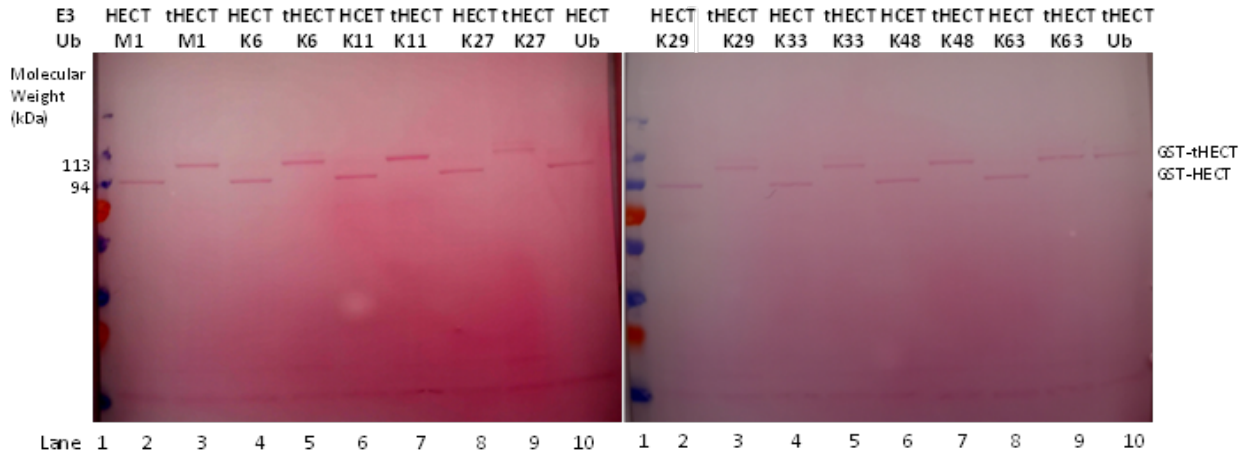

Figure S10. Image of two membranes stained by Ponceau S solution in the in vitro ubiquitination assay with linkage specific monoUb and p53 . Those two membranes were probed by anti-Ub antibody for total ubiquitination level detection which corresponds to the blots in Figure 3.2. Equal loading of GST-tUBM-HECT (113kDa) and GST-HECT (94kDa) was demonstrated by the same size protein bands.

Appendix XI

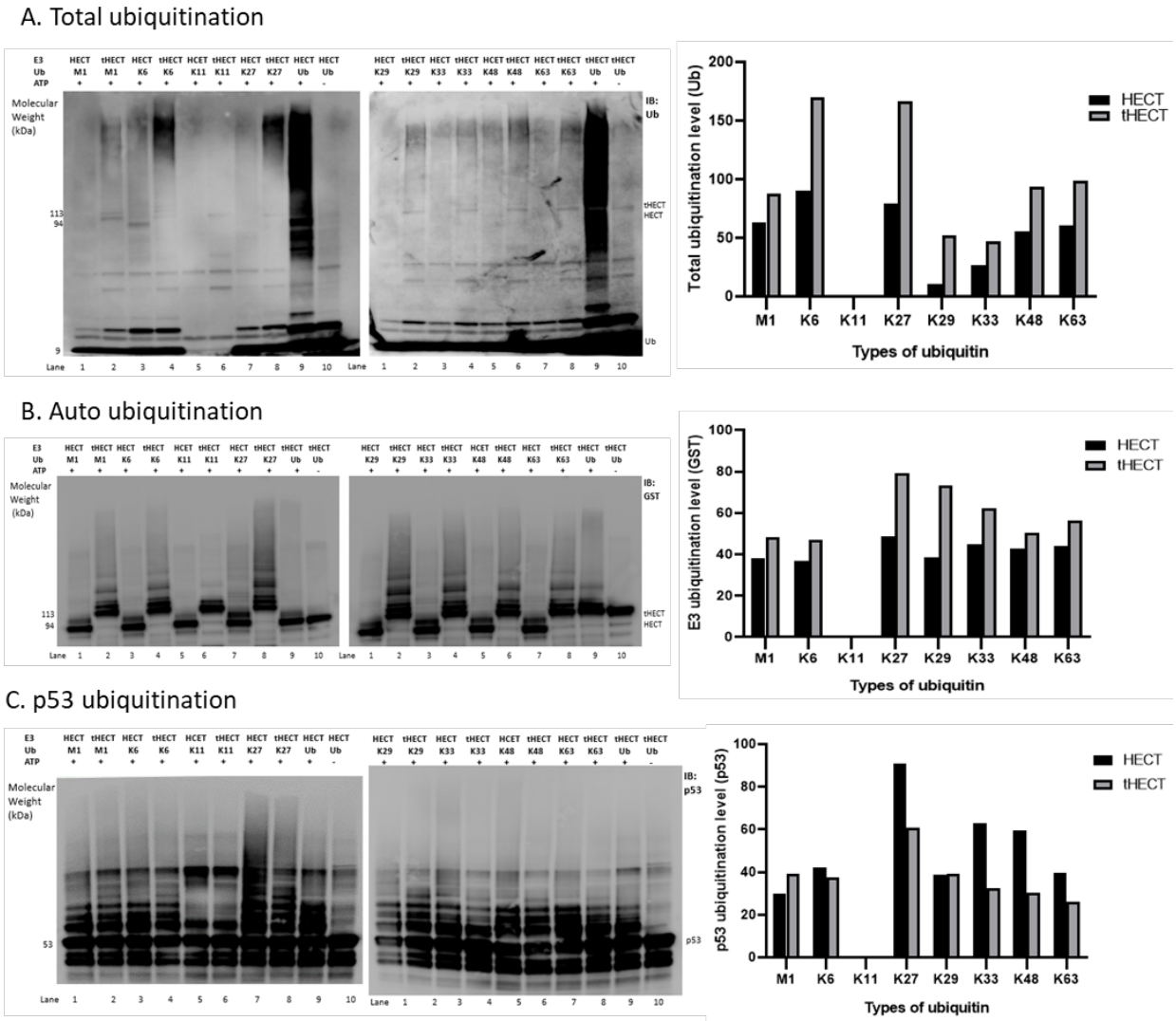

Figure S11. Result of in vitro ubiquitination assay with linkage specific monoUb and p53 repeat1 with negative control. This set of Ub assay was the repeat 1 of Ub assay 1 with the adding negative control omitting ATP in the reaction in the last lane of each blot. **A.** Total ubiquitination probed with anti-Ub Ab and the bar graph illustration. **B.** Auto ubiquitination re-probed with anti-GST Ab from the anti-Ub blots and the bar graph illustration **C.** p53 ubiquitination probed with anti-p53 Ab and the bar graph illustration. Again, K11 linked ubiquitin was not detected by any of three antibodies.

Appendix XII

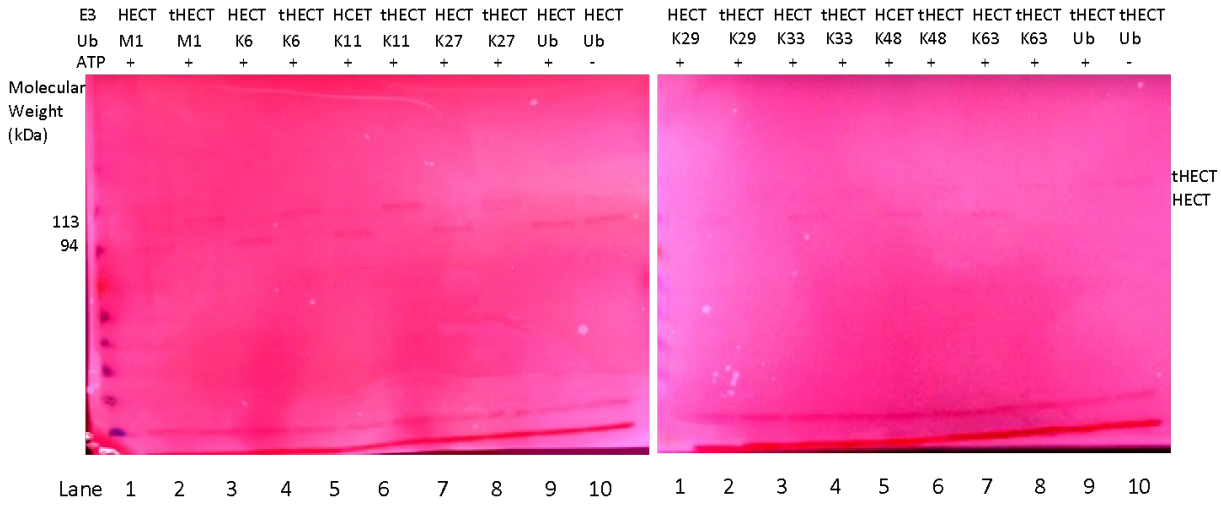

Figure S12. Image of two membranes stained by Ponceau S solution in the in vitro ubiquitination assay with linkage specific monoUb and p53 repeat 1. Those two membranes were probed by anti-Ub antibody for total ubiquitination level detection which corresponds to the blots in Figure S11. Equal loading of GST-tUBM-HECT (113kDa) and GST-HECT (94kDa) was demonstrated by the same size protein bands.

Appendix XIII

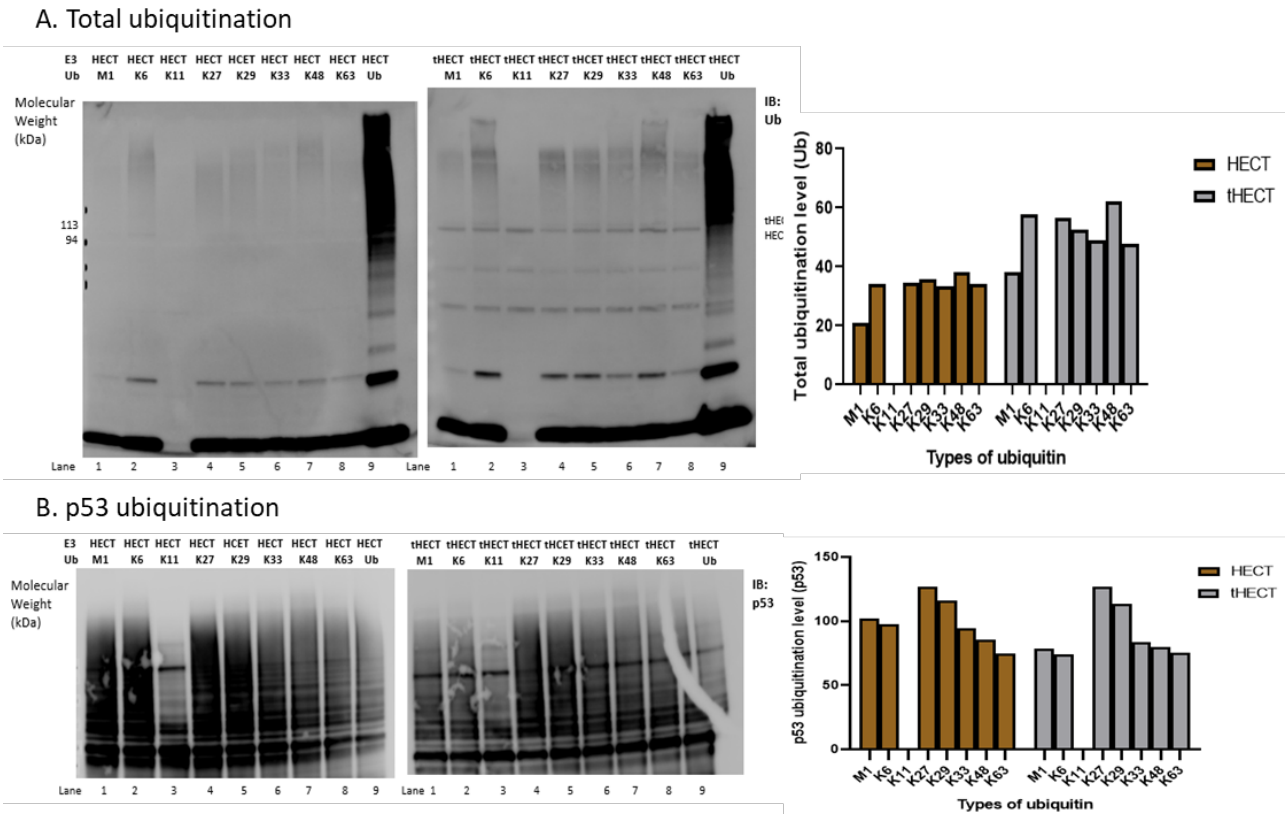

Figure S13. Result of in vitro ubiquitination assay with linkage specific monoUb and p53 repeat 2 in different sample layout. This Ub assay was proceeded with same preparation but different layout contrasting assay1 in order to compare eight types of polyUb levels catalyzed by same E3 on the same membrane. **A.** Left: Result of total ubiquitination probed by anti-Ub Ab in absence/ presence of tUBM domain. Right: Bar graph presentation of the smear intensity of polyubiquitination. K6 and K48 were two most build-up ubiquitin linkages. **B.** Left: p53 ubiquitination result. Right: The intensity of ubiquitinated p53 smear was demonstrated in the bar graph. K11 linked ubiquitin was undetected.

Appendix XIV

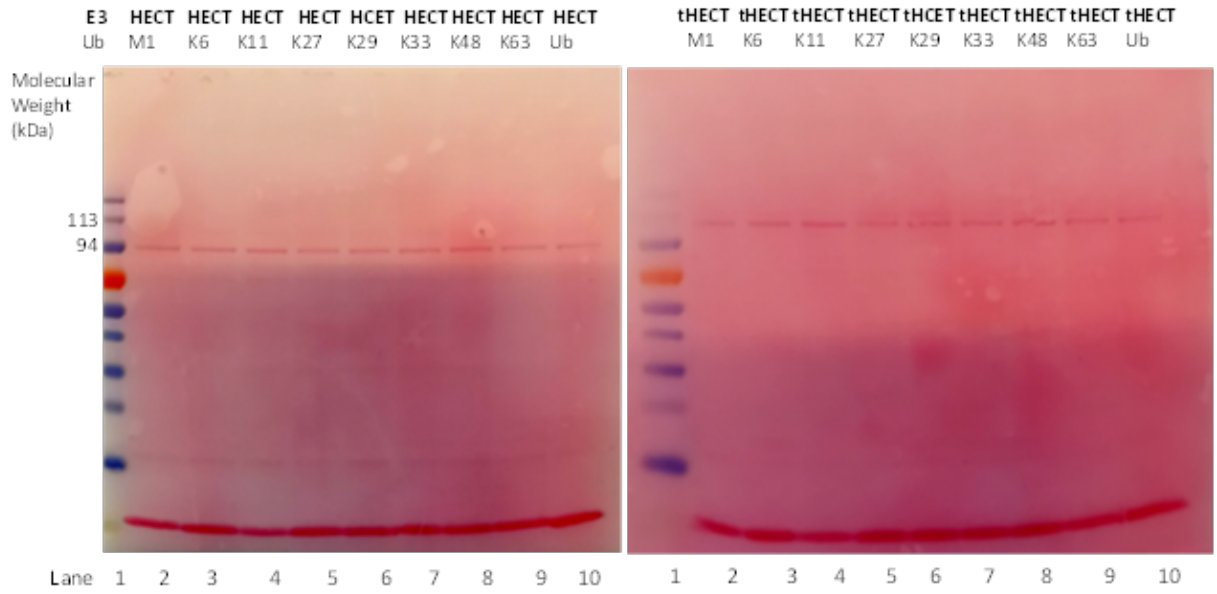

Figure S14. Image of two membranes stained by Ponceau S solution in the in vitro ubiquitination assay with linkage specific monoUb and p53 repeat 2. Those two membranes were probed by anti-Ub antibody for total ubiquitination level detection which corresponds to the blots in Figure S13. Equal loading of GST-tUBM-HECT (113kDa) and GST-HECT (94kDa) was demonstrated by the same size protein bands.

Appendix XV

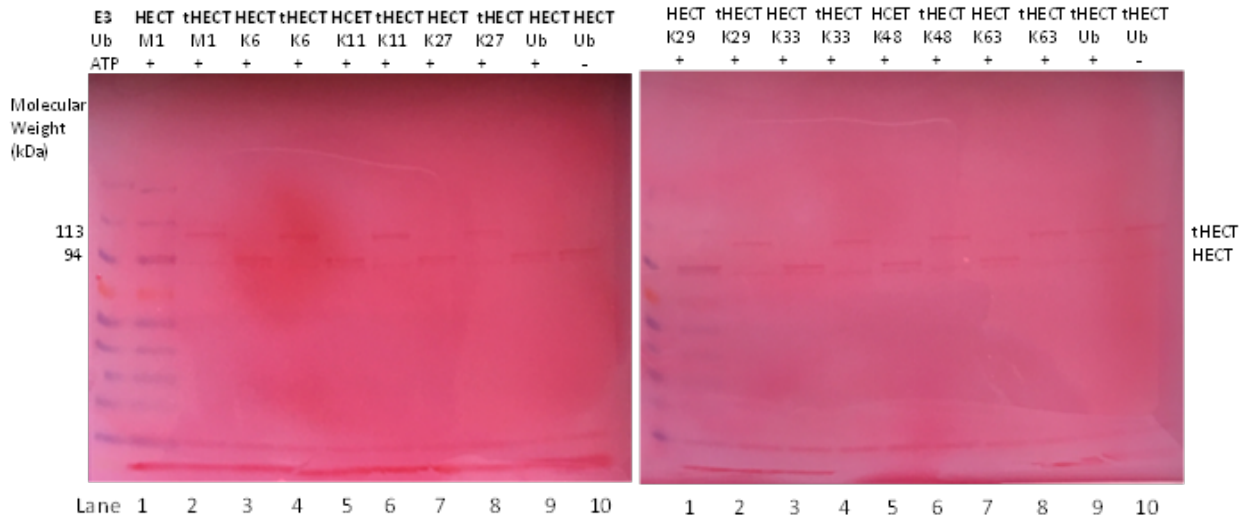

Figure S15. Image of two membranes stained by Ponceau S solution in the in vitro ubiquitination assay with linkage specific monoUb and β-catenin. Those two membranes were probed by anti-Ub antibody for total ubiquitination level detection which corresponds to the blots in Figure 3.4. Equal loading of GST-tUBM-HECT (113kDa) and GST-HECT (94kDa) was demonstrated by the same size protein bands.

Appendix XVI

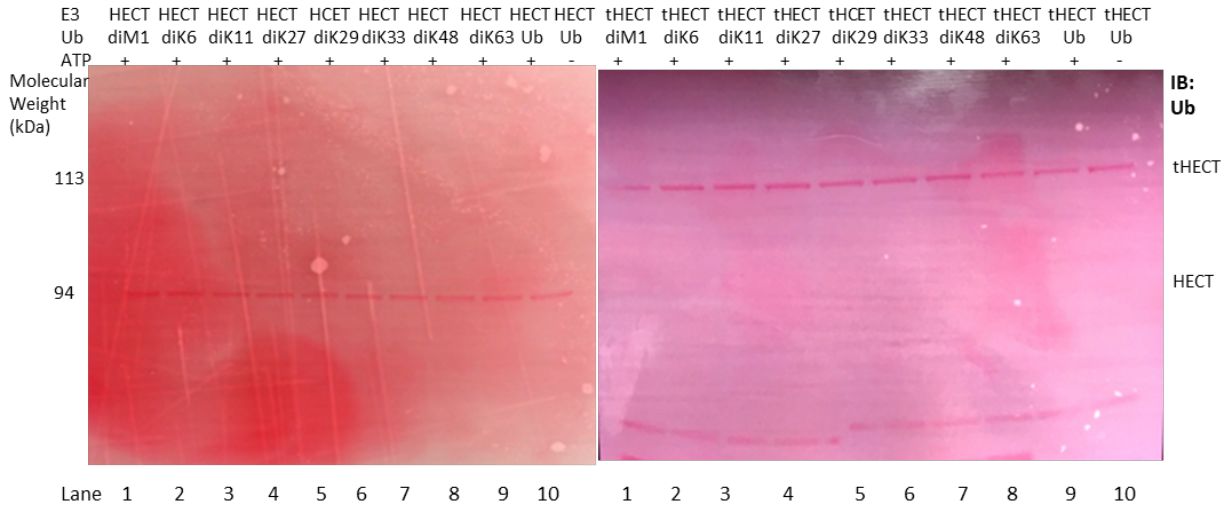

Figure S16. Image of two membranes stained by Ponceau S solution in the in vitro ubiquitination assay with linkage specific diUb and p53 . The membranes stained corelates to the membranes in Figure 3.5. Equal loading was revealed by the same size protein bands.

Appendix XVII

A.

GST tag amino acid sequence

MSPILGYWKI KGLVQPTRLL LEYLEEKYEE HLYERDEGDK WRNKKFELGL EFPNLPYYID
GDVKLTQSMA IIRYIADKHN MLGGCPKERA EISMLEGAVL DIRYGVSRIA YSKDFETLKV
DFLSKLPEML KMFEDRLCHK TYLNGDHVTH PDFMLYDALD VVLYMDPMCL DAFPKLVCFK
KRIEAIPQID KYLKSSKYIA WPLQGWQATF GGGDHPPK

B.

HUWE1 tUBM domain amino acid sequence

TSSEEEDPLA GISLPEGVDP SFLAALPDDI RREVLQNQLG IRPPTRTAPS TNSSAPAVVG
NPGVTEVSPE FLAALPPAIQ EEVLAQQRAE QQRRELAQNA SSDTPMDPVT FIQTLPSDLR
RSVLEDMEDS VLAVMPPDIA AEAQALRREQ EARQRQLMHE RLFGHSSTSA LSA

C.

Constructed linker region between tUBM and HECT domain amino acid sequence

K D P

Figure S17. Amino acid sequence of GST tag and tUBM as well as linker region. **A.** Amino acid sequence of GST based on UniProtKB - P08515 (GST26_SCHJA) Schistosoma japonicum (Blood fluke) GST from UniProt Knowledgebase supported by Swiss Institute of Bioinformatics. 20 lysine residues (red) exist in GST which can be ubiquitin conjugation sites contributing to total and auto HECT mediated ubiquitination level. **B.** Amino acid sequence of tUBM domain (HUWE12951-3123) based on UniProtKB- Q7Z6Z7 human HUWE1. There is no lysine residue in the sequence. **C.** The amino acid sequence of constructed linker region bridging tUBM and HECT domain.

Appendix XVIII

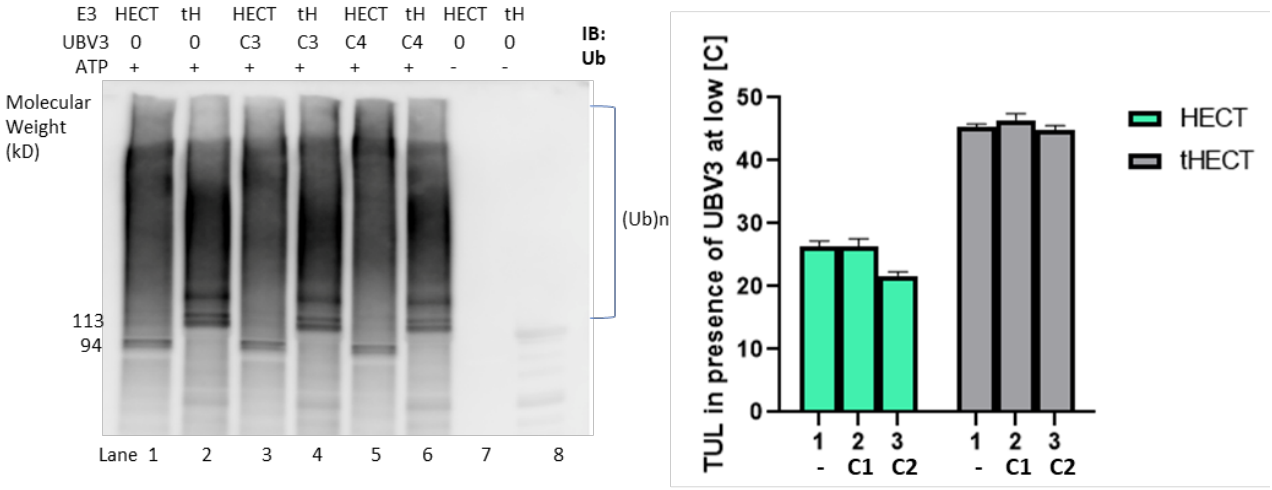

Figure S18. Results of in vitro ubiquitination assay in presence of UbV3 (the 2nd Ub assay with UbV3). The in vitro ubiquitination assay in presence of UbV3 was performed with two different concentrations which were differed from the concentrations in first Ub assay with UbV3 (Figure 5.3). The two concentrations of UbV3 in this assay were C1=0.005µg/µl (0.53µM); C2= 0.01µg/µl (1.06µM). With the concentrations lower than1.06µM, UbV3 did not exert remarkable effect on either HECT or tUBM-HECT. The reaction mixture without ATP was loaded into lane 7,8 serving as negative control.

Appendix XIX

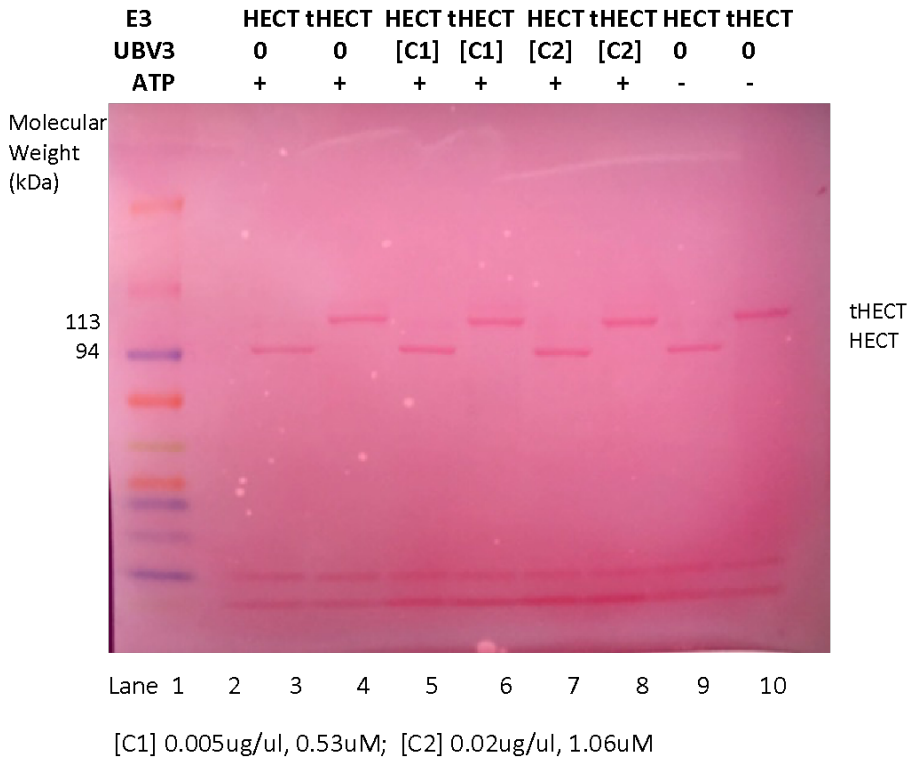

Figure S19. Image of the membrane stained by Ponceau S solution in the in vitro ubiquitination assay in presence of UbV3. The membrane was probed by anti-Ub antibody for total ubiquitination level detection which corresponds to the blots in Figure S18. Equal loading of GST-tUBM-HECT (113kDa) and GST-HECT (94kDa) was demonstrated by the same size protein bands.

Appendix XX

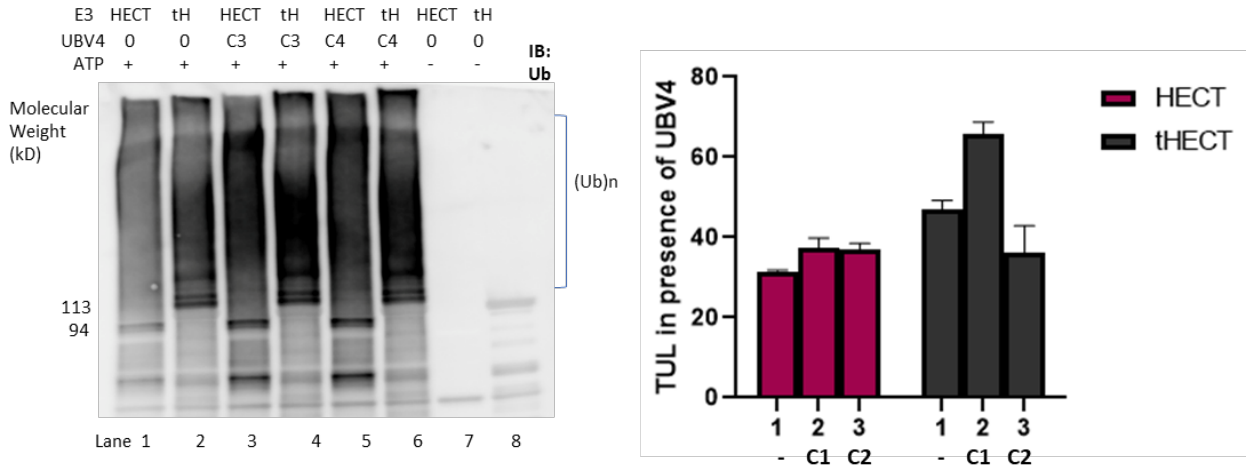

Figure S20. Results of in vitro ubiquitination assay in presence of UbV4 (the 2nd Ub assay with UbV4). The in vitro ubiquitination assay in presence of UbV4 with two concentration was performed. The two concentrations in first assay were C1= 0.015µg/µl (1.60µM); C2=0.03µg/µl (3.19µM). The result showed that at concentration of 1.60µM, UbV4 boosted tUBM further increased total ubiquitination level (lane 3) whereas at 3.19µM, UbV4 lowered the ubiquitination level based on the depressed Ub level (lane 5). Meanwhile, UbV4 also affected HECT catalytic activity through increased ubiquitination level of lane 4. The reaction mixture without ATP was loaded into lane 7,8 serving as negative control.

Appendix XXI

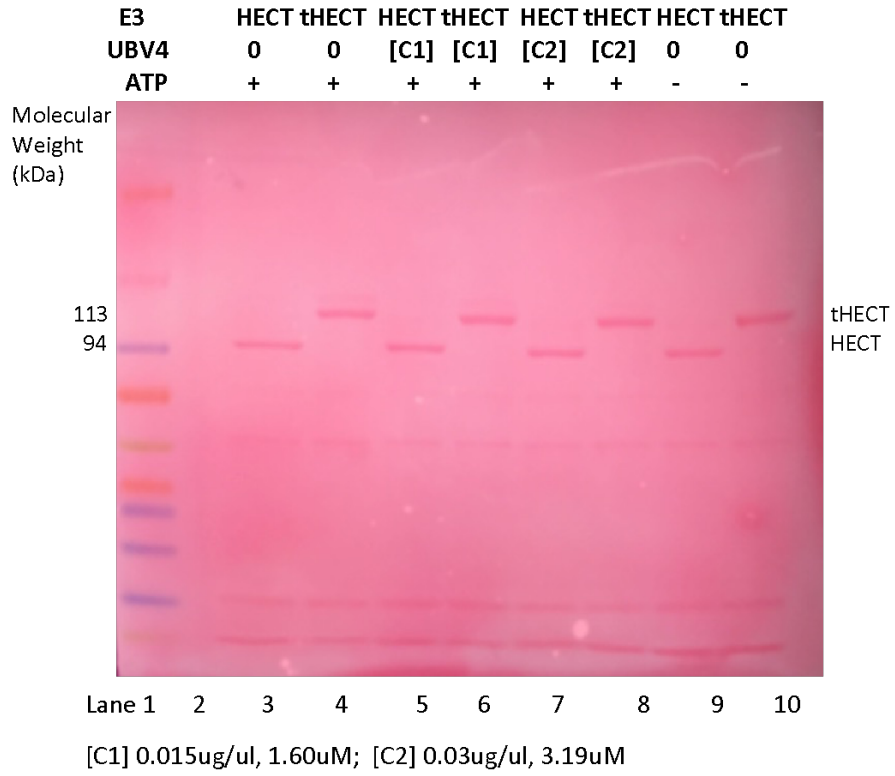

Figure S21. Image of the membrane stained by Ponceau S solution in the in vitro ubiquitination assay in presence of UbV4. The membrane was probed by anti-Ub antibody for total ubiquitination level detection which corresponds to the blots in Figure S20. Equal loading of GST-tUBM-HECT (113kDa) and GST-HECT (94kDa) was demonstrated by the same size protein bands.